

DISSERTATION

**BIOCHEMICAL, BIOPHYSICAL AND STRUCTURAL STUDY OF
THE NUCLEOSOME-MECP2 COMPLEX**

Submitted by

Chenghua Yang

Department of Biochemistry and Molecular Biology

In partial fulfillment of the requirements

For the Degree of Doctor of Philosophy

Colorado State University

Fort Collins, CO

Summer 2009

UMI Number: 3385142

All rights reserved

INFORMATION TO ALL USERS

The quality of this reproduction is dependent upon the quality of the copy submitted.

In the unlikely event that the author did not send a complete manuscript and there are missing pages, these will be noted. Also, if material had to be removed, a note will indicate the deletion.



UMI 3385142

Copyright 2009 by ProQuest LLC.

All rights reserved. This edition of the work is protected against unauthorized copying under Title 17, United States Code.



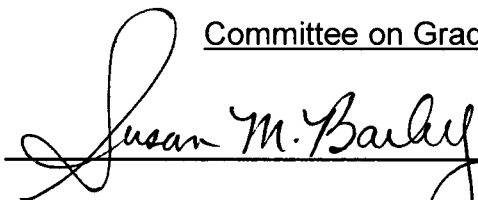
ProQuest LLC
789 East Eisenhower Parkway
P.O. Box 1346
Ann Arbor, MI 48106-1346

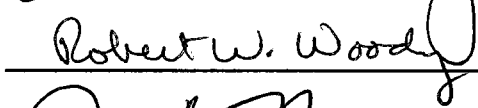
COLORADO STATE UNIVERSITY

July 2, 2009

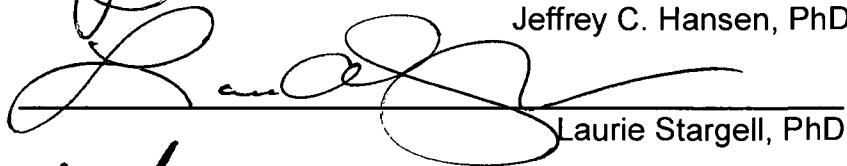
WE HEREBY RECOMMEND THAT THE DISSERTATION PREPARED UNDER OUR SUPERVISION BY CHENGHUA YANG ENTITLED "BIOCHEMICAL, BIOPHYSICAL AND STRUCTURAL STUDY OF THE NUCLEOSOME-MECP2 COMPLEX" BE ACCEPTED AS FULFILLING IN PART THE REQUIREMENTS FOR THE DEGREE OF DOCTOR OF PHILOSOPHY.

Committee on Graduate Work

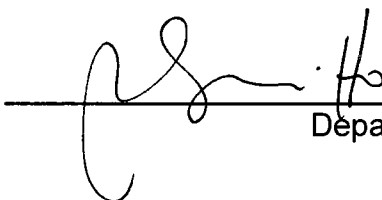

Susan Bailey, PhD


Robert Woody, PhD


Jeffrey C. Hansen, PhD


Laurie Stargell, PhD


Adviser: Karolin Luger, PhD


Department Head: P. Shing Ho, PhD

ABSTRACT OF DISSERTATION

BIOCHEMICAL, BIOPHYSICAL AND STRUCTURAL STUDY OF THE NUCLEOSOME-MECP2 COMPLEX

Methyl-CpG Binding Protein (MeCP2) is an abundant chromatin associated protein that is important in maintaining human health; mutations in this protein cause Rett Syndrome, a neurodevelopmental disease that is a common cause of mental retardation and autism in females. MeCP2 was initially identified as a protein that recognizes the genetic DNA methyl-CpG mark and it was thought to repress gene transcription by recruiting histone deacetylases. Recent studies show that MeCP2 can both repress and activate gene transcription. It also binds chromatin in the absence of the methylation mark, suggesting that its mode of action is more complex than previously assumed.

The observation that MeCP2 compacts nucleosomal arrays *in vitro* and mediates silent chromatin loop formation *in vivo* suggests a novel mechanism by which MeCP2 regulates gene expression. To further characterize the interplay between MeCP2 and chromatin, it is important to understand the interactions between MeCP2 and nucleosomes, the fundamental component of chromatin. We used biochemical and biophysical approaches to study the interplay between MeCP2 and nucleosomes. Gel mobility assays showed that although MeCP2 can interact with a nucleosome with or without extra nucleosomal DNA, it has a higher affinity for nucleosomes with extra nucleosomal DNA. The N-terminal portion of human MeCP2 (amino acids 78-305) is sufficient to establish this

interaction. Size-exclusion chromatography combined with multi-angle light scattering and fluorescence resonance energy transfer (FRET) assays demonstrated that this interaction occurs at a 1:1 molar ratio and that MeCP2 brings the extra nucleosomal DNA ends in a closer proximity. Small angle X-ray scattering (SAXS) revealed the formation of a more compact complex when MeCP2 interacts with nucleosome with (*versus* without) extra nucleosomal DNA, indicating that the extra nucleosomal DNA is important in organizing the MeCP2-nucleosome complex. Our data suggest a model in which MeCP2 compacts chromatin by changing the extra nucleosomal DNA path.

X-ray crystallography is also used to characterize the nucleosome-MeCP2 complex. Crystals of the nucleosomes with extra nucleosomal DNA in complex with MeCP2 were obtained and diffracted to 5.2 Å. Although MeCP2 dissociated from the crystals after soaking in cryo-protectant, the electron density map reveals the path of extra nucleosomal DNA which may be organized by MeCP2.

Chenghua Yang
Department of Biochemistry and Molecular Biology
Colorado State University
Fort Collins, CO 80523
Summer 2009

ACKNOWLEDGEMENTS

I feel very lucky to have the opportunity to pursue a PhD at Colorado State University in Fort Collins – the number one place to live in the United States. I also feel very lucky to join Karolin Luger’s lab and have Karolin Luger as my mentor. During my four-year’s graduate study here, I have many people I want to express my deepest thanks to.

First of all, I would like to express my deepest gratitude to my great mentor, Dr. Karolin Luger, for her advice, inspiration, encouragement and support during my study in her laboratory. From her, I learned from little things including how to write a progress report, how to do presentation, to big things like how to do science and become a good scientist. I think I will benefit from what I have learned from her for my life time.

I would also like to give my special thanks to my wonderful committee members, Dr. Laurie Stargell, Dr. Jeffrey C. Hansen, Dr. Robert Woody, and Dr. Susan Bailey, for their enormous support and help during all my graduate study.

I am very grateful to the past and current members of the Luger laboratory who generously offered their friendship and help to me. They made my study enjoyable in the lab. I really enjoyed working in such a great lab where it feels like a big family. I want to give my special thanks to Dr. Mark van der Woerd who is my “secondary mentor” and taught me crystallography and SAXS. I appreciate Pam Dyer and Dr. Uma Muthurajan for their great advice and help on my research work, they are also my “life mentor”. I want to thank Yunhe Bao, Young-Jun Park, Jayanth Chodaparambil, Vidya Subramanian, Mary Robinson, Wayne

Lilyestrom, and Andy Andrews for their insightful discussion and selfless help. I also appreciate Kitty Brown, Alyson White, Sheena D'Arcy, Mekonnen Lemma Dechassa and Ling Zhang for their genuine friendship. I want to give another special thank to Beth Kasney who made my life in the lab smooth and easier. I also appreciate Keely Sudhoff and Nicholas Clark who made the lab more joyful.

Last but not least, I would like to thank my entire family for their selfless support and love. Without them, I would not have made my way here.

Table of Contents

| | |
|---|------------|
| TITLE PAGE | I |
| SIGNATURE PAGE | II |
| ABSTRACT OF DISSERTATION | III |
| ACKNOWLEDGEMENTS | V |
| CHAPTER 1 | 1 |
| REVIEW OF LITERATURE | 1 |
| 1.1 CHROMATIN STRUCTURE, FUNCTION AND DYNAMICS | 1 |
| 1.2 DNA METHYLATION AND CHROMATIN STRUCTURE..... | 6 |
| 1.3 DNA METHYLATION AND THE METHYL-CPG BINDING PROTEIN (MBP) FAMILY | 8 |
| 1.4 RETT SYNDROME AND MECP2 | 13 |
| 1.4.1 <i>Rett Syndrome</i> | 13 |
| 1.4.2 <i>What is the function of MeCP2? Why does its mutation cause Rett Syndrome?</i> | 17 |
| 1.5 MECP2 AND CHROMATIN STRUCTURE..... | 23 |
| 1.6 SPECIFIC AIMS AND LAYOUT OF THE DISSERTATION..... | 26 |
| CHAPTER 2 | 28 |
| EXTRA NUCLEOSOMAL DNA IN NUCLEOSOMES GUIDES THE ORGANIZATION OF THE NUCLEOSOME-MECP2 COMPLEX | 29 |
| 2.1 ABSTRACT:..... | 29 |
| 2.2 INTRODUCTION | 30 |
| 2.3 EXPERIMENTAL PROCEDURES | 35 |
| 2.3.1. <i>Expression and purification of MeCP2</i> | 35 |
| 2.3.2. <i>DNA for nucleosome reconstitution</i> | 35 |
| 2.3.3. <i>Nucleosome reconstitution</i> | 36 |
| 2.3.4. <i>Electrophoretic mobility shift assays (EMSA)</i> | 37 |
| 2.3.5. <i>Nucleosome competition assay</i> | 37 |
| 2.3.6. <i>Analytical Ultracentrifugation</i> | 38 |
| 2.3.7. <i>Multi-angle Light scattering (SEC-MALS) assay</i> | 38 |
| 2.3.8. <i>Fluorescence resonance energy transfer (FRET) assay</i> | 39 |
| 2.3.9. <i>Small angle X-ray scattering (SAXS) data collection and analysis</i> | 40 |
| 2.4 RESULTS..... | 41 |
| 2.4.1. <i>MeCP2 binds to nucleosomes (146 NCP and 165NCP)</i> | 41 |
| 2.4.2. <i>Sedimentation properties of the NCP-MeCP2 complex</i> | 43 |
| 2.4.3. <i>Stoichiometry of the NCP-MeCP2 complex</i> | 46 |
| 2.4.4. <i>MeCP2 prefers nucleosome with extra nucleosomal DNA</i> | 49 |
| 2.4.5. <i>MeCP2 brings extra nucleosomal DNA ends in 165NCP in a closer proximity</i> .53 | 53 |
| 2.4.6. <i>Small angle X-ray scattering (SAXS) studies of the NCP-MeCP2 complex</i> .58 | 58 |
| 2.5 DISCUSSION..... | 65 |
| 2.5.1. <i>Extra nucleosomal DNA is not necessary for MeCP2 to interact with nucleosomes, but it is important to organize the nucleosome-MeCP2 complex</i> | 65 |
| 2.5.2. <i>MeCP2 does not bridge mono-nucleosomes</i> | 71 |
| 2.5.3. <i>Implications for how MeCP2 compacts chromatin</i> | 73 |

| | |
|--|------------|
| 2.6 ACKNOWLEDGEMENT | 75 |
| CHAPTER 3 | 77 |
| ARE THERE ANY INTERACTIONS BETWEEN MECP2 AND HISTONES WITHIN NUCLEOSOMES?..... | 77 |
| 3.1 ABSTRACT..... | 77 |
| 3.2 INTRODUCTION | 78 |
| 3.3 MATERIALS AND METHODS | 80 |
| 3.3.1 Preparation of MeCP2 for pull-down assay | 80 |
| 3.3.2 Refolding of histone dimer, tetramer or octamer | 81 |
| 3.3.3 Pull-down assay with intein tag | 81 |
| 3.3.4 Isothermal Titration Calorimetry (ITC) | 82 |
| 3.3.5 Sedimentation velocity | 82 |
| 3.3.6 Gel filtration combined with multi angle light scattering (SEC-MALS) | 83 |
| 3.4 RESULTS..... | 83 |
| 3.4.1 MeCP2-Intein fusion protein can pull down histone complexes. | 84 |
| 3.4.2 His-tagged histone complexes do NOT pull down MeCP2. | 89 |
| 3.4.3 The interaction between MeCP2 and histones was not detected by Isothermal Titration Calorimetry (ITC). | 91 |
| 3.4.4 Sedimentation velocity did not give a conclusive result about the interaction between MeCP2 and histones | 93 |
| 3.4.5 The interaction between MeCP2 and histones cannot be detected by gel filtration..... | 95 |
| 3.5 DISCUSSION | 99 |
| 3.6 ACKNOWLEDGEMENT | 101 |
| CHAPTER 4 | 102 |
| CRYSTALLOGRAPHIC STUDIES OF NUCLEOSOME-MECP2 COMPLEX.. | 102 |
| 4.1 INTRODUCTION | 102 |
| 4.2 MATERIALS AND METHODS | 104 |
| 4.2.1 Nucleosome reconstitution..... | 104 |
| 4.2.2 MeCP2 expression and purification..... | 105 |
| 4.2.3 Expression and purification of Selenium labeled MeCP2 | 105 |
| 4.2.4 Electrophoresis mobility shift assay (EMSA) for interactions between MeCP2 and nucleosome | 106 |
| 4.2.5 Crystallization of nucleosome..... | 106 |
| 4.2.6 Soaking MeCP2 MBD fragment into nucleosome crystals..... | 107 |
| 4.2.7 Co-crystallization of nucleosome-MeCP2 complex..... | 107 |
| 4.2.8 Heavy atom tetrakis(acetoxymethyl)-methane (TAMM) soaking procedure for nucleosome-MeCP2 complex | 108 |
| 4.2.9 Data collection and structure refinement | 109 |
| 4.3 RESULTS AND DISCUSSION | 110 |
| 4.3.1 Nucleosome crystals soaking with MeCP2 fragment | 110 |
| 4.3.2 Co-crystallization of nucleosome-MeCP2 complex..... | 117 |
| 4.4 DISCUSSION | 134 |
| 4.5 ACKNOWLEDGEMENT | 137 |
| CHAPTER 5 | 138 |
| SUMMARY AND FUTURE DIRECTIONS..... | 138 |

| | |
|--------------------------|------------|
| APPENDIX I | 144 |
| APPENDIX II | 145 |
| REFERENCES..... | 146 |

CHAPTER 1

REVIEW OF LITERATURE

1.1 Chromatin structure, function and dynamics

DNA is the genetic information carrier in cells. In mammalian cells, DNA is about 2 meters long and is packed into the cell's nucleus which is only about 6 μm in diameter on average. To achieve this, DNA is organized into DNA-protein complexes known as chromatin. Chromatin also serves as a mechanism to control gene expression and DNA replication by physically limiting the access of transcription factors as well as of the DNA replication and repair machinery to DNA.

Structurally there are two different forms of chromatin: euchromatin and heterochromatin. Euchromatin is a less compact form, or extended form, of chromatin structure, where genes are frequently transcribed. The other form, heterochromatin, is a more compact form, or condensed form, of chromatin structure, and contains genes that are infrequently transcribed in the cell (reviewed in (Ehrenhofer-Murray, 2004)).

While chromatin is the basic organizational form of DNA in the nucleus, nucleosomes are the basic building blocks and repetitive units of chromatin. A conventional Nucleosome Core Particle (NCP) consists of 146-147 base pairs of

DNA wrapped around a histone octamer core in 1.65 left-handed super helical turns (figure 1.1) (Luger et al., 1997). The histone octamer contains two copies each of the four major type histones, H2A, H2B, H3 and H4. The octamer is made up of histone H3/H4 tetramer, which organizes 80 base pairs of nucleosomal DNA, and two histone H2A/H2B dimers, which are located on either side of H3/H4 tetramer and organize ~30 base pairs of nucleosomal DNA at the two ends. The chromatin fiber also contains a fifth histone, the linker histone (usually referred as linker histone H1 or its variant H5), which can bind to the nucleosomal DNA at its “entry-exit” region (Hamiche et al., 1996a)(Bednar et al., 1998) and protect about 10 base pairs of linker DNA on either side (reviewed in (Thomas, 1999))(Nikitina et al., 2007a). Hundreds of thousands of nucleosomes repeat in an array and form a beads-on-a-string structure with a diameter of about 10 nm (the 10nm chromatin fiber), which is also called chromatin’s primary structure. This 10nm chromatin fiber further folds into a fiber with an approximate diameter of 30 nm: the 30nm chromatin fiber. This usually happens in the presence of linker histone (Robinson et al., 2006; Robinson and Rhodes, 2006). The 30-nm chromatin fiber is also referred to as the secondary chromatin structure and it folds further into a tertiary structure via unknown mechanisms (figure 1.2).

Although the detailed mechanisms of how chromatin folds into its higher order structure are unknown, in general, there are two different pathways by which chromatin condenses into high order structures: the intrinsic pathway and the protein-mediated pathway. The intrinsic pathway refers to the dynamic behavior

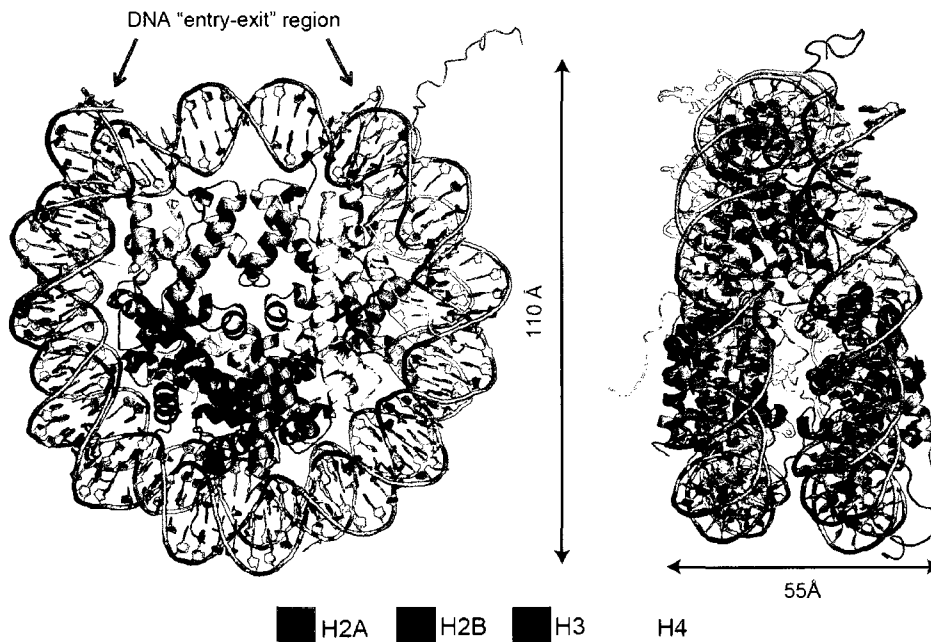
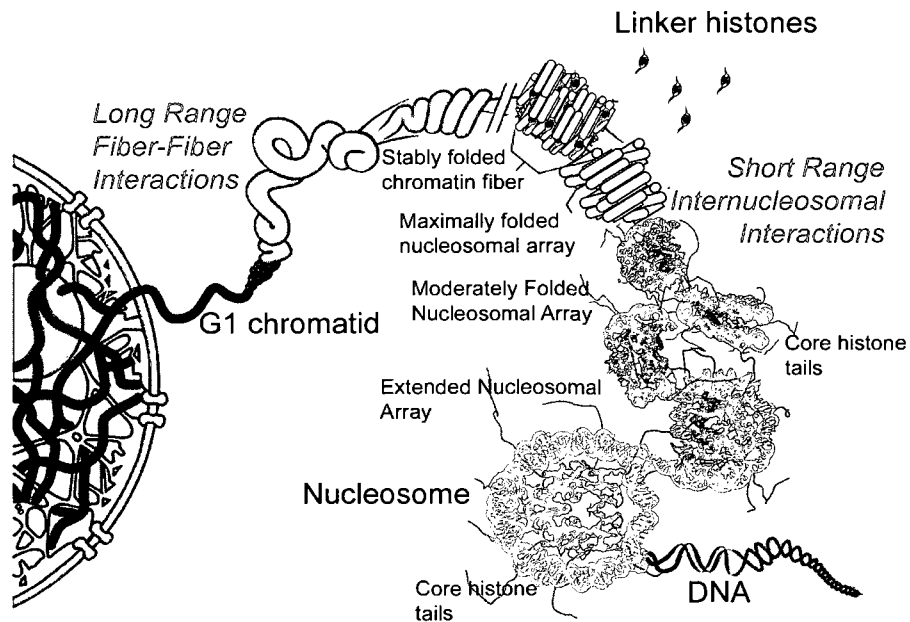


Figure 1.1: Structure of the Nucleosome. Front view (left) and side view (right) of the nucleosome. The dimensions of a single nucleosomal unit are indicated along the side of the mononucleosome structure. The color scheme used for the protein octamer core is explained below the structure. This figure is adapted from PDB file 1AOI (Luger et al., 1997).



Adapted from Hansen, 2002

Figure 1.2: Hierarchy of DNA compaction. The basic unit of chromatin—the nucleosome is represented at the bottom of the DNA compaction ladder. Nucleosomes in an array form the “beads-on-a-string” structure, the primary chromatin structure. This beads-on-a-string structure further folds into a fiber with a diameter of about 30 nm, the secondary chromatin structure, usually in the presence of linker histones. The 30nm fiber compacts further into a higher order chromatin structure, the tertiary structure, by unknown mechanisms (Hansen, 2002).

of regularly spaced nucleosomal arrays. It has been established that all the core histones within the nucleosomal histone octamer and one or more of the core histone N-terminal tail domains (NTDS) are extensively involved in the intrinsic chromatin condensation pathway (Hansen, 2002). For example, the “acidic charge patch” on the surface of H2A-H2B in one nucleosome can interact with the H4 NTD from a neighboring nucleosome, thereby inducing the intrinsic folding of chromatin (Dorigo et al., 2004; Luger et al., 1997; Zhou et al., 2007). Richmond and his colleagues showed that the histone H4 NTD is essential for the folding of the 10nm fiber into the 30nm fiber (Dorigo et al., 2003). A recent study employed atomic force microscopy (AFM) and showed that without histone tails, nucleosomal arrays did not aggregate at high salt concentrations, which is in contrast with the behavior of nucleosomal arrays composed of nucleosomes with intact histone N-terminal tails (Hizume et al., 2009). These results demonstrate that attractive interactions between nucleosomes through their histone tails are critical in the formation of chromatin secondary structure.

The fifth histone, the linker histone (such as H1 and H5) is also involved in the intrinsic chromatin condensation. Linker histones are abundantly associated with chromatin. In different cell types, the stoichiometry of linker histones to nucleosome core particles is approximately one to one (Bates and Thomas, 1981) (Woodcock et al., 2006). Linker histones can bind to the DNA “entry-exit” region of nucleosomes and form a “stem” like structure, which is very important in stabilizing the 30nm chromatin fiber from the 10nm fiber (Routh et al., 2008).

The other important pathway for chromatin condensation is the protein-mediated pathway. It has been shown that many non-histone nucleosome-binding proteins can mediate chromatin folding. For example, Methyl-CpG binding protein 2 (MeCP2) is an abundant chromatin associated protein. It has been shown that MeCP2 is also a chromatin architectural protein that can compact a nucleosomal array into its higher order structure in a different way from how H1 compacts chromatin (Georgel et al., 2003). Other chromatin architectural proteins, including myeloid and erythroid nuclear termination (MENT), heterochromatin protein 1 α (HP1 α) and polycomb group protein complex (PCC), have also been shown to mediate the compaction of chromatin to a higher order structure (Fan et al., 2002; Francis et al., 2004; Springhetti et al., 2003).

DNA that is packed in chromatin has to be accessible to cellular processes including DNA transcription, replication and repair. Therefore, the chromatin structure has to be dynamic during these processes. Indeed, chromatin fiber is highly dynamic during cellular processes.

1.2 DNA methylation and chromatin structure

In eukaryotes, DNA methylation is a major and important epigenetic modification of genomes. This modification usually occurs at position 5 of cytosines when a cytosine is followed by a guanosine (CpG). In eukaryotes, most of the CpG sites are methylated except in regions called CpG islands where DNA sequences have a high frequency of CpG dinucleotides in a stretch of about 500-2000 base pairs (Bird, 1986). Methylation of CpG islands has been found to occur in the

inactivated X chromosome of female mammals and subsequently represses associated genes (Riggs and Pfeifer, 1992). Methylation of CpG dinucleotides is crucial for mammalian development and plays an important role in inactivation of the X-chromosome and genomic imprinting (Jaenisch, 1997). Early studies have indicated that DNA methylation directs the formation of nuclease-resistant chromatin and represses gene activity as a consequence (Keshet et al., 1986)(Cedar, 1988)(Boyes and Bird, 1991)(Bird, 1992)(Razin, 1998)(Bird and Wolffe, 1999). Thus, the general consensus regarding DNA methylation is that it is associated with gene repression and heterochromatin formation.

Theoretically, DNA methylation can repress gene expression through three different mechanisms. First, methylation on cytosine bases can physically block the association of transcription factors to their specific DNA recognition sites. It has been shown that some transcription factors cannot bind to their target sequences when they are methylated (Comb and Goodman, 1990; Iguchi-Ariga and Schaffner, 1989). Second, proteins that can recognize the methylation mark on CpG sites can bind to the methylated CpG sites and then either exclude the binding of transcription factors to the same sites or recruit other transcription repressors to repress transcription (Hendrich and Bird, 1998). Third, methylated DNA with the help of other proteins that bind to the methylated DNA can change the chromatin structure directly or indirectly, which in turn could limit the access of transcription machinery to the DNA and repress gene transcription (Razin, 1998). It has been shown that, in native chromatin, methylated DNA sequences

are more susceptible to micrococcal nuclease digestion, which suggests a change in chromatin structure (Antequera et al., 1989).

1.3 DNA methylation and the Methyl-CpG Binding Protein (MBP) family

The information contained in the DNA methylation mark is interpreted by a family of proteins called methyl-CpG binding protein family (MBP family) which can recognize the methyl-CpG sites. Proteins in this family share a common methyl-CpG-binding domain (MBD domain), the protein motif that is responsible for recognizing and binding to methylated CpG dinucleotides. To date, there are five mammalian protein members identified in this family: MeCP2, MBD1, MBD2, MBD3 and MBD4 (figure 1.3).

Initially MeCP1 and MeCP2 were the first proteins identified in this family with the ability to recognize methylated CpG (Lewis et al., 1992; Meehan et al., 1989). MeCP1 is a large multisubunit protein complex; it was originally identified as a nuclear factor that can specifically bind to DNA containing methylated CpGs (Meehan et al., 1989). MeCP2 (Methyl-CpG-Binding Protein 2) is a single protein with a molecular weight of 52.4 kDa. It is a chromatin associated protein that can bind to DNA with a single methylated CpG pair (Lewis et al., 1992). So MeCP2 was the first true member of the MBP protein family. Two functional domains have been well characterized: a methyl-CpG-binding domain (MBD) that can specifically recognize the methylated CpG sites (Nan et al., 1993) and a transcription repression domain (TRD), which is important for the silencing of gene transcription (Nan et al., 1997).

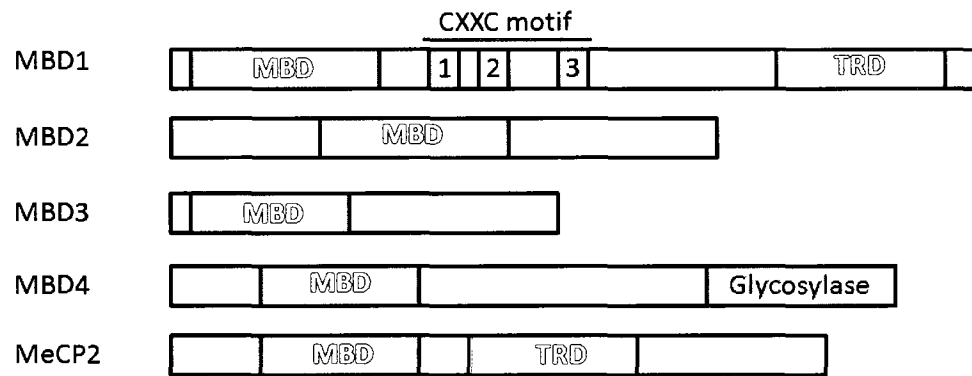


Figure 1.3: Schematic map of MBD family proteins. All the proteins in this family have a common MBD domain. CXXC motif: the cysteine-rich motif in MBD1. MBD: Methyl-CpG-binding domain. TRD: transcription repression domain.

Based on the conserved amino acid sequence of the MBD domain in MeCP2, a database search for sequence homologues of the MBD domain led to the identification of four other proteins in the MBP family: MBD1 (formerly called PCM1: Protein Containing MBD), MBD2, MBD3 and MBD4 (Cross et al., 1997; Hendrich and Bird, 1998). A schematic map of the mammalian MBP family of proteins is shown in figure 1.3.

MBD1, a protein of 70 kDa, has two or three cysteine-rich regions (CXXC1, CXXC2, CXXC3 motifs) between the MBD motif on the N-terminus and the TRD motif on the C-terminus (see figure 1.3). Due to alternative splicing in the region of CXXC domains and the C-terminus, MBD1 has at least 5 isoforms (Fujita et al., 1999). Depending on the presence or absence of the CXXC3 motif, different MBD1 isoforms have different roles. For example, with the presence of all three CXXC motifs, MBD1 isoforms MBD1v1 and MBD1v2 can repress transcription from both methylated and unmethylated promoters. In the absence of the CXXC3 motif, MBD1 isoforms MBD1v3 and MBD1v4 only repress transcription from methylated promoters (also reviewed in (Nakao et al., 2001)). Thus, the CXXC3 motif may have a role in binding to unmethylated DNA.

MBD2 is a component of the MeCP1 protein complex which also contains histone deacetylases (Cross et al., 1997; Ng et al., 1999). Both MBD2 and MBD4 can specifically bind to methylated DNA in *vitro* or in *vivo*. In mouse cells, they both co-localize with hypermethylated satellite DNA foci (Hendrich and Bird, 1998). Although MBD3 also has a MBD domain that shares high homology to

MBD2, surprisingly, MBD3 does not bind methylated DNA *in vitro* and *in vivo*. Instead, MBD3 forms a Mi-2/NuRD complex with nucleosome remodeling complex and histone deacetylase, and the complex can be tethered to methylated DNA by the presence of MBD2 (Wade et al., 1999)(Zhang et al., 1999). MBD4 can bind to hemimethylated DNA or mismatched methylated CpG-TpG pairs, and thus is proposed to function as a part of the DNA repair system (Hendrich et al., 1999)(Riccio et al., 1999).

To date, the structure of the MBD domain of human MBD1 was solved by NMR (Ohki et al., 2001) and the structure of the MBD of human MeCP2 were solved by NMR (Wakefield et al., 1999) and X-ray crystallography (Ho et al., 2008). The MBD structures from both methods are easily aligned and consist of a wedge shape with antiparallel β -stands forming one face of the wedge and α -helices forming the other face (figure 1.4). Interestingly, both MBD structures have largely disordered regions. The structures of MBDs have shed light on how the MBD domain interacts with methylated CpG pairs. The X-ray crystal structure of the MBD in hMeCP2 revealed that it recognizes the CpG methylation mark by hydrogen-bond interactions through water molecules, rather than by hydrophobic interactions as predicted before.

How do the MBP family proteins interpret the methylation on DNA after they recognize the methylation mark? It has been shown that, except for MBD1 and MBD4, all other MBDs including MeCP2, MBD2 and MBD3 are associated with histone deacetylase complexes and are involved in the compaction of chromatin

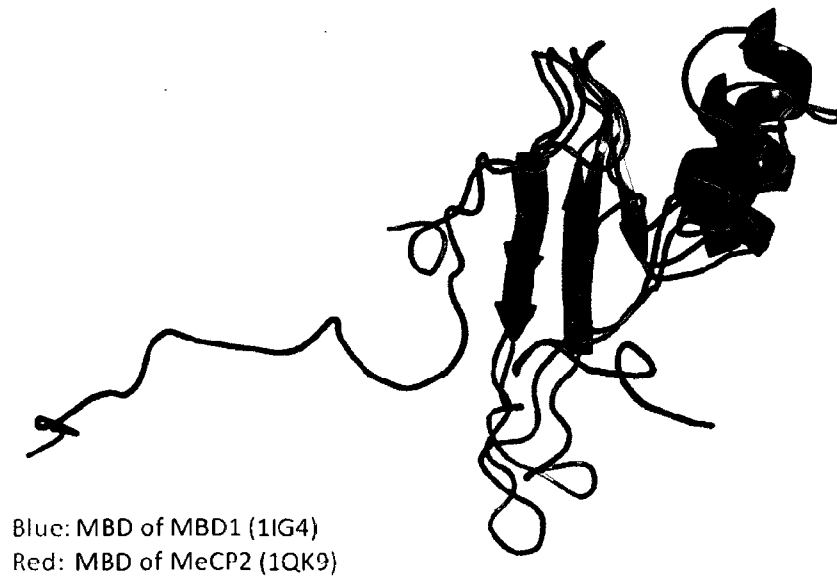


Figure 1.4: NMR structures of the MBD domains of human MBD1 and MeCP2. The two solution structures are aligned. Both structures consist of a wedge shape with antiparallel β -stands forming one face of the wedge and α -helices forming the other face.

into inactive heterochromatin, leading to transcriptional repression (Jones et al., 1998)(Nan et al., 1998)(Ng et al., 1999)(Zhang et al., 1999)(Wade et al., 1999). However, the detailed mechanism of how MBDs repress transcription remains unclear. After *MECP2* is identified as a disease-related gene, mutations in which cause Rett syndrome—a neurodevelopmental disease, studies on MeCP2 have bloomed afterwards.

1.4 Rett syndrome and MeCP2

1.4.1 Rett Syndrome

Rett Syndrome (RTT) is a postnatal neurodevelopmental disease first described by Andreas Rett, an Austrian pediatrician, in 1966 (Rett, 1966). It was not commonly recognized in the medical community until 17 years later. Dr. Hagberg, a Swedish neurologist, reported 35 cases of RTT (Hagberg et al., 1983). It is now appreciated that RTT is one of the common causes of mental retardation and autism in females. The incidence of RTT is estimated to be about 1 in every 10,000-15,000 females (Hagberg, 1985).

Patients with classic RTT usually show normal development after birth until 6 to 18 months of age, when they start to develop regression symptoms, including the loss of already gained ability to speak, walk and use hands purposefully. Affected individuals gradually develop stereotypic hand wringing, extended gazing, irritability, ataxia and gait apraxia (Hagberg et al., 1983). Microcephaly, mental retardation, seizures, autism and hyperventilation during wakefulness are also

common symptoms in RTT patients (Hagberg et al., 1983). Females affected with RTT usually can survive to adulthood, but sudden death does occur, probably due to the breathing dysfunction and cardiac abnormalities such as abnormally long QT_C interval (Guideri et al., 1999; Sekul et al., 1994).

Since most RTT patients are females and males with RTT usually have a partial or complete Klinefelter (47, XXY) karyotype, or die in early life (Schwartzman et al., 2001; Schwartzman et al., 1998), before the early 1990s it was postulated that RTT is an X-linked syndrome. Many studies set out to map the mutated gene(s) in RTT. Since most RTT cases are sporadic (only about 1% of RTT cases are familial cases), it was not feasible to use conventional genome-wide linkage analysis. Instead, a focused exclusion-mapping approach was used to map RTT mutation gene(s) based on the hypothesis that RTT is an X-linked disease. Initially, the RTT mutation gene was narrowed down to the region distal to Xq27.3 (Archidiacono et al., 1991; Curtis et al., 1993; Ellison et al., 1992; Schanen and Francke, 1998; Schanen et al., 1997; Sirianni et al., 1998). Finally RTT mutations were defined in the Methyl-CpG-Binding protein 2 gene (*MECP2*) (Amir et al., 1999), which had been previously mapped to human Xq28 (Quaderi et al., 1994)(D'Esposito et al., 1996)(Vilain et al., 1996). Studies have shown that approximately 70-75% of RTT patients have mutations in the *MECP2* gene (Shahbazian and Zoghbi, 2001). About two thirds of the mutations in *MECP2* are caused by C to T transitions at eight CpG dinucleotides of paternal origin (Trappe et al., 2001; Wan et al., 1999). The mutation types include nonsense, missense,

deletion and frame-shift mutations. Most mutations are located in MBD and TRD regions of MeCP2 (figure 1.5).

Since *MECP2* is located on the X chromosome, it is subjected to X-chromosome inactivation (XCI) in females to compensate for the dosage of the extra X chromosome (Adler et al., 1995). Although several studies had focused on the phenotype-genotype correlation, due to the XCI, it is difficult to correlate genotype with phenotype, even through many mutations in MeCP2 have been identified to cause RTT. In general, patients carrying missense mutations have milder symptoms than those carrying truncation/deletion mutations; and small truncations cause milder symptoms compared to large truncations (Cheadle et al., 2000; Monros et al., 2001). However, large truncations can also be found in patients with very mild symptoms (Monros et al., 2001). This may be due to skewed X-chromosome inactivation, which happens to favor the inactivation of the X-chromosome with a mutated *MECP2* gene. The opposite effect can also happen, causing severe RTT symptoms with a missense mutation.

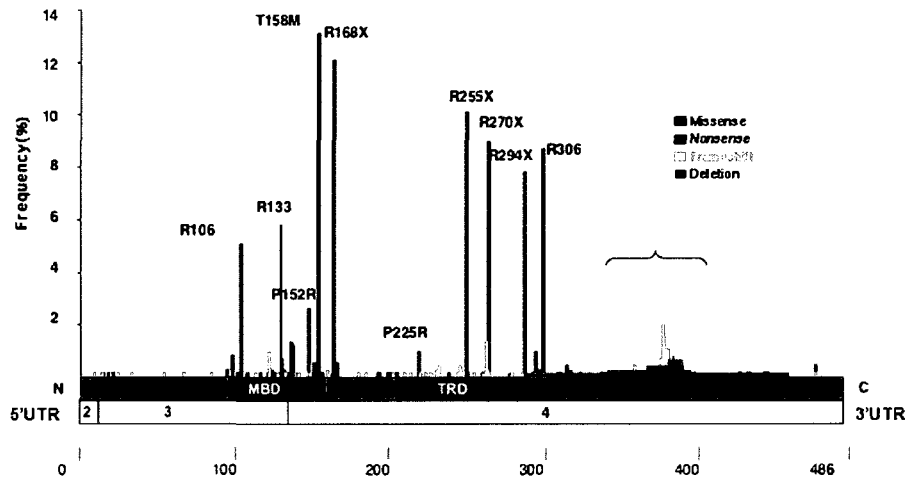


Figure 1.5: Location and frequency of mutations in MeCP2 in patients with Rett Syndrome. The spectrum of the Rett Syndrome causing mutations covers the entire protein. Most of the mutations cluster in the MBD and TRD domains of MeCP2. (Adapted from www.MeCP2.org.uk)

1.4.2 What is the function of MeCP2? Why does its mutation cause Rett Syndrome?

1.4.2a: Tissue distribution of MeCP2

Although MeCP2 is widely expressed in all tissues, it has a higher expression level in the brain (Akbarian et al., 2001; LaSalle et al., 2001). Within the brain, MeCP2 is mostly expressed in neurons (Akbarian et al., 2001; LaSalle et al., 2001). It has been shown that MeCP2 expression correlates with neuron maturation (Akbarian et al., 2001; Shahbazian et al., 2002; Smrt et al., 2007). This also explains why the brain is most affected in RTT patients. MeCP2 is also expressed in glia cells in the brain (Ballas et al., 2009). Astrocytes carrying MeCP2 mutation failed to support the normal dendritic morphology of neurons, suggesting a non-cell autonomous effect of astrocytes on normal neuron growth and maturation. Thus, the normal expression of MeCP2 is important in both neurons and glia cells.

1.4.2b: The classic paradigm of MeCP2 function

It has been known for more than a decade that DNA methylation correlates with transcription repression and changes in chromatin structure (see section 1.2). This common conception has led to the search for proteins which can interpret and mediate the effects of DNA methylation. In line with this idea, MeCP2 was identified and purified by Lewis and colleagues in 1992 as the first Methyl-CpG-binding protein (Lewis et al., 1992). They also found that the distribution of

MeCP2 along the chromosome coincides with the distribution of Methyl-CpG sites. Meehan *et al.* tested the possible role of MeCP2 *in vitro* and found that purified MeCP2 inhibited transcription from both methylated and unmethylated DNA templates (Meehan *et al.*, 1992). They hypothesized that MeCP2 normally binds to methylated DNA in the chromatin context, and contributes to long-term transcription repression. One year later, Nan *et al.* isolated a minimal methylated-CpG binding domain, namely MBD domain, by deletion analysis. They showed that the peptide from residue 78 to 162 in human MeCP2 only bound to methylated DNA, but not non-methylated DNA, thus defining the MBD as the minimum region of MeCP2 that specifically recognizes methylated DNA. The approximate dissociation constant of MBD domain to methylated DNA is $\sim 10^{-9}$ M (Nan *et al.*, 1993).

In 1997, Nan *et al.* showed that native MeCP2 purified from rat brain specifically repressed methylated gene transcription *in vitro*. Their data also showed that MeCP2 had some activation effect on non-methylated genes, but they did not further explore this phenomenon. Again, using deletion analysis, they mapped a region in MeCP2 that is responsible for the transcriptional repression function, the transcription repression domain (TRD). The TRD ranges from residue 207 to 310, and can repress transcription at a distance away from the location of genes *in vitro* and *in vivo* (Nan *et al.*, 1997).

But how does MeCP2 repress transcription? To explore the mechanism of transcriptional repression by MeCP2, Nan *et al.* employed a pull-down assay.

They fused different fragments of MeCP2 to glutathione S-transferase (GST) and found that GST-MeCP2 fusion protein can pull down a corepressor complex containing mSin3A, histone deacetylases 1 and 2 (HDAC1 and HDAC2) from HeLa cell nuclear extract. The corepressor-interacting region in MeCP2 was mapped between residue 108 and 392 (Nan et al., 1998). The interaction between MeCP2 and corepressors including mSin3A and HDACs indicates that MeCP2 silences transcription in a HDAC dependent manner. In addition, the observation that the HDAC inhibitor, trichostatin A (TSA), can relieve part of the repression effect of MeCP2 further supports this mechanism (Nan et al., 1998). Thus, a link between DNA methylation and histone deacetylation was established by MeCP2.

Based on those studies, a classic paradigm for MeCP2 function has emerged and was held to be true for many years: the function of MeCP2 is to bind to methylated DNA and recruit histone deacetylases, thus mediating transcriptional repression (Jones et al., 1998; Nan et al., 1998). However, a later study revealed that in rodent tissues, cultured cells, and *Xenopus laevis* oocytes, only a small amount of mammalian MeCP2 interacts with Sin3A and that this interaction is not stable (Klose and Bird, 2004). In addition, the HDAC inhibitor TSA can alleviate in part, but not completely, the repressive effect of MeCP2 (Jones et al., 1998; Nan et al., 1998), suggesting that MeCP2 may also have mechanisms to repress transcription in a HDAC independent manner (Yu et al., 2000). The findings that MeCP2 is also associated with other corepressors including c-ski (Kokura et al.,

2001) and N-CoR in addition to mSin3A further suggest other repression mechanisms for MeCP2.

1.4.2c: The function of MeCP2 is more complicated than previously expected

Recent studies suggest that the function of MeCP2 may be even more complicated than previously thought. For example, in searching for the targets of MeCP2, no substantial up-regulation of a discrete set of genes was found in genome wide gene expression profiling studies in MECP2/Rett syndrome mutations (Tudor et al., 2002) (Colantuoni et al., 2001) (Ballestar et al., 2005) (Jordan et al., 2007). Although some potential MeCP2 targets were identified, there was very little overlap between the misregulated genes from different studies (Tudor et al., 2002) (Colantuoni et al., 2001) (Ballestar et al., 2005) (Jordan et al., 2007), which was probably due to the use of different methods, tissues or cell lines, and the different developmental stages examined. For example, the commonly recognized MeCP2 target gene, brain-derived neurotrophic factor (BDNF), was up-regulated in MeCP2-deficient neuronal cultures (Chen et al., 2003), but was down-regulated in MeCP2-deficient brain (Chang et al., 2006).

For a large-scale mapping of neuronal MeCP2-binding sites, Yasui *et al.* used differentiated human neuronal cell line SH-SY5Y cells, which have been shown to have double MeCP2 expression level,. The results were unexpected: of all the regions examined, 59% of the MeCP2 binding sites were outside of genes; 63%

of MeCP2-bound promoters were actively expressed; and only 6% of MeCP2-bound promoters were highly methylated (Yasui et al., 2007). These results obviously contradicted the original paradigm of MeCP2 function as a methylated DNA-specific binding protein and a global transcriptional repressor. The paradigm of MeCP2 function was further challenged by another large scale examination of gene expression patterns in the hypothalamus of mice with MeCP2 deficient or overexpressed. Chahrour *et al.* revealed that in mice hypothalamus ~85% of MeCP2 regulated genes were activated by MeCP2 (Chahrour et al., 2008). Taken together, these two results argue against the MeCP2 function originally thought: first, DNA methylation may not be absolutely necessary for MeCP2 to bind to chromatin; second, MeCP2 may both function as an activator and a repressor to gene transcription.

Recently, Adams *et al.* identified High-mobility group like domain (HMGD) 1 and 2, C-terminal domain α and β (CTD α and CTD β) in human MeCP2 based on trypsin digestion experiments (Adams et al., 2007), but the functions of these domains remain unknown. Buschdorf *et al.* found that the proline-rich C-terminal region of MeCP2 can specifically bind to Group II WW domains of splicing factors formin-binding protein 11 (FBP11) and HYPC. They localized this Group II WW domain binding region from residue 325 to the C-terminus (Buschdorf and Stratling, 2004). The WW domain is a well known protein module that mediates protein-protein interaction by binding to proline-rich sequence containing ligands (Kato et al., 2004). This indicates that MeCP2 may be involved in protein-protein interactions via its WW domain-binding region.

Recent studies revealed some other functions of MeCP2. For example, by immunoprecipitation and mass spectrometry, Yong *et al.* showed that MeCP2 interacts with the RNA-binding protein Y box-binding protein 1 (YB-1) and it has a role in regulating RNA splicing (Young *et al.*, 2005). Kaludov found that MeCP2 can directly interact with transcription factor IIB (TFIIB) and interfere with the assembly of the transcriptional pre-initiation complex (PIC) (Kaludov and Wolffe, 2000), thereby regulating transcription initiation. MeCP2 has also been shown to regulate chromatin structure by compaction (Georgel *et al.*, 2003) and forming chromatin loops (Horike *et al.*, 2005).

1.4.2d: Regulation mechanism of MeCP2 function

Protein phosphorylation plays an important role in regulating the function of countless proteins. Some of the MeCP2 functions also appear to be regulated by phosphorylation. In active neurons, MeCP2 is phosphorylated at serine 421 (S421) (Zhou *et al.*, 2006), while de-phosphorylated at serine 80 (S80) (Tao *et al.*, 2009). In resting neurons, the opposite happens. Tao *et al.* also demonstrated that mutation of MeCP2 at S80 to alanine attenuates MeCP2-chromatin association at several gene promoters in resting neurons (Tao *et al.*, 2009), suggesting that phosphorylation of MeCP2 at S80 serves as one of the mechanisms to regulate the interaction between MeCP2 and chromatin.

1.4.2e: Structure of MeCP2

To date, the only structural information available for MeCP2 are the NMR (Wakefield et al., 1999) and X-ray structures (Ho et al., 2008) of the MBD domain in complex with a methylated DNA oligomer (figure 1.4). In the structure solved by NMR, a conserved hydrophobic pocket was proposed as the candidate for the interaction with the methyl group on cytosine. However, the X-ray crystal structure revealed that the MBD of MeCP2 interacts primarily with hydration water molecules around the CpG methylation mark in the major groove of DNA. As shown in figure 1.4, only a small portion of the MBD of MeCP2 adopted well ordered secondary structure; large parts of it are relatively flexible loops. Together with the published CD data, which showed that MeCP2 is an intrinsically disordered protein, this potentially explains why there is no structure of the entire protein to date.

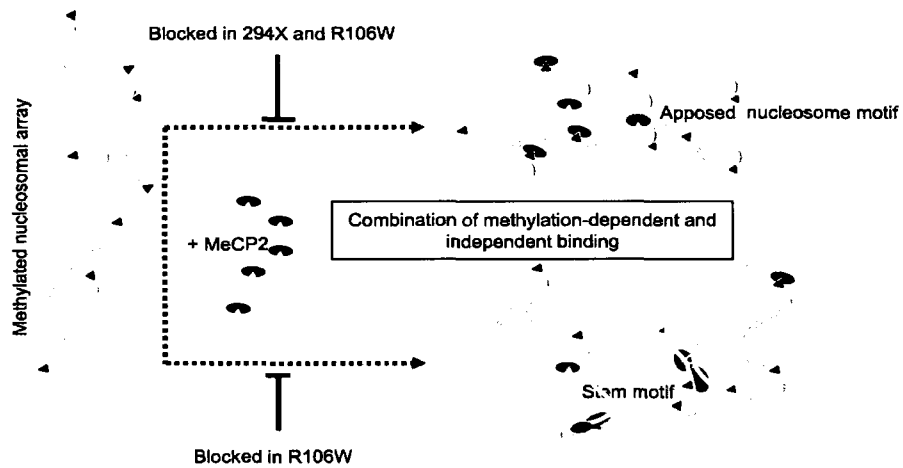
1.5 MeCP2 and chromatin structure

The early correlation between MeCP2 and chromatin structure was from the observation that, in mouse cells, MeCP2 is most concentrated in pericentromeric heterochromatin, suggesting a role for MeCP2 in forming inert chromatin (Nan et al., 1996).

In 1999, Chandler *et al.* primarily applied DNase I footprinting assays and showed that MeCP2 can stably associate with mono-nucleosomes *in vitro* by showing that MeCP2 protected nucleosomal DNA from DNase I digestion

(Chandler et al., 1999). This interaction involves its C-terminal region in addition to the MBD domain. The interaction between MeCP2 and mono-nucleosomes was further confirmed by Nikitina *et al.* by electrophoretic mobility shift assay (EMSA) analysis (Nikitina et al., 2007a). They also showed that MeCP2 protected ~11 bp linker DNA from Micrococcal nuclease (Mnase) digestion, indicating that the MeCP2 binding site on nucleosomes is close to the linker DNA “entry-exit” region, similar to how histone H1 interacts with nucleosomes (Hamiche et al., 1996b; Nikitina et al., 2007a; Toth et al., 2001). Together with the finding that MBD also binds to unmethylated four-way DNA junctions with a similar affinity to methylated DNA (Galvao and Thomas, 2005), it is reasonable to propose that MeCP2 could have recognized certain structural features on the nucleosome rather than the methylation mark to interact with nucleosome. This could also explain why MeCP2 can abundantly associate with chromatin, and probably be involved in compacting chromatin.

Indeed, early in 2003, Georgel *et al.* showed that MeCP2 is capable of compacting biochemically defined nucleosomal arrays containing 12 nucleosomes, the “mini chromatin”, into a higher order structure (Georgel et al., 2003). This compaction can happen independently of DNA methylation and in the absence of monovalent or divalent cations, which is different from other chromatin-condensation proteins such as H1. Horike *et al.* showed that MeCP2 was involved in the formation of a silent chromatin loop between genes (Horike et al., 2005), another possible mechanism by which MeCP2 could regulate chromatin structure and gene transcription. Recently Nikitina *et al.* proposed two different



(Adapted from Nikitina, 2007, MCB)

Figure 1.6: Two possible mechanisms of how MeCP2 compacts chromatin. In the first mechanism, MeCP2 compacts chromatin by bringing nucleosomes together forming a cluster of nucleosomes; In the second mechanism, MeCP2 compacts chromatin by forming a linker DNA “stem” at the nucleosome “entry-exit” site (Nikitina et al., 2007b).

models of how MeCP2 may compact chromatin (figure 1.6): one, by bringing nucleosomes together forming a cluster of nucleosomes; second, by forming a linker DNA “stem” at the nucleosome entry-exit site (Nikitina et al., 2007b). The two models are not exclusive and thus may exist at the same time. However, the detailed mechanism of how MeCP2 interacts with nucleosome (are the histones within nucleosomes involved in this interaction?) and how MeCP2 compacts chromatin still remain unclear.

1.6 Specific aims and layout of the dissertation

The work in this dissertation focuses on studying the interaction between the nucleosome and MeCP2. Various biochemical and biophysical methods, including gel filtration, light scattering, analytical ultracentrifugation, fluorescence resonance energy transfer, and small angle X-ray scattering have been used to study this interaction. We also wish to look at the interaction at the atomic level by crystallizing the nucleosome-MeCP2 complex. Finally this study will shed light on the mechanism of how MeCP2 functions to promote the compaction of chromatin, and how mutations in MeCP2 cause Rett Syndrome.

Chapter 2 employs different biochemical and biophysical techniques to analyze the nucleosome-MeCP2 complex. The results in this chapter suggest that a single MeCP2 molecule binds to a single nucleosome at the DNA “entry-exit” region and brings linker DNA ends closer to form a “stem” structure, which leads to the compaction of chromatin.

In chapter 3, pull-down assays and various in-solution assays like gel filtration and isothermal titration calorimetry were used to investigate if histones within nucleosomes also participate in the interaction with MeCP2.

Chapter 4 is directed to study the nucleosome-MeCP2 complex at atomic resolution by X-ray crystallography. In chapter 4 we show that it is feasible to crystallize the nucleosome-MeCP2 complex. The crystals of the 165NCP-MeCP2B complexes diffracted to 5.2 Å. However, there is a need to improve the crystallization conditions and optimize the cryo-protection procedures to get better diffracting crystals and prevent the dissociation of MeCP2 from crystals.

CHAPTER 2

This chapter will be published as a paper with the following authorships:

Chenghua Yang, Mark van der Woerd, and Karolin Luger

(Chenghua Yang conducted all the experiments; Mark van der Woerd provided technical support.)

EXTRA NUCLEOSOMAL DNA IN NUCLEOSOMES GUIDES THE ORGANIZATION OF THE NUCLEOSOME-MECP2 COMPLEX

2.1 Abstract:

Methyl-CpG Binding Protein (MeCP2) is an abundant chromatin associated protein that is important in maintaining human health; mutations in this protein cause Rett Syndrome, a neurodevelopmental disease that is a common cause of mental retardation and autism in females. MeCP2 was initially identified as a protein that recognizes the genetic DNA methyl-CpG mark and it was thought to repress gene transcription by recruiting histone deacetylases. Recent studies show that MeCP2 can both repress and activate gene transcription. It also binds chromatin in the absence of the methyl mark, suggesting that its mode of action is more complex than previously assumed.

The observation that MeCP2 compacts nucleosomal arrays *in vitro* and mediates silent chromatin loop formation *in vivo* suggests a novel mechanism by which MeCP2 regulates gene expression. To further characterize the interplay between MeCP2 and chromatin, it is important to understand the interactions between MeCP2 and nucleosomes, the fundamental component of chromatin. We used biochemical and biophysical approaches to study the interplay between MeCP2 and nucleosomes. Gel mobility assays showed that although MeCP2 can interact with a nucleosome with or without extra nucleosomal DNA, it has a higher affinity for nucleosomes with extra nucleosomal DNA. The N-terminal portion of human MeCP2 (amino acids 78-305) is sufficient to establish this

interaction. Light scattering and fluorescence resonance energy transfer (FRET) assays demonstrated that this interaction occurs at a 1:1 molar ratio and that MeCP2 brings the extra nucleosomal DNA ends closer together. Small angle X-ray scattering (SAXS) revealed the formation of a more compact complex when MeCP2 interacts with nucleosome with (*versus* without) extra nucleosomal DNA, indicating that the extra nucleosomal DNA is important in organizing the MeCP2-nucleosome complex. Our data suggest a model in which MeCP2 compacts chromatin by changing the extra nucleosomal DNA path.

2.2 Introduction

In mammalian genomes, DNA methylation of CpG di-nucleotides is a key epigenetic modification that is important for the regulation of gene activity and chromatin structure (Bird and Wolffe, 1999; Chen et al., 1998). In many cases these DNA methylation sites are recognized by a family of protein factors that have a highly conserved methyl-CpG binding domain (MBD). Methyl-CpG binding protein 2 (MeCP2) is the family member with a strong relevance to human health. Many mutations in MeCP2 are related to a neurodevelopmental disease, the Rett syndrome (Amir et al., 1999; Hagberg et al., 1983; Rett, 1966), which is a main cause of mental retardation and autistic behavior in girls and young women. The incidence of Rett syndrome is about 1 in every 10,000 to 15,000 female births (Hagberg, 1985).

Human MeCP2 isoform e2 is composed of 486 amino acids and exhibits a high degree of intrinsic disorder (Adams et al., 2007). Two functional domains in

MeCP2 have been well characterized: a MBD positioned from amino acid residues 76 to 163 (Chandler et al., 1999) and a transcription repression domain (TRD; amino acids 203 to 310) (Kaludov and Wolffe, 2000). Additional domains were proposed based on trypsin digestion experiments and sequence homology (Adams et al., 2007), for example high-mobility group like domains (HMGD) 1 and 2, and a C-terminal domain α and β (CTD α and CTD β). Their functions remain unknown. A group II WW-binding domain localized from residue 325 to the C terminus was mapped in MeCP2 by GST pull-down assay (Buschdorf and Stratling, 2004). The WW-domain is a well known protein module that mediates protein-protein interaction by binding to proline-rich sequence containing ligands (Kato et al., 2004). This indicates that MeCP2 may be involved in protein-protein interactions by its WW-binding domain.

MeCP2 binds DNA in a non-specific manner. In addition to binding to DNA regions containing methyl-CpG sites, MeCP2 promotes the compaction of chromatin fibers in the absence of methylation (Georgel et al., 2003). Recombinant human MeCP2 is capable of binding to both naked DNA and to biochemically defined nucleosomal arrays in the absence of methylated DNA (Georgel et al., 2003).

The classic paradigm for MeCP2 function is to bind to methylated DNA and recruit histone deacetylases, thus mediating transcriptional repression (Jones et al., 1998)(Nan et al., 1998). However, no substantial up-regulation of a discrete set of genes was found in genome-wide gene expression profiling studies in MECP2/Rett syndrome mutations (Colantuoni et al., 2001; Tudor et al., 2002)

(Ballestar et al., 2005; Jordan et al., 2007). Although some potential MeCP2 targets were identified, there was very little overlap between the mis-regulated genes from different studies (Tudor et al., 2002)(Colantuoni et al., 2001)(Ballestar et al., 2005)(Jordan et al., 2007). This lack of overlap may be explained by the use of different tissues or cell lines, by examination at different time points, or by the different analysis methods used. Two recent genome-wide promoter analyses of MeCP2 binding revealed that only a small portion of MeCP2 binding sites are highly methylated and MeCP2 can function as both an activator and a repressor of transcription (Yasui et al., 2007)(Chahrour et al., 2008). However, how MeCP2 activates or represses gene transcription remains unclear.

To date, the only structural information for any part of MeCP2 are NMR (Wakefield et al., 1999) and X-ray structures (Ho et al., 2008) of the MBD domain in complex with a methylated oligonucleotide. Both approaches reveal that only a small portion of the MBD of MeCP2 has a folded structure; the rest of the protein appears to be mostly disordered. CD data of the entire MeCP2 molecule indicate that MeCP2 is a largely disordered protein (Adams et al., 2007), consistent with predictions (<http://bip.weizmann.ac.il/fldbin/findex>) (Prilusky et al., 2005). This explains the absence of structural data on MeCP2 other than on the MBD. Intrinsically disordered proteins usually adopt a structure upon interaction with their functional partners. MeCP2 interacts with a variety of macromolecules and macromolecular complexes, including unmethylated and methylated DNA (Adams et al., 2007; Kaludov and Wolffe, 2000; Nan et al., 1993), nucleosomes

and chromatin (Chandler et al., 1999; Georgel et al., 2003; Nikitina et al., 2007a; Nikitina et al., 2007b), transcriptional co-repressors (Nan et al., 1998) (Jones et al., 1998), a histone H3 methyltransferase (Fuks et al., 2003); Dnmt1 DNA methyltransferase (Kimura and Shiota, 2003), and RNA splicing factors (Buschdorf and Stratling, 2004).

The biological function of MeCP2 in health and disease is unknown. A key role of MeCP2 may be to dramatically modulate chromatin structure by acting as a chromatin architectural protein (Georgel et al., 2003) (Nikitina et al., 2007b). However, the mechanism by which MeCP2 modulates chromatin structure is not clear. Since the nucleosome is the fundamental building block of chromatin, an investigation into the interactions between MeCP2 and the nucleosome is a key to understand the molecular details of its role as a chromatin architectural protein.

Early studies have shown that MeCP2 forms discrete complexes with nucleosomal DNA via the methyl-CpG-binding domain (MBD) in a methyl-CpG dependent manner, and the carboxyl-terminal segment of MeCP2 is important in binding both to naked DNA and to the nucleosome core particle (Chandler et al., 1999). However, *Xenopus Laevis* MeCP2 was used in this study, and the interaction between MeCP2 and nucleosomes were investigated by the DNase I footprinting assays. More recently, Nikitina *et al.* primarily applied gel shift assays and found that MeCP2 interacts with the nucleosome independent of methylation, but the presence of the extra nucleosomal DNA in the nucleosome is essential for this interaction (Nikitina et al., 2007a). The nucleosome-MeCP2-

nucleosome “sandwich” structure was observed by EM. They also showed that MeCP2 protected ~11 bp from Mnase digestion, indicating that the MeCP2 binding site on nucleosomes is close to the linker DNA “entry-exit” region. However, the details of how MeCP2 interacts with nucleosomes (e.g. the stoichiometry of the interaction, whether the interaction involves the eviction of histones within nucleosomes) still remains unclear.

Here, we have used biochemical and biophysical approaches to further investigate the interaction between MeCP2 and nucleosomes. Since there are many different structural sites within the nucleosome, for example the major and minor grooves in the double-helical DNA, and the DNA entry-exit sites of a nucleosome, we chose to use non-methylated DNA to obtain unbiased structural information of MeCP2-nucleosome interaction. We have used gel mobility assays and competition assays to show that MeCP2 prefers nucleosomes with extra nucleosomal DNA over those without extra nucleosomal DNA. The N-terminal portion of MeCP2 (amino acids 78-305) is sufficient for this interaction. Light scattering and fluorescence resonance energy transfer (FRET) assays indicate that nucleosomes form a 1:1 complex with MeCP2, and MeCP2 is capable of bringing the extra nucleosomal DNA ends closer together. Small angle X-ray scattering (SAXS) revealed the formation of a more compact complex when MeCP2 interacts with nucleosome with extra nucleosomal DNA (versus without). Our data suggest a model in which MeCP2 compacts chromatin by altering the path of the extra nucleosomal DNA, probably not by bridging nucleosomes, and suggests conformational changes of the intrinsically disordered MeCP2 upon

interaction with the nucleosome. This can have profound effects on the type and stability of chromatin higher order structure.

2.3 Experimental procedures

2.3.1. Expression and purification of MeCP2.

Recombinant full length human MeCP2 (isoform e2) was expressed and purified as described (Adams et al., 2007) in the IMPACT system (New England Biolabs). The purified full length MeCP2 and fragments 1-305 and 78-305 were dialyzed into storage buffer (10 mM Tris, pH 7.5, 10% glycerol, 10 mM NaCl, 0.25 mM EDTA, 1 mM β -mercaptoethanol), and stored at 4 °C.

2.3.2. DNA for nucleosome reconstitution.

The DNA fragments used to reconstitute nucleosomes were either 147-bp palindromic DNA fragments derived from human α -satellite DNA (Luger et al., 1997) or 146-bp and 165-bp DNA fragments derived from the strong positioning '601' DNA sequence (Lowary and Widom, 1998). The preparation of DNA for nucleosomes used in electrophoretic mobility shift assays (EMSA), analytical ultracentrifugation (AUC), light scattering and small angle X-ray scattering assay (SAXS) has been described before (Dyer et al., 2004).

Fluorescently labeled DNA fragments of different lengths (146-bp or 165-bp) used in FRET or competition assays were prepared by PCR amplification. The template

(ATCGGACCCTATCGCGAGCCAGGCCTGAGAATCCGGTGCCGAGGCCGCTCAATTGGTCG

TAGACAGCTCTAGCACCGCTTAAACGCACGTACGCGCTGTCCCCCGGTTTTAACCGCCA
AGGGGATTACTCCCTAGTCTCCAGGCACGTGTCAGATATATACATCCAGGCCTTGTGTCC
CGAAATTCATATTAATTAATACTAGAT) is a 206-mer DNA sequence derived from
the 601 nucleosome positioning sequence and inserted into the pUC19 plasmid.
The primers were designed to amplify 146 base pair or 165 base pair DNA
fragments in the centered nucleosome positioning sequence: 146bp-Forward: 5'-
Alexa-488-CCT GAG AAT CCG GTG CCG AGG CCG CTC -3', 146bp-Reverse:
5'- Alexa-546-CCT GGA TGT ATA TAT CTG ACA CGT GCC TG -3'; 165bp-
Forward: 5'- Alexa-488-CGA GCC AGG CCT GAG AAT CCG GTG -3', 165bp-
Reverse: 5' – Alexa-546-CGA CAC AAG GCC TGG ATG TAT ATA TCT G
-3'. Alexa-488 or -546 labeled primers were purchased from IDT. Single or
double end labeled 146-bp or 165-bp DNA were prepared by PCR using iproof
polymerase (BioRad). Large scale PCR was done in 96 well plates with
denaturing at 98°C for 10 seconds, annealing at 62°C for 15 seconds and
extension at 72°C for 15 seconds. PCR products were ethanol precipitated and
purified over a MonoQ column.

2.3.3. Nucleosome reconstitution.

Nucleosomes were reconstituted with 146, 147 or 165 base pair DNA and
recombinant *Xenopus laevis* histones by salt gradient method as described
before (Dyer et al., 2004). For convenience, we denote the nucleosomes used in
this study 146NCP, 147NCP or 165NCP, for nucleosomes reconstituted with
146, 147 or 165 base pair DNA respectively. 147NCPs are reconstituted with 147

bp α -satellite DNA, 146NCPs and 165NCPs are reconstituted with 146 or 165 bp 601 DNA.

2.3.4. Electrophoretic mobility shift assays (EMSA).

147NCP or 165NCP (15 μ M) were incubated with increasing amounts of MeCP2 in binding buffer (10 mM Tris, pH 7.5, 1 mM EDTA, 1 mM DTT, and 0, 100 or 300 mM NaCl) in 10 μ l reaction volumes at room temperature for 30 minutes. The products were electrophoresed on pre-run 5% polyacrylamide gel (mono/bis ratio of 35:1) in 0.2X TB (45 mM Tris, 45 mM borate pH 8.3) at 150 V for 75 minutes at 4°C.

2.3.5. Nucleosome competition assay.

146NCP was pre-incubated with MeCP2-WT at a 1 to 1.5 molar ratio in binding buffer (10 mM Tris pH 7.5, 100 mM NaCl, 2% Glycerol, 0.2 mM TCEP) at room temperature for 30 minutes. Then increasing amounts (0.25 to 1 molar ratio) of Alexa Fluor 488 labeled 165NCP was added to the pre-incubated 146NCP-MeCP2WT complex and incubated at room temperature for another 30 minutes before resolving on a 5% native PAGE gel. The reverse competition assay was done under identical conditions. The products were electrophoresed on pre-run 5% polyacrylamide gel (mono/bis ratio of 35:1) in 0.2X TB (45 mM Tris, 45 mM borate pH 8.3) at 150 V for 75 minutes in 4°C. The gel was visualized both by fluorescence view and Ethidium Bromide staining.

2.3.6. Analytical Ultracentrifugation.

For sedimentation velocity experiments, approximately 600 nM 147NCP or 165NCP alone or in complex with MeCP2 at 1:1.5 or 1:3 ratio was used. Sedimentation velocity experiments were done in a Beckman XL-I or XL-A analytical ultracentrifuge with absorbance detection at 260 nm. Scans were collected at a radial step resolution of 0.003 cm. Boundaries were analyzed using the Ultrascan software (version 7.3). This analysis gives an integral distribution of sedimentation coefficients, $g(s)$. Sedimentation coefficients were corrected to that in water at 20°C. The solvent densities were calculated in Ultrascan. The partial specific volumes of the samples were calculated from the primary DNA and amino acid sequence within Ultrascan.

2.3.7. Multi-angle Light scattering (SEC-MALS) assay.

Size exclusion chromatography (SEC) combined with MALS (Wyatt technologies) was performed at the Advanced Light Source (ALS) in Berkeley, California. A Superose-6 PC 3.2/30 column (2.4ml total volume) (GE Healthcare) with a flow rate of 40 μ l/min was used to separate the sample before performing the MALS measurement. MALS measures the amount of light scattered by the molecules. The concentration of molecules is also determined by MALS by measuring the refractive index or UV absorbance. Since the light scattered by a molecule is proportional to the molecular mass times the concentration, the molar mass of the molecules is therefore determined with ASTRA software provided with the instrument. The SEC-MALS assays were performed by using 25 μ l

147NCP or 165NCP respectively alone, or each of these in complex with MeCP2-WT. Samples were at least 90% homogeneous as determined by EMSA and were injected at a concentration of 11.5 μ M. The molar mass for each molecule was determined by ASTRA.

2.3.8. Fluorescence resonance energy transfer (FRET) assay.

Alexa-488 and Alexa-546 fluorophore pairs with a Förster distance (R_0) of 64 Å (the diameter of a nucleosome is ~110 Å) were chosen to label the two ends of the DNA in 165NCP. Fluorescence was measured using a Horiba Jobin Yvon Fluorolog-3 spectrofluorometer. All measurements were done at room temperature. Clear four-sided cuvettes with path length of 1 cm were used (Fisher, catalog # 14-955-130). A protein additive of 0.1 mg/ml BSA was used in each measurement to avoid adhesion of the dye or sample to the cuvettes. Labeled nucleosomes were added first to both the sample and reference cuvettes. Non-labeled MeCP2-WT was titrated to the sample cuvette and MeCP2 buffer to the reference cuvette thereafter. After each addition of MeCP2, 10 minutes of incubation were allowed before taking the measurement. An excitation wavelength of 488 nm was used for all the FRET experiments. A series of emission scans from 400 to 700 nm was taken after each addition of MeCP2. The fluorescence emission spectra were measured relative to the lamp intensity and corrected for the instrument response and buffer signal. To correct for the concentration differences and change of the signal with the addition of MeCP2, spectra were normalized at the emission maximum of the donor (518 nm). Numerical treatment of the collected data was done with Microsoft Office Excel.

2.3.9. Small angle X-ray scattering (SAXS) data collection and analysis.

SAXS data for all nucleosome samples and nucleosome-MeCP2 complexes were measured at the SIBYLS beamline (12.3.1) at ALS with an X-ray energy of 10 keV ($\lambda=1.2398 \text{ \AA}$). A Mar CCD detector was used to record the scattering data. A 15 μl sample was placed in a 1mm thick chamber with two windows of 25 μm mica. The distance between the sample and the detector was 1.5 m.

MeCP2-WT, 146NCP, 165NCP each at 7.5 mg/ml, MeCP2-WT in complex with 146NCP or 165NCP at 9.4 mg/ml (the concentration of NCP remains the same in the complex when compared with the NCP sample alone) were prepared as stock solutions. Additional samples for the data collection were acquired by diluting the stock solutions to 2/3 and 1/3 with reference buffer. The intensity curves were measured at all three different concentrations, and corrected for buffer scattering. Repeat exposures were taken to check for radiation damage, while two different exposures, typically of 6 and 60 seconds in duration, were taken to optimize the signal-to-noise ratio and avoid detector saturation. Initial data processing was performed with the program PRIMUS (Konarev et al., 2003). The radius of gyration R_g was estimated by Guinier analysis in PRIMUS, or from analysis with GNOM; the maximum particle dimension was estimated by indirect Fourier transform with the program GNOM (Svergun et al., 2001).

2.4 Results

2.4.1. MeCP2 binds to nucleosomes (146 NCP and 165NCP).

It was shown before that MeCP2 interacts with nucleosomes. However, it was not clear if the interaction between MeCP2 and nucleosomes involves the displacement of histones within the nucleosomes, whether the extra nucleosomal DNA in nucleosome and C-termini of MeCP2 are indispensable for the interaction. To further investigate how MeCP2 interacts with nucleosomes, we reinvestigated the interaction with electrophoretic mobility shift assays (EMSA) and checked the components in the complex on SDS gel.

Nucleosomes reconstituted with 147 bp α -sat DNA (147NCP) or alternatively with strong nucleosome positioning 165 bp "601" DNA (165NCP) (Lowary and Widom, 1998) were incubated with increasing amounts of wild-type (wt) MeCP2 (molar ratio of MeCP2 to 147NCP ranged from 0 to 2). The product(s) of 147NCP with MeCP2 were resolved on a 5% native polyacrylamide gel (Figure 2.1A). The incubation of 147NCP with increasing amounts of MeCP2-WT clearly resulted in a progressive reduction of free 147NCP and the appearance of discretely shifted and super-shifted bands. The same behavior was observed with MeCP2 fragment 1-305 or 78-305 (Figure 2.1B) and MBD or TRD (appendix I). To identify the components of the shifted bands in the EMSA assay, the upper bands and lower bands were cut and electro-eluted out before loading onto an 18% SDS gel as indicated in Figure 2.1C and 2.1D. All four histones as well as MeCP2 were present both in the upper and lower bands. These results clearly

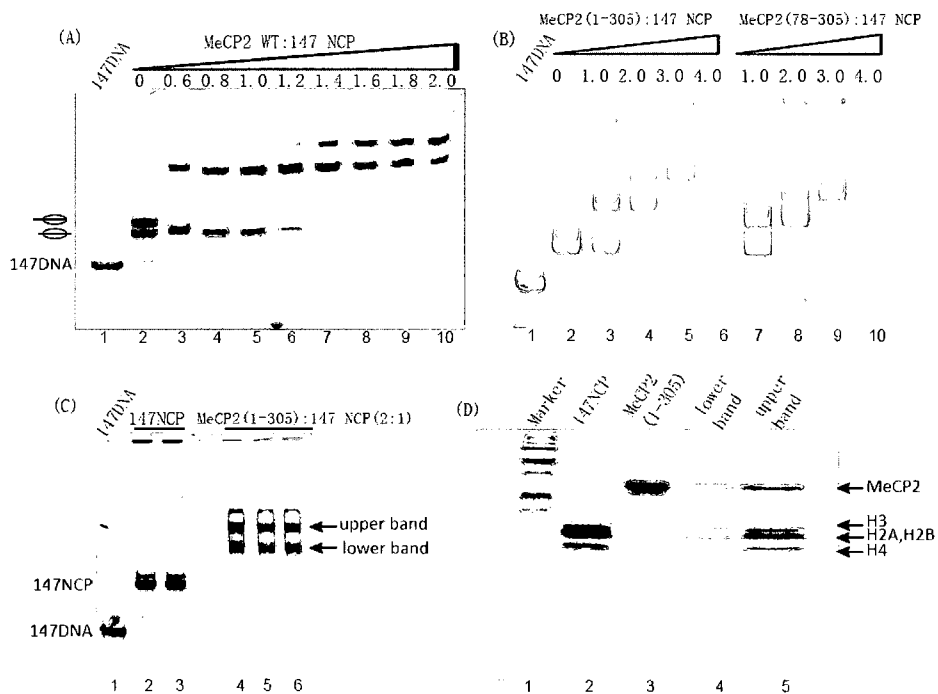


Figure 2.1: MeCP2 forms defined complexes with nucleosomes *in vitro*. (A) Increasing amounts (at molar ratios from 0 to 2.0) of WT MeCP2 were added to 147NCP resulting in a dramatic retardation of the mobility of 147NCP. (B) The same mobility retardation was observed when MeCP2 N-terminal fragments (amino acid 1-305 or 78-305) were added to 147NCP, indicating that the N-terminal portion of MeCP2 is sufficient for this interaction. (C and D) To check the content in the shifted bands, upper and lower bands (panel C) were cut and eluted out before loading onto 18%SDS gel. Panel D showed that both bands contain MeCP2 as well as all four core histones.

demonstrate that MeCP2 is capable of making complexes with 147NCP under the conditions tested, and that no histones were displaced upon the interaction with MeCP2. This EMSA experiment was repeated under conditions with higher salt, 150 mM or 300 mM NaCl, the same results were observed. Similar EMSA and component check experiments were done for 165NCP and MeCP2, and the same results were obtained. Thus extra nucleosomal DNA in nucleosomes is not needed for the interaction.

2.4.2. Sedimentation properties of the NCP-MeCP2 complex.

To test the hypothesis that the upper band shown in Fig. 2.1 represents two nucleosomes that are cross-bridged by MeCP2, we employed analytical ultracentrifugation (AU). This method is used to characterize the size and shape of molecules in solution. The sedimentation properties of mono-nucleosomes, di-nucleosomes, tri-nucleosomes, have been published (Butler and Thomas, 1998). Mono-nucleosomes and di-nucleosomes have sedimentation coefficients (s-value) of ~11s and ~13-15s, respectively (Butler and Thomas, 1998). Full length MeCP2 has also previously been shown by AUC to be a monomer with an s-value of 2s (Adams et al., 2007). Since the difference in the sedimentation coefficient between mono- and di-nucleosomes is significant we should be able to observe a significant change in the s-value if MeCP2 bridges two nucleosomes together and forms a nucleosome-MeCP2-nucleosome “sandwich” structure as suggested by Nikitina *et al* (Nikitina et al., 2007b). To investigate if this “sandwich” complex exists under our condition, AUC was used to characterize the NCP-MeCP2 complex. A solution of 147NCP was mixed with MeCP2-WT to

form a 1:1.5 or 1:3 molar ratio complex at room temperature. Initial sedimentation velocity experiments were performed at low salt concentration (10 mM Tris, pH 7.5, 1 mM EDTA, 1 mM DTT). The $g(s)$ plots of the diffusion-corrected sedimentation coefficient distributions are shown in figure 2.2A. Under our conditions, 147NCP sediments at $\sim 11.2s$, which is in agreement with published data (Butler and Thomas, 1998). However, when the 147NCP complexes with MeCP2-WT at two different ratios (1:1.5 and 1:3.0), the two complexes sediment at $\sim 10.4s$ and $\sim 10.7s$, respectively, slower than 147NCP alone (figure 2.2A). Native PAGE of the samples after the sedimentation velocity runs verified that under the two conditions, the complexes migrate exclusively in the lower and upper band, respectively, with little contamination with free NCP (Figure 2.2C). Similar sedimentation velocity experiments were done for 165NCP and the 165NCP-MeCP2-WT complex, either in low salt or in 100 mM salt. 165NCP sediments at $11.2s$, similar to 147NCP; while the 165NCP-MeCP2 complex sediments at $\sim 11s$ at low salt or 100 mM salt concentration (figure 2.2B). These results clearly show that both the 147NCP-MeCP2 complex and the 165NCP-MeCP2 complex sediment slower when compared to NCP alone, having a higher frictional coefficient (since the molecular weight increases in the complex, the frictional coefficient has to increase more to offset the increase in molecular weight and results in a smaller s -value). However, the complexes sediment significantly slower than the di-nucleosomes (with an S -value of 13-15s), making the possibility that MeCP2-WT forms a “sandwich” structure involving two mono-nucleosomes unlikely.

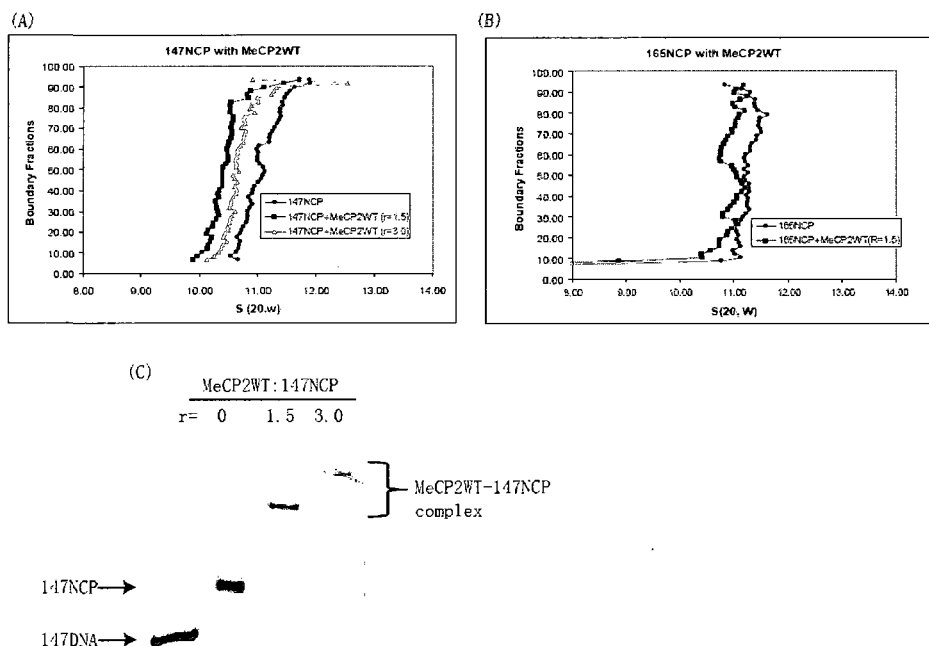


Figure 2.2: MeCP2 does not bridge nucleosomes. (A) Sedimentation velocity analysis of 147NCP and 147NCP-MeCP2 complexes. 147NCP sediments at ~11s. When MeCP2 is mixed with 147NCP at two different ratios (1:1.5 and 1:3.0), they sediment at ~10.4s and ~10.7s, respectively, slower than 147NCP alone. (B) Sedimentation velocity analysis of 165NCP-MeCP2 complex at two different salt conditions. 165NCP sediment at ~11.3s. 165NCP-MeCP2 complex sediment at ~10.8s at 5 mM NaCl, and ~11s at 100 mM salt concentration. (C) The 147NCP-MeCP2 complexes were checked in a 5% native gel after the sedimentation experiment. The complexes are still intact after the sedimentation.

2.4.3. Stoichiometry of the NCP-MeCP2 complex.

The stoichiometry of the various NCP-MeCP2 complexes in the first shifted band was further investigated using size exclusion chromatography combined with multi-angle light scattering. MeCP2-WT was titrated into 147NCP or into 165NCP to make a NCP-MeCP2 complex that migrated to ~90% in the first shifted band (refer to figure 2.6A). MeCP2WT, 147NCP, 147NCP-MeCP2-WT, 165NCP or 165NCP-MeCP2-WT was injected individually into a Superose 6 size exclusion column connected to a light scattering detector. The chromatogram shows a single peak for each sample (Figure 2.3, right y-axis). The analysis of molar mass in the center part of the peak reveals a mono-disperse species for MeCP2WT, 147NCP (figure 2.3, left y-axis), 147NCP-MeCP2WT and 165NCP, and a slightly poly-disperse species for 165NCP-MeCP2WT complex. For MeCP2WT, 147NCP and 165NCP, the molar mass in the center part of the peak measured by light scattering (56.00 kDa, 198.0 kDa and 202.8 kDa, respectively) is very close to the molecular weight calculated based on the DNA and protein sequence (52.44 kDa, 205.0 kD and 208.95 kD, respectively; Table 2.1). These results validate the method used to measure the molar mass of the molecules.

For the 147NCP-MeCP2-WT and 165NCP-MeCP2-WT complex, the measured molar mass (251.4 kD and 253.9 kD, respectively) was close to the calculated molecular weight (257.9 kD and 261.4 kD) assuming a 1:1 ratio

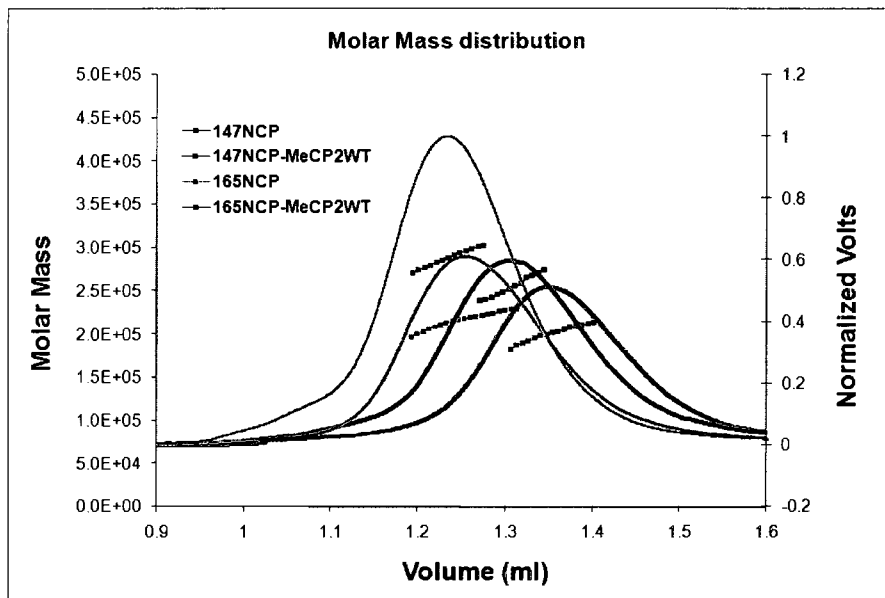


Figure 2.3: Size exclusion chromatography combined light scattering profile of NCPs and their complexes with MeCP2WT. The light scattering profiles are shown in continuous curves. Right y-axis is the normalized scattered light signal. All four samples showed single peaks in the light scattering profiles. The molar mass are calculated for each peak and shown as dotted lines with the same color as the light scattering profile peak. The flat dotted lines indicated the mono-disperse of the sample over the peak.

Table 2.1: Summary of SEC-MALS

| | Molecular Weight (kD) | | rH (Å) |
|-----------------------|-----------------------|--------------------|---------------|
| | Observed | Calculated | |
| BSA | 66.47(± 2%) | 67.0 | ----- |
| MeCP2WT | 56.00(± 4%) | 52.44 | ----- |
| 147NCP | 198.0 (± 2%) | 205.0 | 57(±2) |
| 147NCP-MeCP2WT | 251.4 (± 2%) | 257.9 (1:1) | 66(±2) |
| 166NCP | 202.8 (± 1%) | 208.95 | 61(±1) |
| 166NCP-MeCP2WT | 253.9 (± 0.6%) | 261.4 (1:1) | 73(±2) |

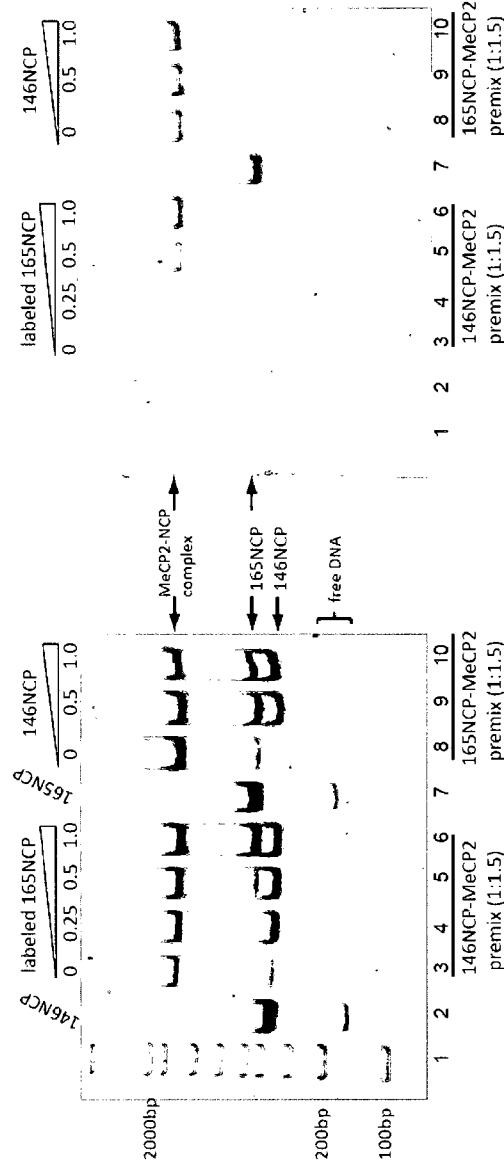
complex formation. This suggests a one-to-one stoichiometry in both NCP-MeCP2 complexes in the first shifted band.

2.4.4. MeCP2 prefers nucleosome with extra nucleosomal DNA.

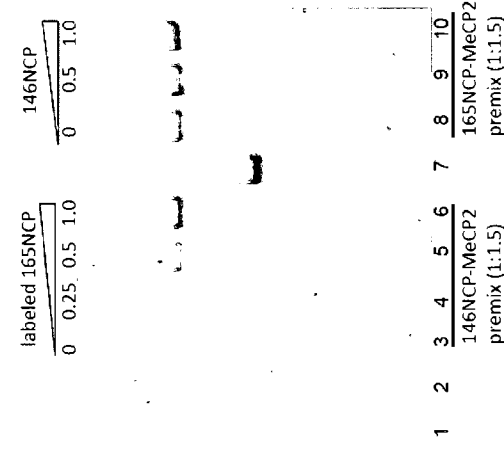
After establishing that MeCP2 can interact with nucleosomes with or without extra nucleosomal DNA, it is important to know if MeCP2 has a preference for nucleosomes with or without extra nucleosomal DNA. A competition assay was used to answer this question.

Nucleosomes made with a 146 base pair “601” DNA fragment (146NCP) were pre-incubated with MeCP2-WT at a molar ratio varying from 1 to 1.5. Increasing amounts of fluorescently labeled nucleosomes reconstituted with a 165 bp “601” DNA fragment (165 NCP) were added to the pre-incubated 146NCP-MeCP2-WT (0.25 to 1.0 molar ratio of 165 NCP to 146 NCP) and incubated at room temperature for another 30 minutes before resolving the complexes on a 5% native PAGE gel (Figure 2.4). With the addition of increasing amounts of fluorescently labeled 165 NCP to the pre-formed 146NCP-MeCP2WT complex, there was an increase in the amount of 165 NCP-MeCP2-WT complex and at the same time an increase in the appearance of free 146 NCP (Figure 2.4A and 2.4B, lane 3-6). However, when increasing amounts of 146 NCP were added as a competitor to the pre-formed 165 NCP-MeCP2-WT complex, the amount of 165 NCP-MeCP2WT complexes almost remained unchanged (Figure 2.4A and 2.4B, lane 8-10). The quantification of fluorescence intensity in the 165NCP-MeCP2-WT complex bands (figure 2.2B, lane 4-6 and 8-10) is shown in figure 2.4C.

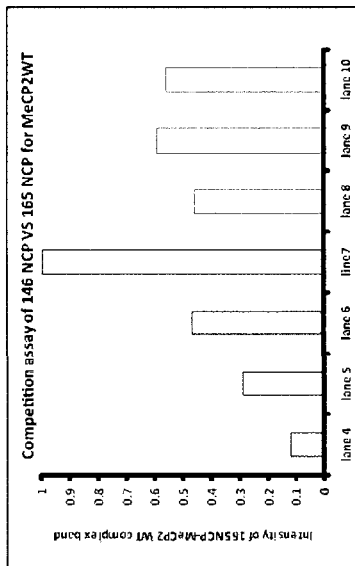
(A) (Stained with Ethidium Bromide)



(B) (Fluorescence view)



(C)



(D) (Stained with Ethidium Bromide)

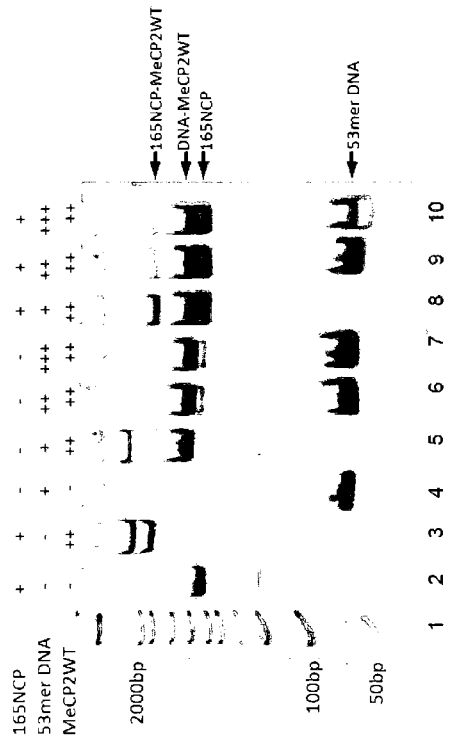


Figure 2.4: MeCP2 has higher affinity for 165NCP than 146NCP. (A) When MeCP2 is pre-incubated with 146NCP, and an increasing amount of fluorescently labeled 165NCP is then added to the premix as a competitor, 146NCP is competed off from MeCP2 and is replaced with 165NCP in the complex. However, when 146NCP is added as competitor to the pre-incubated 165NCP-MeCP2 complex, it cannot compete off 165NCP from the complex. (B) Fluorescence view of the same gel as in panel A. It shows the increase in fluorescently labeled 165NCP-MeCP2 complex when 165NCP is added as a competitor, but no significant change is seen in the 165NCP-MeCP2 complex when 146NCP is added as competitor. (C) The quantification of the fluorescently labeled 165NCP-MeCP2 complex. (D) Competition assay between 53 mer DNA and 165NCP showed that MeCP2 prefers free 53mer DNA over 165NCP even though there is ~10 bp linker DNA on each side of the 165NCP.

There is a four-fold increase in the 165NCP-MeCP2-WT complex band intensity when a four-fold increase of 165 NCP competitor was added from lane 4 to lane 6. However, there is no such change in lane 8 to 10 when unlabeled 146NCP was added to the pre-formed 165NCP-MeCP2-WT complex at a similar ratio. These results indicate that 165 NCP can compete 146 NCP away from the pre-formed 146 NCP-MeCP2 complex, but 146 NCP cannot compete 165 NCP away from the pre-formed 165NCP-MeCP2 complex.

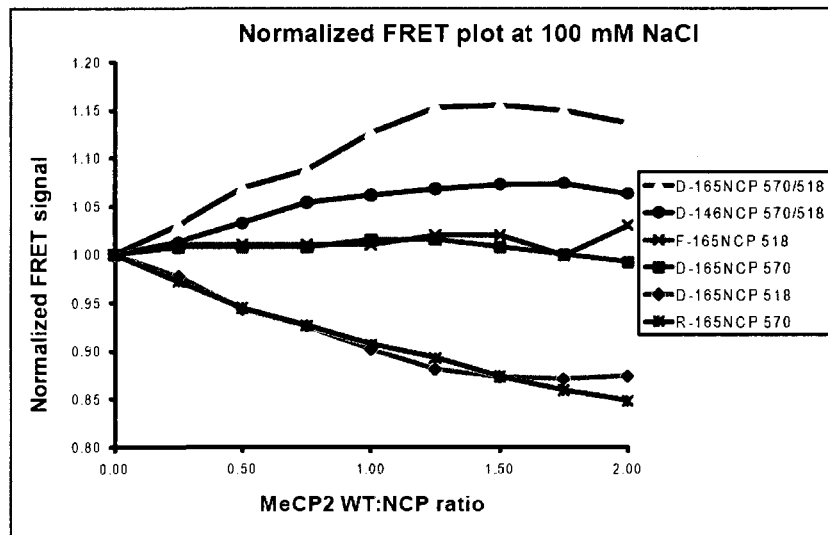
Competition assay was also performed between 165NCP and free 53 mer DNA. Figure 2.4D showed that when free 53 mer DNA was added to the preformed 165NCP-MeCP2WT complexes, there was a decrease in the 165NCP-MeCP2WT complexes and an increase in the 53mer DNA-MeCP2WT complexes; at the same time, free 165NCP increases (figure 2.4D, lane 8-10). This suggests that 165NCP was competed away by the free 53 mer DNA.

2.4.5. MeCP2 brings extra nucleosomal DNA ends in 165NCP in a closer proximity.

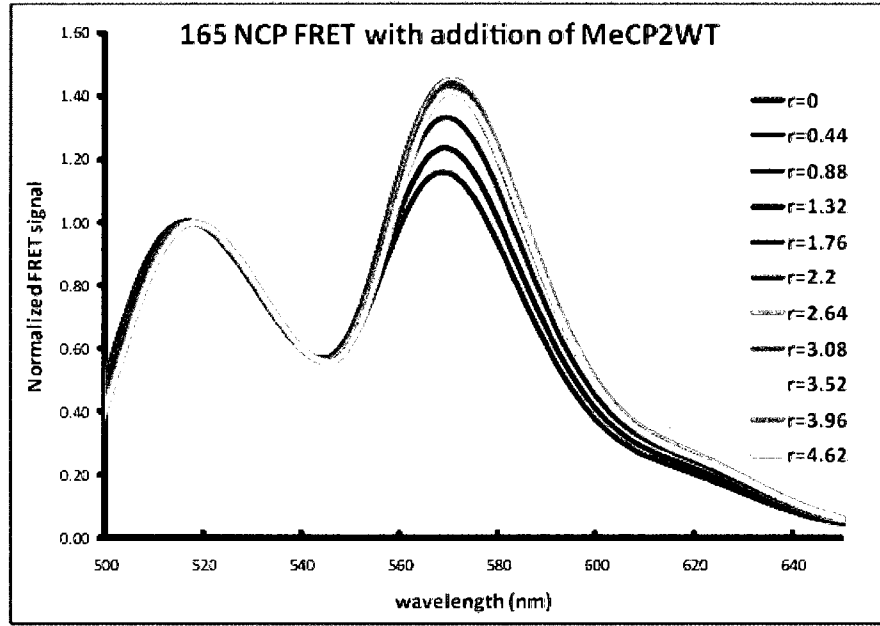
Although MeCP2 can interact with nucleosomes without extra nucleosomal DNA, it has higher affinity for NCP with extra nucleosomal DNA, 165NCP, than for NCP without extra nucleosomal DNA, 146NCP. To investigate the effect of MeCP2 on extra nucleosomal DNA, fluorescence resonance energy transfer (FRET) was employed. An Alexa-488 and Alexa-546 fluorophore pair with a Förster distance (R_0) of 64Å was chosen to label the two 5' ends of the DNA in 165NCP. Full length MeCP2 was added incrementally to doubly labeled 165NCP

(D-165NCP), and a series of emission scans (from 400 to 700 nm) was taken after exciting the samples at 488 nm. The emission signal was first corrected for the fading and dilution of the fluorophores over time. A significant decrease in the donor emission (Alexa-488) and a slight increase in the acceptor emission (Alexa-546) were observed with the addition of MeCP2 (Figure 2.5A) (figure 2.5A plotted the emission peak at 518 nm or 570 nm as a function of addition of MeCP2 at 100 mM NaCl, and it was normalized by dividing the emission intensity at each titration point by that at the first data point, so all the data started at 1). The possibility of donor quenching by MeCP2 was ruled out by titrating MeCP2 into the donor only labeled 165NCP (F-165NCP) and no quenching of the donor emission was observed (figure 2.5A). When MeCP2 was added to the acceptor only labeled 165NCP (R-165NCP), a significant decrease in the acceptor emission was observed. This could explain when MeCP2 was added to the D-165NCP, only a slight increase in the acceptor emission was observed. The fluorophore emission spectra were normalized by dividing the fluorescence intensities by the value recorded at 518 nm where donor emission peaks. The normalized spectra are shown in figure 2.5B. The normalized peak intensity at 570 nm (the acceptor emission peak) was subsequently plotted as a function of MeCP2 addition, shown in figure 2.5C. A 24% increase in the FRET efficiency between the two fluorophores in the DNA ends was observed when an increasing amount of full length MeCP2 was added into D-165NCP in 50 mM salt (figure 2.5C). Since fluorescence resonance energy transfer is very sensitive to the distance between the two fluorophores, the 24% change in the FRET signal

(A)



(B)



(C)

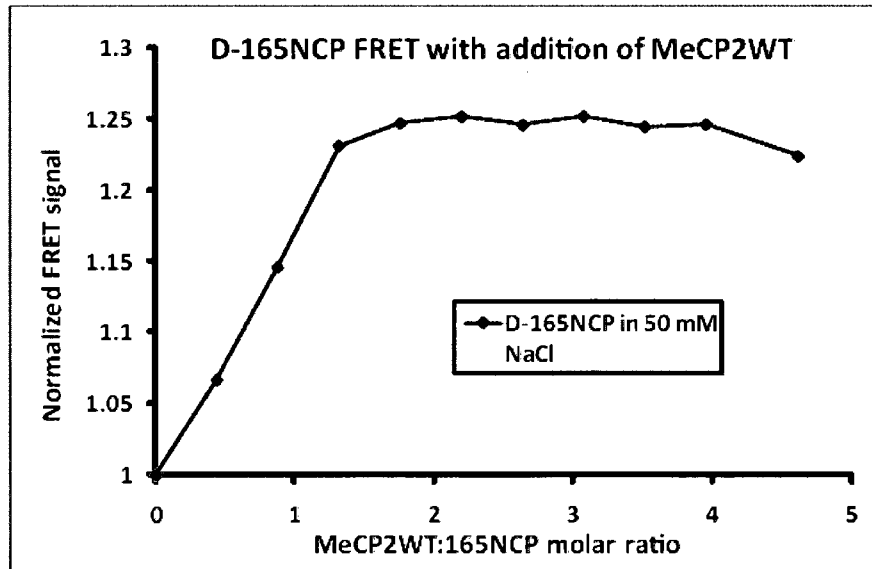


Figure 2.5: Fluorescence resonance energy transfer (FRET) assay suggests that MeCP2 can bring linker DNA ends in closer proximity. The two linker DNA ends of 165NCP were labeled with Alexa 488 and Alexa 546 fluorophores respectively. The fluorophores were excited at 488 nm, and the emission spectra were recorded as increasing amounts of full length MeCP2 were added. (A) shows the plots of emission peak intensities at 518 nm or 570 nm as a function of MeCP2WT concentration. (B) shows the normalized emission spectra of doubly labeled 165NCP as a function of MeCP2 addition. The emission spectra were normalized by dividing the peak signal at 518nm. (C) The emission peak at 570 nm was plotted as a function of the addition of MeCP2. The plot shows that FRET signal increases by ~24% when MeCP2 is added to fluorescently labeled 165NCP. The plateau starts at about 1:1 ratio of MeCP2 added, suggesting only one MeCP2 can bind to the linker DNA region and pull the linker DNA ends closer.

indicates a change in the relative distance between the two extra nucleosomal DNA ends of nucleosomes when MeCP2 is added. When the same experiment was repeated at 100 mM salt, a 15% increase in the FRET efficiency was observed (figure 2.5A). When doubly labeled 146NCP (lacking extra nucleosomal DNA) was used in the same FRET experiment in 100 mM salt, only a 7% increase in FRET efficiency was observed (figure 2.5A). In all the FRET experiments, a common plateau at about a 1:1 molar ratio of MeCP2 to NPC was observed, whether MeCP2 was added to 165NCP or 146NCP, in 50 mM salt or 100 mM salt. This finding is in agreement with our data obtained by SEC-MALS.

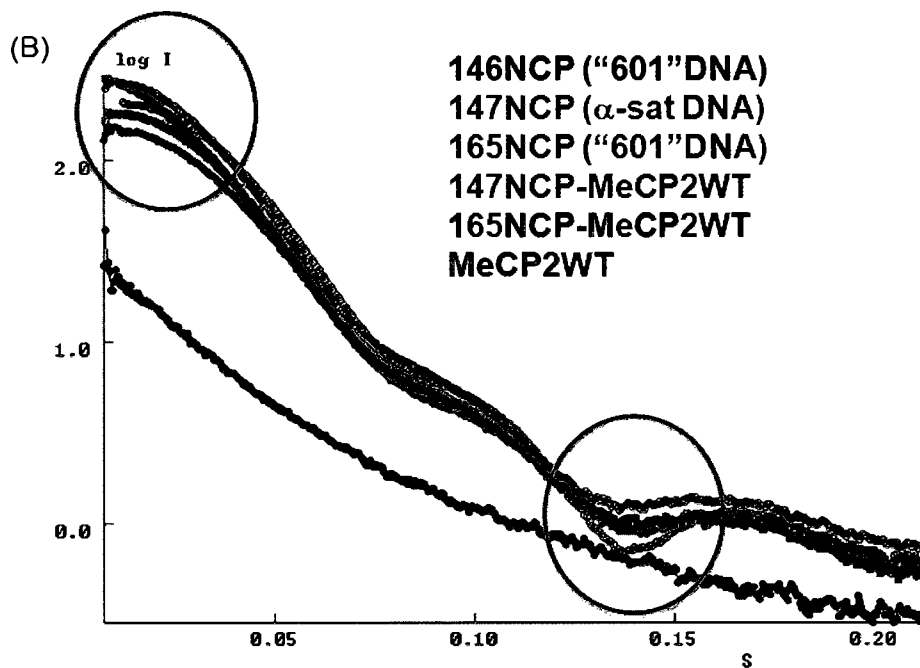
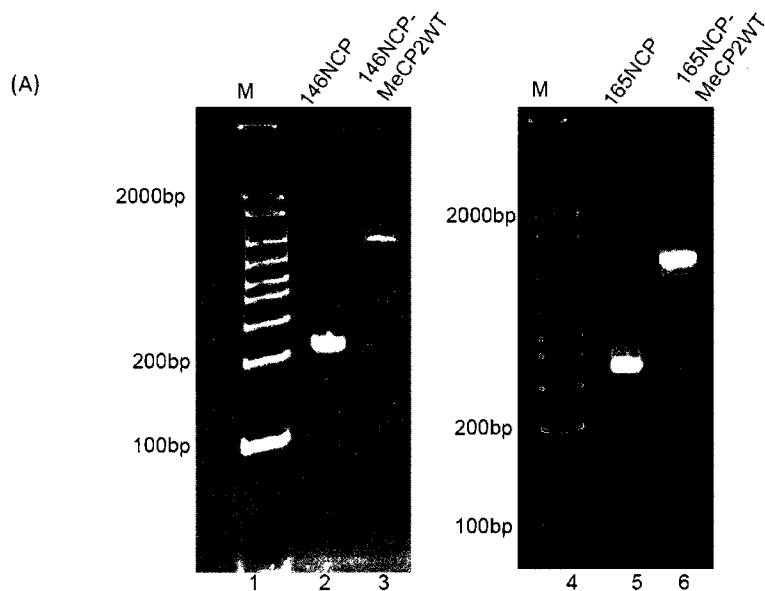
2.4.6. Small angle X-ray scattering (SAXS) studies of the NCP-MeCP2 complex.

SAXS provides low resolution structural information on macromolecules. We applied SAXS to the two nucleosomes under investigation here, to full length MeCP2, and to the complexes of the two. The following molecules and complexes were prepared: MeCP2-WT, 147NCP, and 165NCP at 7.5 mg/ml; MeCP2-WT in complex with 147NCP or 165NCP at 9.4 mg/ml (the concentration of NCP is the same in the complex as in the NCP sample) (figure 2.6A). Additional dilutions were made with sample buffer to obtain samples diluted to 2/3 and 1/3 for the data collection. Data were collected at the ALS beam line 12.3.1. Each sample was exposed for 6, 60 seconds and 6 seconds, in sequence. The scattering profiles at two six-second exposures were compared and no radiation damage was detected in the samples.

Scattering curves $I(q,C)$ recorded from a short exposure (6 seconds, data range $0.0071 < q < 0.05 \text{ \AA}^{-1}$) and from a long exposure (60 seconds, data range $q > 0.03 \text{ \AA}^{-1}$) were merged with PRIMUS (Konarev et al., 2003) to obtain an optimal complete scattering curve. At high concentrations (7.5mg/ml), the Guinier analysis of the data shows anti-aggregation or particle-particle repulsion, consistent with the highly charged character of the nucleosome. At low concentration (2.5 mg/ml), this inter-particle repulsion is minimized. Therefore further analysis of the scattering data was based on (merged) curves recorded at 2.5 mg/ml. These curves were used to derive the radius of gyration (R_g), maximum particle dimension and particle volume.

To facilitate the visual comparison of the scattering curves, the curve representing the 165NCP-MeCP2-WT complex was multiplied by a factor of 0.86 to superimpose it onto other curves as closely as possible. All the original scattering curves are shown in figure 2.6B. Generally the overall shape of the scattering curves for 147NCP, 165NCP, 147NCP-MeCP2-WT and 165NCP-MeCP2-WT complex are similar (Figure 2.6B). However, in the low q region the curves are distinct as indicated in the circle in Figure 2.6B. In this low q region, the radius of gyration (R_g) was estimated using a Guinier plot (Konarev et al., 2003), limiting the data to $qR_g < 1.3$, assuming non-interacting particles.

The maximum particle dimension (D_{max}) was estimated with the program GNOM (Svergun et al., 2001) (figure 2.6C). Both R_g and D_{max} values are listed in Table 2.2.



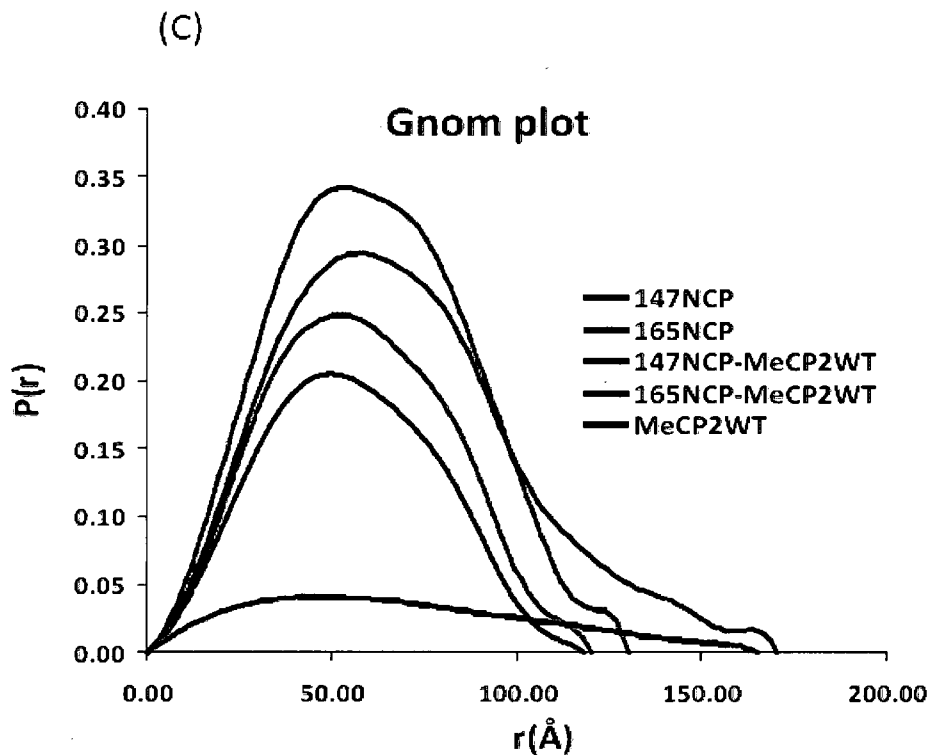


Figure 2.6: Small angle X-ray scattering (SAXS) reveals a more compact structure for MeCP2 complexes with 165NCP as opposed to 146NCP. (A) Samples for the SAXS experiment were run on 5% native TBE gel. It shows that all the samples are ~90% homogenous. (B) The scattering profile (I vs q) for NCP, MeCP2WT and NCP-MeCP2WT complexes. The overall shape of the scattering curves for the NCP and NCP-MeCP2WT complexes are very similar except the regions indicated in the circle. The curve of MeCP2WT is very different from the others. (C) Distance distribution function ($P(r)$ function) plot of NCP, MeCP2 and NCP-MeCP2 complexes. Maximum dimensions (D_{\max}) of the molecules are estimated by calculating the distance distribution function $P(r)$. The $P(r)$ plots here are derived with GNOM program with best statistics.

Table 2.2: Summary of SAXS data

| | Rg(Guinier)(Å) | D_{max}(Gnom) (Å) | Volume(Porod) (Å³) |
|--------------------------|-----------------------|----------------------------------|--------------------------------------|
| MeCP2WT | 67.0 ±2.02 | 165 ±2 | 1.40E+05 |
| 146NCP("601"DNA) | 41.6 ± 0.51 | 110±3 | 3.45E+05 |
| 147NCP(α-sat DNA) | 44.3 ±0.25 | 118 ±3 | 3.54E+05 |
| 147NCP-MeCP2WT | 54.7 ±0.56 | 170 ±2 | 5.71E+05 |
| 165NCP("601"DNA) | 42.1 ±0.23 | 120 ±2 | 4.03E+05 |
| 165NCP-MeCP2WT | 46.5 ±0.12 | 130 ±2 | 4.78E+05 |

Since MeCP2 is an intrinsically disordered protein and is very flexible by itself, it is not trivial to determine reliable values for Dmax. MeCP2-WT has a radius of gyration (Rg) of approximately 54-67 Å, and a Dmax of 163-350 Å. These results are consistent with previously published data that MeCP2-WT has a very elongated, largely unfolded structure. MeCP2 has been observed by gel filtration with a Stokes radius of ~60 Å and frictional coefficient of ~2.4 (Klose and Bird, 2004) and, with the help of EM, as an oblate ellipsoid with a dimension of 55 x 26 Å (Nikitina et al., 2007b).

The Rg and Dmax values for the two different nucleosomes, 147NCP and 165NCP, are similar, although the 165NCP includes 19 more DNA base pairs than 147NCP (see Table 2.2). The Dmax values reported here are slightly smaller than those published by Mangenot (Mangenot et al., 2002). The Dmax values for 165NCP and 146NCP were reported to be 138 ± 5 Å and 137 ± 5 Å, respectively; while we find 120 ± 2 Å for 165NCP and 118 ± 3 Å for 147NCP. Three factors contribute to the differences: First, the samples we used are prepared in a different way and therefore may have slightly different characteristics. The nucleosomes described in the literature are isolated from calf thymus or chicken erythrocyte nuclei and the sample used likely consisted of a mixture of nucleosomes with different DNA lengths. By contrast, our nucleosomes were reconstituted with purified DNA and recombinant *Xenopus* histones and therefore have a well-defined DNA length and are homogenous. It is well known that SAXS is sensitive to the presence of non-homogeneities, particularly if these are larger than the particle of interest. Second, the salt

concentrations are different in the two cases (50 mM versus 5 mM). It has been demonstrated by Mangenot that salt concentrations can drastically change the Dmax value because the salt concentration directly influences the conformation of the histone tails (Mangenot et al., 2002). Third, the methods for the determination of Dmax in GNOM could be different. Two methods can be used to determine Dmax in GNOM program. Dmax, by definition, is the maximum dimension of the particle. Thus in the P(r) function plot, Dmax can be determined when the probability of finding a dimension within the particle larger than Dmax becomes zero. When running the Gnom program, we are asked to give a Dmax input first. For each run with a different Dmax input, the statistics for evaluate the Dmax is different. The other way to determine Dmax is to choose the Dmax input which will give the best statistics. Our reported Dmax was determined by the second method, giving the best statistics, which is usually smaller than the Dmax determined by the first way.

In both Dmax determination methods, the trend holds true for the 165NCP-MeCP2WT complex and 147NCP-MeCP2WT complex. When MeCP2 forms a complex with 147NCP, the Rg (~54.7 Å) of the complex is much larger than the Rg when it complexes to 165NCP (Rg ~46.5 Å). The P(r) distribution in 147NCP-MeCP2WT complex shows a very large extension, which reflects a fairly large Dmax value (~170 Å). The P(r) distribution for 165NCP-MeCP2WT complex only shows a minor extension when compared to the 165NCP alone, and the Dmax is much smaller than that of 147NCP-MeCP2WT complex. The maximum extension

of 165NCP-MeCP2WT complex is estimated to be 130 Å, which is about 40 Å shorter than the 147NCP-MeCP2WT complex.

2.5 Discussion

2.5.1. Extra nucleosomal DNA is not necessary for MeCP2 to interact with nucleosomes, but it is important to organize the nucleosome-MeCP2 complex.

It has been reported that extra nucleosomal DNA is essential for MeCP2 interactions (Nikitina et al., 2007a). Without extra nucleosomal DNA, MeCP2 cannot interact with mono-nucleosome. Here we show that MeCP2 does clearly bind to mono-nucleosomes without extra nucleosomal DNA (Figure 2.1), but it has a higher affinity for nucleosomes with extra nucleosomal DNA (Figure 2.4).

The SAXS data (Table 2.2) show that MeCP2 is an elongated, largely unfolded molecule in solution, in the absence of a binding partner; these results are consistent with the observations reported in the literature (Klose and Bird, 2004)(Adams et al., 2007). However, when MeCP2 binds to a nucleosome, the SAXS data show that the maximum dimension of the nucleosome-MeCP2 complex is smaller than the sum of the dimensions of the two components making the complex (Table 2.2). Furthermore, the maximum particle size for the 165NCP-MeCP2 complex is significantly smaller than that for the 147NCP-MeCP2 complex, in spite of the fact that the 165NCP contains 19 additional base pairs of DNA (approximately 10 base pairs extra on each DNA terminus). Based on the D_{max} derived from Gnom, *ab initio* models can be calculated with Gasbor (Svergun et al., 2001) or Dammin (Svergun, 1999) programs. Usually 10-20

individual models were calculated and averaged. Figure 2.7 shows the procedures of how to calculate/reconstruct *ab initio* models. Figure 2.8 shows the surface representations of the averaged *ab initio* models for NCPs and their complex with MeCP2WT which were calculated by Gasbor and averaged over 10 models. It clearly demonstrates that 147NCP and 165NCP have similar sizes and shapes, but the sizes and shapes for the two complexes are different: the 147NCP-MeCP2 complex is more elongated than the 165NCP-MeCP2 complex, although the 147NCP-MeCP2 complex has less material. The nucleosome crystal structure (from PDB 1AO1) was superimposed with the *ab initio* models as an indication of the size for a 146NCP.

Based on these observations we can propose two possible models: one in which MeCP2 and 165NCP in complex have a large interaction interface, thus reducing the total particle size, and a second in which MeCP2 becomes better organized (folded) in complex with 165NCP. These two models do not contradict each other and may in fact apply at the same time. The results obtained from FRET experiments support a model in which the extra nucleosomal DNA is brought closer together upon addition of MeCP2 to 165NCP. This suggests that the extra nucleosomal DNA and MeCP2 directly interact and that the extra nucleosomal DNA is important in organizing the nucleosome-MeCP2 complexes. In this study, we did not identify which domain in MeCP2 is responsible for the interaction with extra nucleosomal DNA. In future studies, it will be important to map out which domain in MeCP2 is responsible for the interaction with the extra nucleosomal

Procedures of averaged *ab initio* models reconstruction

Scattering profile



Gnom

P(r) function



Gasbor or Dammin

Individual *Ab initio* models



Damaver

Average

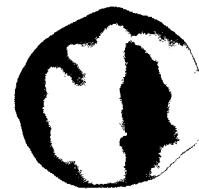
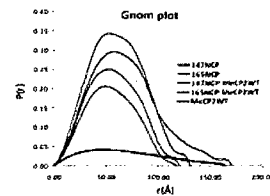
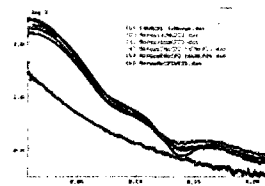


Figure 2.7: Procedures of averaged *ab initio* models reconstruction from SAXS scattering data. Scattering profile is transformed to distance distribution function (P(r) function) by Gnom. Gnom output file is the input file for the Gasbor or Dammin programs which reconstruct individual *ab initio* models. The individual *ab initio* models are averaged by Damaver program.

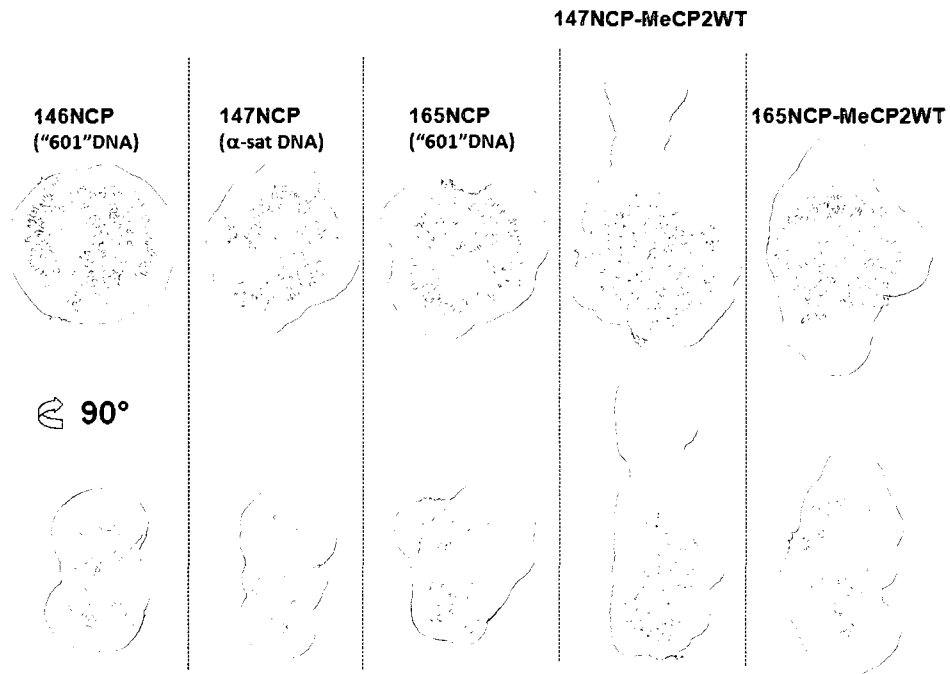


Figure 2.8: Surface representation of the averaged *ab initio* models calculated by Gasbor. It shows both the front view (top row) and side view (bottom view) for each molecule. Nucleosome crystal structure (PDB 1AO1) were superimposed with the *ab initio* models by "supcomb" program. The models at the top row shows that 147NCP and 165NCP have similar size and shape; while models at the bottom row clearly shows that the 147NCP-MeCP2 complex has more elongate shape when compared with the 165NCP-MeCP2 complex.

DNA in the nucleosome, and which domain in MeCP2 is responsible for the interaction with the nucleosomal part or histone part.

From the SEC-MALS and FRET experiment results, it clearly shows that the nucleosome-MeCP2 complex in the first shifted band (figure 2.1) consists of one nucleosome and one MeCP2. With the calculated molar mass and the sedimentation coefficient observed by sedimentation velocity assay, we can simulate the frictional ratio, f/f_0 , which reflects the shape of the sedimenting molecules. The simulated f/f_0 for NCPs and their complexes with MeCP2 were shown in table 2.3. 147NCP and 165NCP have similar f/f_0 values, suggesting the two NCPs have similar overall shape, as would be expected. However, when they complex with MeCP2WT, the 165NCP-MeCP2WT complex has a smaller f/f_0 value and axial ratio than that of the 147NCP-MeCP2WT complex (f/f_0 value: 1.39 VS 1.46; axial ratio: 8.4 VS 10.1), indicating that the 165NCP-MeCP2WT complex is less elongated or more compact than the 146NCP-MeCP2WT complex, although the 165NCP-MeCP2WT complex has 19 more base pairs of DNA. This is in agreement with the SAXS data. Taken together, the results from SAXS, SEC-MALS and sedimentation assays, indicate the role of extra nucleosomal DNA in organizing the nucleosome-MeCP2 complex, since the only difference between the two NCP-MeCP2 complexes is the 19bp extra nucleosomal DNA.

Table 2.3: AUC f/f_0 simulation and comparison with SAXS data

| | Sedimentation Velocity | | | | SAXS | |
|----------------|--|--------------------------|-------------|---------|----------|-----------|
| | Molecular weight (kDa) (calculated) | $s_{20,w}$ (observed) | Axial ratio | f/f_0 | Dmax (Å) | Rg (Å) |
| 147NCP | 205.0 | 11.2s | 4.0 | 1.16 | 118±3 | 44.3±0.25 |
| 147NCP-MeCP2WT | 257.9 (1:1) | 10.4s | 10.1 | 1.46 | 170±2 | 54.7±0.56 |
| 165NCP | 208.95 | 11.2s | 4.5 | 1.19 | 120±2 | 42.1±0.23 |
| 165NCP-MeCP2WT | 261.4 (1:1) | 11.0s | 8.4 | 1.39 | 130±2 | 46.5±0.12 |

2.5.2. MeCP2 does not bridge mono-nucleosomes.

Recently Nikitina proposed two different modes of how MeCP2 may compact chromatin based upon electron microscopy. One of the modes is by bringing nucleosomes together, forming a cluster of nucleosomes (Nikitina et al., 2007b). However, our current data show that under our conditions, MeCP2 does not bring mono-nucleosomes together.

Supporting evidence is derived from three experimental methods:

First, the AUC data suggest MeCP2 does not bridge nucleosomes together. Sedimentation properties of mono-, di-, tri-nucleosomes have been investigated extensively before (Butler and Thomas, 1998). Mono-nucleosomes sediment at ~11s. The sedimentation coefficient of di- and tri- nucleosomes depends on the ionic strength of the solution. Over the salt conditions tested in our experiments (5-100 mM), di-nucleosomes sediment at ~13-15s, tri-nucleosomes sediment at ~16-18s. If MeCP2 bridges two nucleosomes together, we should expect to observe a sedimentation coefficient around 13-15s, considering that the molar mass of nucleosome is four fold larger than that of MeCP2. However, our AUC data do not support this model; instead, sedimentation coefficients smaller than those of mono-nucleosomes alone were observed in the MeCP2 complexes with 147NCP or 165NCP. Since the sedimentation coefficient (s) is proportional to the molecular mass over frictional coefficient f (M/f), s increases if M/f increases and vice versa. In our case the complex formation of the nucleosome with MeCP2 is confirmed by native PAGE gel (Figure 2.2B). Therefore M increases upon

complex formation, but at the same time, the overall s decreases, which indicates that frictional coefficient f must increase much more to offset the increase in M so that M/f decreases. Considering that MeCP2 is an intrinsically disordered protein it is reasonable to propose that there is still a portion of MeCP2 that is not ordered when it interacts with mono-nucleosomes, so the frictional coefficient increases significantly when the complex is formed, compared to the mono-nucleosomes alone. From SAXS data, we already showed that the NCP-MeCP2 complexes were elongated, and the simulated frictional ratio f/f_0 from the sedimentation velocity also agreed that the NCP-MeCP2 complexes were elongated (table 2.3). This explains why we observed a smaller s -value even when the molecular mass increases in the complex. More importantly, no larger species that sediment at $\sim 13s$ or higher s -value (representative of di- or multi-nucleosomes) are observed.

Second, when the nucleosome-MeCP2 complexes (with either 147NCP-MeCP2 complex or 165NCP-MeCP2) were subjected to size exclusion chromatography combined with light scattering, the molecular weights are indicative of a complex formation at a 1:1 ratio (table 2.1). These results also suggest the absence of di-nucleosomes or nucleosome clusters in the complex.

Third, when MeCP2 was added to the fluorescently labeled 165NCP, the FRET signal increases first and levels off after about a one-to-one ratio MeCP2 was added, suggesting only one MeCP2 binds to the extra nucleosomal DNA region and changes the distance between extra nucleosomal DNA ends.

In summary, none of our data suggest the formation of di-nucleosomes or nucleosome clusters in the nucleosome-MeCP2 complex. Thus, the compaction of chromatin by MeCP2 is likely not achieved by bridging the nucleosomes together, unless the compaction by bridging the nucleosomes is cis-dependent. In the EMSA experiments multiple shifted bands are observed when increasing amounts of MeCP2 are added to the nucleosomes. As demonstrated by light scattering the first shifted band consists of one nucleosome and one MeCP2 molecule in complex, and FRET result show that only one MeCP2 binds to the entry-exit region in nucleosome. Since MeCP2 can protect ~11 base pair extra nucleosomal DNA in the nucleosome entry-exit region (Nikitina et al., 2007a), we attribute the complex in the first shifted band in Figure 1 to one MeCP2 binding to one nucleosome in the dyad region. AUC shows that even the complex in the second shifted band does not contain multiple nucleosomes, but does have a higher sedimentation coefficient. Furthermore, the complex in the second shifted band can be changed to the first shifted band when more nucleosomes are added (data not shown). We therefore attribute this complex to be multiple MeCP2 molecules binding to one nucleosome non-specifically in addition to binding specifically to the dyad region.

2.5.3. Implications for how MeCP2 compacts chromatin.

Many previous studies have shown that MeCP2 has a similar function to the linker histones H1 or H5 (McBryant et al., 2006; Nikitina et al., 2007a; Woodcock, 2006). Both MeCP2 and linker histones are chromatin architectural proteins which can compact chromatin, they have a high correlation with methylated DNA

(Ball et al., 1983); and they all likely bind to nucleosomes close to the DNA entry-exit region and protect about 11 base pair extra nucleosomal DNA in nucleosomes (Hayes and Wolffe, 1993; Nikitina et al., 2007a). Toth *et al* have shown that incorporation of linker histone H1 pulls the extra nucleosomal DNA ends closer together (Toth et al., 2001), while Hamiche *et al* visualized by EM the “stem”-like structure in the linker histone H5 containing mononucleosome (Hamiche et al., 1996). To investigate if MeCP2 has a similar function as the linker histone in this respect, we performed FRET assays. As shown in Figure 2.5, when MeCP2 was added to fluorescently labeled 165NCP, a significant increase in FRET signal was observed, which is similar to the result when H1 is added (Toth et al., 2001). Since the FRET signal is inversely related to the sixth power of the distance between the two fluorophores, the increase in the FRET signal suggests a decrease in distance between the two fluorophores. A similar effect was observed for H1 on extra nucleosomal DNA ends (Toth et al., 2001). Together with the 1:1 stoichiometry obtained by SEC-MALS and FRET assays, and the observation that MeCP2 does not bridge nucleosomes, our data suggest that one MeCP2 molecule binds to the DNA “entry-exit” region of one nucleosome, pulls the DNA ends closer and possibly forms a “stem” at the entry-exit region. Our model also suggests that MeCP2 compacts chromatin by altering the path of the extra nucleosomal DNA, in addition to bridging nucleosomes, and this may be the initial step in the compaction of chromatin by MeCP2. This aspect of compaction mechanism by MeCP2 is similar to that of H1. To further confirm the validity of this model, more investigations are needed. Extensive

high-resolution AFM or EM images may contribute to test the validity of this model. Although the EM images of MeCP2 in complex with mono-nucleosomes and nucleosomal arrays have been acquired (Georgel et al., 2003) (Nikitina et al., 2007a), there were 2-4 MeCP2 molecules present per nucleosome in the complex, resulting in highly compacted chromatin arrays. Our study shows that MeCP2 is capable of forming a complex with nucleosome at a 1:1 ratio. In order to visualize the “stem” structure, a 1:1 ratio or under-saturated complex with MeCP2 may be added, with the intention of forming an array that is not too compacted. In the EM images of MeCP2 in complex with mono-nucleosomes, no “stem”-like structure was observed. This may be because that the length of the extra nucleosomal DNA in the mono-nucleosomes is not long enough to observe the “stem” structure formation. Hamichie *et al* used mono-nucleosomes reconstituted with 256 bp DNA and showed the “stem” structure formation upon H5 binding (Hamiche et al., 1996). The similar experiment can be repeated with MeCP2 to see if the “stem” structure formation can be observed.

2.6 Acknowledgement

We thank the International Rett Syndrome Foundation and American Heart Association for financial support. We thank Dr. Valerie H. Adams for generously providing us with the MeCP2 plasmids. We thank Kitty Brown, Drs Wayne Lilyestrom, Uma Muthurajan, as well as Drs Robert Woody and Steven McBryant for discussions. Drs Michal Hammel and Robert P. Rambo (ALS) are acknowledged for help in collecting and analyzing SAXS and the light scattering data.

X-ray scattering and diffraction technologies and their applications to the determination of macromolecular shapes and conformations at the SIBYLS beamline at the Advanced Light Source, Lawrence Berkeley National Laboratory, are supported in part by the DOE program Integrated Diffraction Analysis Technologies (IDAT) and the DOE program Molecular Assemblies Genes and Genomics Integrated Efficiently (MAGGIE) under Contract Number DE-AC02-05CH11231 with the U.S. Department of Energy. Efforts to apply SAXS and crystallography to characterize eukaryotic pathways relevant to human cancers are supported in part by National Cancer Institute grant CA92584.

CHAPTER 3

ARE THERE ANY INTERACTIONS BETWEEN MECP2 AND HISTONES WITHIN NUCLEOSOMES?

3.1 Abstract

Pull-down assays are widely used in biological research to either confirm interactions between proteins or probe for new protein-protein interactions in cells. Tags including Glutathione S-Transferase (GST) tag are usually fused to “bait” proteins and used to immobilize the “bait” proteins to a solid phase like specifically coated beads. One weakness of the pull-down assay using the tag-protein fusion protein is that the fusion protein could have adopted a new conformation which is different from that of the “bait” proteins alone so that the interactions detected by this method could be particular to this novel conformation, not the “bait” protein itself. Here we present such an example. In this study, we showed that intein-tagged MeCP2 interacts with histone dimers and tetramers under 300 mM salt; however, this interaction could not be demonstrated by any other solution-state method in the absence of the intein tag. Thus we conclude that the interaction with histones detected by the intein-tag pull-down assay is specific to the intein-MeCP2 fusion protein and not to MeCP2.

3.2 Introduction

Pull-down assays are widely used in biological research to determine physical interactions between two or more proteins. They can serve as a discovery tool in identifying new proteins in endogenous environment to interact with a given protein, or as a tool to confirm the interaction between proteins indicated by other methods, such as immunoprecipitation.

In pull-down assays, a “bait” protein is usually expressed as a fusion protein with a “tag” peptide or protein and immobilized to a solid phase through the “tag”. Potential “prey” proteins are added to and incubated with “bait” protein. After a series of wash steps to remove the non-specific “prey” proteins, the entire complex is eluted from the solid phase and evaluated on SDS-PAGE gel.

Glutathione S-Transferase (GST) tag, polyhistidine tag and maltose tag are commonly used tags in the pull-down assays. The GST tag itself is a 220-amino-acid containing protein and has been used in numerous studies to screen for protein-protein interactions. Nan *et al* employed a GST pull-down assay to confirm the interaction between MeCP2 and co-repressors. After the observation that MeCP2 co-immunoprecipitated with mSin3A, they used GST-MeCP2 fusion protein to pull down mSin3A. They found that GST-MeCP2 fusion protein can pull down mSin3A, but not HDAC1 and HDAC2 (Nan et al., 1998).

The Intein tag is another commonly used tag in protein purification and pull-down assays. Like genes having introns and exons, proteins also have inteins and exteins. Inteins are segments of proteins that can excise themselves and rejoin the remaining parts (the exteins) (Anraku et al., 2005), in analogy to RNA splicing. This self-cleavable

property of inteins is commonly applied to protein affinity purification. IMPACT (Intein Mediated Purification with an Affinity Chitin-binding Tag) (New England BioLabs) is a relatively new system which utilizes intein as an affinity tag during protein purification. In this system it is very easy to separate the target protein from the affinity tag because the affinity intein tag can cleave itself from the target protein. Alternatively, it can also be used as an affinity tag for pull-down assays.

Although there are many advantages of using pull-down assays to study the interactions between proteins, there are disadvantages as well. First, because the tag is not a natural part of the “bait” protein, the interactions detected with the protein-tag fusion protein may be specific to the artificial fusion protein, not the native protein; second, the tag, especially a protein tag like GST tag which is about 24 kD, may block the interaction interface between “bait” and “prey” proteins, so pull-down assays may fail to detect interactions due to the tag; third, weak and transient interaction may not be detected by pull-down assays; fourth, conditions in pull-down assays may not properly simulate biological situations, so the interactions detected by pull-down assay may not exist under native conditions.

Here we show an example that the interaction detected by pull-down assays may be an artifact of the fusion protein. Previously it has been shown that MeCP2 is a chromatin architectural protein and it can stably associate with the nucleosome, the basic unit of chromatin. It was known that MeCP2 is a DNA binding protein and it can also interact with DNA within the nucleosomal context. The nucleosome consists of DNA as well as a histone core containing two copies each of histone H2A, H2B, H3 and H4 (Luger et al., 1997). To understand the molecular details of how MeCP2 interacts with nucleosomes, we hypothesize that the histone core within nucleosomes also participates in the

interaction with MeCP2. To do this, intein-tagged pull-down assays were applied. My results showed that intein-tagged MeCP2 interacts with histone dimers and tetramers under 300 mM salt, but not with intein-tag alone. Only histone complexes interact with intein-tagged MeCP2, not individual unfolded histones. As such, our results are entirely self-consistent and controlled. However, this interaction could not be demonstrated by other in-solution state methods in the absence of the intein tag. Therefore, we conclude that the interaction with histones detected by the intein-tag pull-down assay is specific to the intein-MeCP2 fusion protein, not MeCP2.

3.3 Materials and methods

3.3.1 Preparation of MeCP2 for pull-down assay

Recombinant human MeCP2 isoform e2 (full length and its fragments) gene was cloned in pTYB1 vector in the IMPACT (Intein Mediated Purification with an Affinity Chitin-binding Tag) system from New England BioLabs. MeCP2 was fused with intein tag at the C-terminal region. The expression clones for full length MeCP2 and its fragments were a gift from the Hansen lab in our department. The expression of MeCP2 was as described before (Adams et al., 2007; Georgel et al., 2003). Expression host cell BL21-CodonPlus(DE3)-RP (Stratagene) from *E. coli* host strain was used for the expression. Typically three liter cultures were grown and induced with 0.4 mM IPTG for two hours when cell growth reached OD₆₀₀~0.4. Cells were then spun down and harvested. Cell pellets were resuspended in ~40 ml Chitin Binding Protein Buffer (CBP buffer) (25 mM Tris pH 7.5, 500 mM NaCl, 10% glycerol, 2 mM PMSF, 0.5% Triton x100) and sonicated. Cell debris were pelleted by centrifugation and the supernatant was applied onto 5 ml chitin beads previously equilibrated with CBP buffer, and incubated with the chitin beads in a 50 ml conical tube on a rocker at 4 °C overnight. The beads were washed with 50

ml CBP buffer three times by spinning. 6 ml of bead suspension after the last wash were aliquoted into 100 μ l each for the pull-down assay.

3.3.2 Refolding of histone dimer, tetramer or octamer

Xenopus laevis histone H2A, H2B, H3 and H4 were over-expressed in bacteria and purified as described before (Dyer et al., 2004). Equimolar amounts of unfolded H2A and H2B for histone dimer, or H3 and H4 for histone tetramer, or all four histones for histone octamer, were mixed and refolded into histone dimer, tetramer or octamer by dialysis into refolding buffer (2 M NaCl, 10 mM Tris pH 7.5, 1 mM EDTA, 5 mM β -mercaptoethanol) and purified by size exclusion chromatography in the same buffer.

3.3.3 Pull-down assay with intein tag

MeCP2-Intein fusion protein was prepared and bound to chitin beads as described above. One aliquot of MeCP2-Intein fusion protein bound chitin beads was washed in the tube with 1 ml MeCP2 buffer (10 mM Tris pH7.5, 50 mM NaCl), or CBP buffer with 100 mM NaCl or 300 mM NaCl three times by spinning. The supernatant was removed after the last spin, 0.8 nmol test protein (H2A, H2B, H3, H4, histone dimer, histone tetramer, or histone octamer) was added and incubated with the bead suspension at 4 $^{\circ}$ C on a rocker for 3 hours. Beads were washed with 1 ml of their corresponding buffer five times. After the last spin, about one third volume of the protein loading dye with β -ME was added to the beads and incubated at 95 $^{\circ}$ C for 5 minutes. The beads were pelleted, and 15 μ l of the supernatant was loaded onto an 18% SDS-PAGE gel.

3.3.4 Isothermal Titration Calorimetry (ITC)

The ITC experiments were performed using a MicroCal VP-ITC. All solutions were prepared using deionized water and degassed for 10 minutes before loading into the ITC instrument. MeCP2 and histone tetramer were dialyzed into ITC buffer (25 mM Tris pH 7.5, 300 mM NaCl, 0.25 mM EDTA, 10% Glycerol). 1.8 ml MeCP2 were injected into sample cell, while 200 μ l histone tetramer were loaded in the syringe with a concentration about ten-fold higher than that of MeCP2. The sample cell was stirred when histone tetramer was injected into the sample cell with 6 μ l per injection and 300-second intervals between injections. Data were analyzed and fitted by the software provided by MicroCal.

3.3.5 Sedimentation velocity

Before the AUC experiment, H2A/H2B dimer and MeCP2 WT were dialyzed into the same buffer (10 mM Tris pH 7.5, 100 mM NaCl, 2% glycerol, 0.2 mM TCEP). In the sedimentation velocity experiments, H2A/H2B dimer and MeCP2 WT at 3 μ M each, or a mixture of dimer and MeCP2wt at 1:1 molar ratio were used. Sedimentation velocity experiments were done with Beckman XL-I analytical ultracentrifuge with absorbance detection at 230 nm. Scans were collected at a radial step resolution of 0.003 cm. Boundaries were analyzed using the method of Demeler *et al* (Demeler *et al.*, 2000; Demeler and van Holde, 2004) with the Ultrascan program (version 7.3). This analysis gives an intergral distribution of sedimentation coefficients, G(s). Sedimentation coefficients were corrected to that in water at 20 °C. The solvent densities were calculated in Ultrascan. The partial specific volumes of the samples were calculated from the primary amino acid sequence using Ultrascan.

3.3.6 Gel filtration combined with multi angle light scattering (SEC-MALS)

A Superose 6 3.2/30 gel filtration column was pre-equilibrated in gel filtration buffer solution (GF buffer) (10 mM Tris pH 7.5, 0.25 mM EDTA, 100 mM NaCl, 0.2 mM TCEP, 2% glycerol). Proteins (e.g. MeCP2, histone dimer, histone tetramer) were purified first and dialyzed into the GF buffer before loading onto the gel filtration column. 40 μ l of each protein were loaded onto the column at approximately 2 mg/ml and detected with UV absorbance at 280 nm. The elution profiles were plotted. The gel filtration column is connected to a multi angle light scattering (MALS) instrument (Wyatt technologies). MALS measures the amount of light scattered by the molecules. The concentration of molecules is determined by MALS by measuring the refractive index or UV absorbance. Since the light scattered by a molecule is proportional to the molecular mass times the concentration, the molar mass for each elution peak of the molecules is therefore determined with ASTRA software provided with the instrument.

3.4 Results

MeCP2 is an abundant chromatin associated protein and studies have shown that it can interact with the nucleosome, the basic building block of chromatin. The nucleosome is a DNA-protein complex which consists of 146-147 base pairs of DNA wrapped around a histone octamer core (Luger et al., 1997). There are two copies each of core histone proteins H2A, H2B, H3 and H4 in the histone octamer. MeCP2 is a DNA binding protein, it can bind DNA via its Methyl-CpG Binding Domain (MBD). It has long been assumed that MeCP2 interacts with chromatin via its DNA binding domain. The possibility that MeCP2 interacts with the histone component of the nucleosome has not been investigated, although precedents for other proteins exist in the literature (Barbera et al., 2006). Nikitina *et al* showed that MeCP2 is in close proximity to histone H3 when it is in

complex with mono-nucleosomes (Nikitina et al., 2007), suggesting that MeCP2 might interact with core histones within nucleosomes. To test the hypothesis that MeCP2 interacts with histones, we applied pull-down assays with different histone complexes.

3.4.1 MeCP2-Intein fusion protein can pull down histone complexes.

In the MeCP2 expression system as described before (Georgel et al., 2003), MeCP2 has an intein tag fused to its C-terminal end. The intein tag can bind to the chitin beads, thus immobilizing MeCP2. The schematic of this pull down assay system is shown in figure 3.1A. Pull-down assays were performed with MeCP2-intein and different forms of histones in 100 mM or 300 mM NaCl. The results of pull-down assays done at 300 mM salt are shown in figure 3.1B and 3.1C. MeCP2-intein fusion protein clearly pulled down the histone dimer, tetramer and octamer in 100 mM and 300 mM salt, suggesting interaction between MeCP2-Intein fusion protein and histone dimers or tetramers. Two important controls were done and confirmed that we were observing a specific binding event. First, the immobilized intein tag alone did not pull down histones under the same conditions (data not shown). Second, individual histones, H2A, H2B, H3 and H4, which are likely to be disordered without their respective dimerization partners, were pulled down by MeCP2 at 100 mM NaCl, but not at 300 mM NaCl when histone dimer and tetramer can be pulled down (figure 3.1C). The interaction between MeCP2 and histones were interrupted in 500 mM salt (figure 3.1D), indicating a rather high affinity. These results suggested the exciting possibility that concerted interaction of the MBD with DNA, and other regions of MeCP2 with the histone octamer surface confer positional specificity and additional affinity to the complex of MeCP2 with the nucleosome. Previous studies showed that the latency-associated nuclear antigen (LANA) peptide interacts with H2A/H2B dimer in the acidic patch on the surface (Barbera et al., 2006)

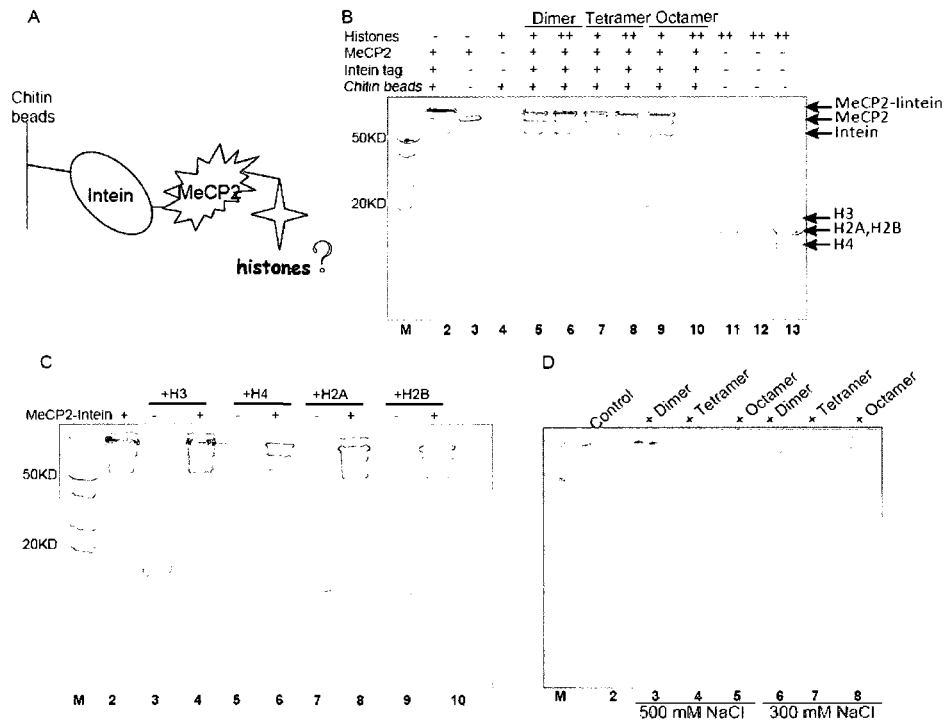


Figure 3.1: Intein-tagged WT-MeCP2 pull-down assays in 300 mM NaCl. Panel A shows the schematic cartoon for the pull-down assays. Panel B and C show the pull-down results at 300 mM NaCl. At 300 mM salt, intein-tagged MeCP2 can pull down folded histones in dimer, tetramer and octamer forms, but not in individual histone forms (H3, H4, H2A or H2B alone). Panel C shows that interactions between intein-tagged MeCP2 and folded histones were disrupted at 500 mM salt.

so considering the pI for MeCP2 and histones are both basic, it is possible that MeCP2 may interact with H2A/H2B dimers in the acidic patch. We then used the acidic patch mutant H2A/H2B dimer which neutralized histone surfaces (Chodaparambil et al., 2007) and repeated the pull-down assay under the same condition. The acidic mutant dimer can still be pulled down by MeCP2 (see figure in appendix II), suggesting the acidic patch is not the determinant in the interaction between MeCP2 and histone H2A/H2B dimer. When the all-tailless histone octamer was used in the pull-down assay, no effect on the interaction between MeCP2 histones was observed, indicating that the tails of histones are not important in the interaction either.

To map out which region(s) or fragment(s) of MeCP2 are responsible for the interactions with histones, different fragments of MeCP2 were used to repeat the pull-down assays. The annotation for the fragments of MeCP2 is shown in figure 3.2.

MeCP2 fragments B and C, encompassing MBD and TRD domains, both can pull down histone dimers and tetramers at 300 mM salt (figure 3.3A), but neither fragment I (MBD) or fragment D (TRD) fused to intein tag individually can pull down histones at 300 mM salt (figure 3.3B). This suggests that the combination of these two domains is involved in the interaction with histones, and the individual domains are not sufficient to pull down histones.

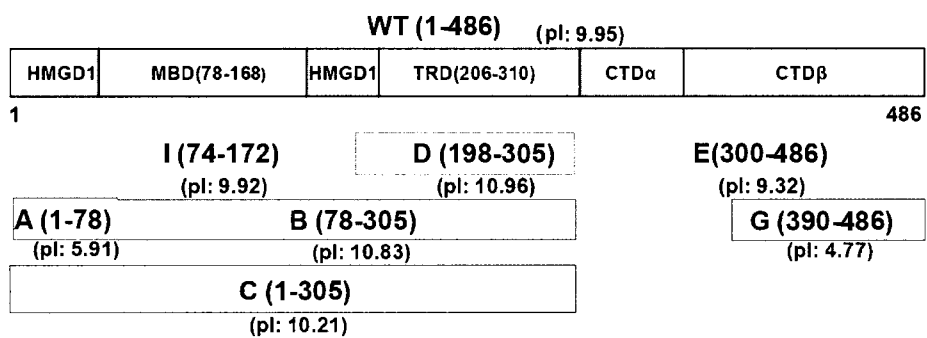


Figure 3.2: Annotation for MeCP2 and its fragments.

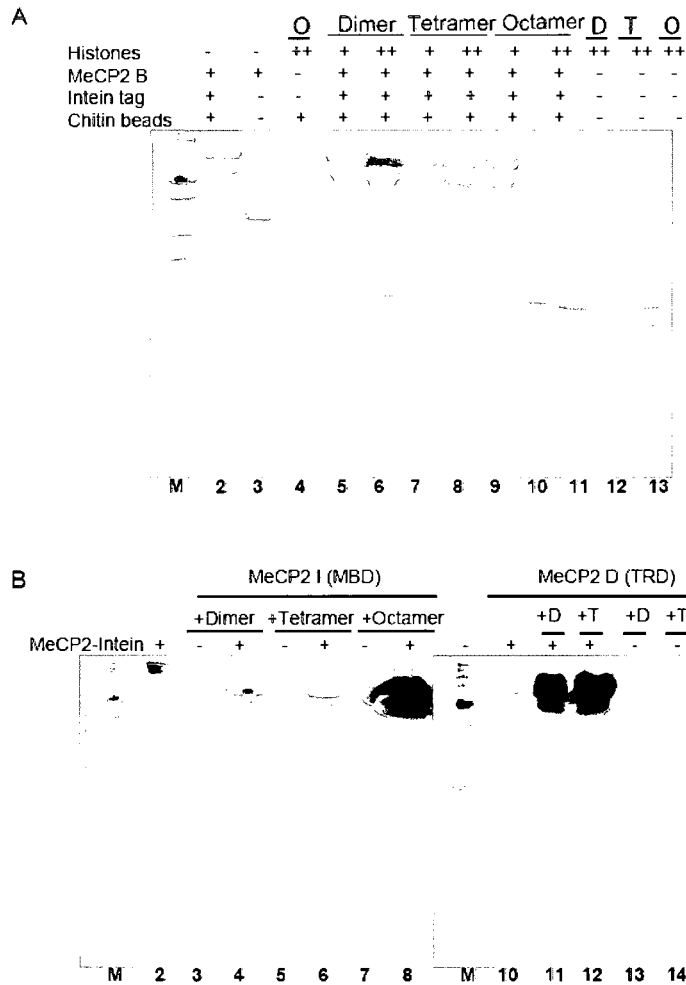


Figure 3.3: Intein-tagged MeCP2 fragments B, I and D pull-down assays in 300 mM NaCl. Panel A shows the pull-down results of intein-tagged MeCP2 B at 300 mM NaCl. At 300 mM salt, intein-tagged MeCP2 B can pull down folded histones in dimer, tetramer and octamer forms as the WT-MeCP2 does. Panel B shows that intein-tagged MeCP2 I and D both failed to pull down histone dimer, tetramer and octamers under the same condition as MeCP2 B did.

The C-terminal part of MeCP2 was also tested in the interaction with histones. MeCP2 fragment E (a.a. 300-486) can pull down histone dimer and tetramer at 300 mM salt, but fragment G (a.a. 390-486) cannot pull down histone dimer or tetramer under the same condition.

Taken together, the results from intein-tag pull-down assays show that MeCP2 is likely to interact with folded histone complexes, and there are multiple domains of MeCP2 which can interact with histones.

3.4.2 His-tagged histone complexes do NOT pull down MeCP2.

To further confirm the interaction between MeCP2 and histones shown by the intein-tagged MeCP2 pull-down assay, we did the reverse pull-down assay. Since MeCP2 fragment B in fusion with intein-tag can pull down histones, and the yield of MeCP2 B is much greater than full length MeCP2, MeCP2 fragment B was used in the reverse pull-down assay. Mouse H2A/H2B is his-tagged and immobilized onto nickel beads. Pull-down assay was done under the same condition as in the intein-tagged MeCP2 pull down assay. From the result shown in figure 3.4, MeCP2 B can bind to the nickel beads nonspecifically; his-tagged mouse H2A/H2B dimer can bind to nickel beads fairly well. However, no significant amount of MeCP2 B in addition to what was already bound nonspecifically was pulled down by his-tagged mouse H2A/H2B dimer. This result suggested that within the his-tagged histone system, there is no significant interaction between the mouse H2A/H2B dimer and MeCP2 B. Although this his-tagged mouse H2A/H2B dimer pull-down assay was not the exact reverse pull-down assay to the intein-tagged MeCP2 system, H2A/H2B dimer is highly conserved between mouse and *Xenopus*.

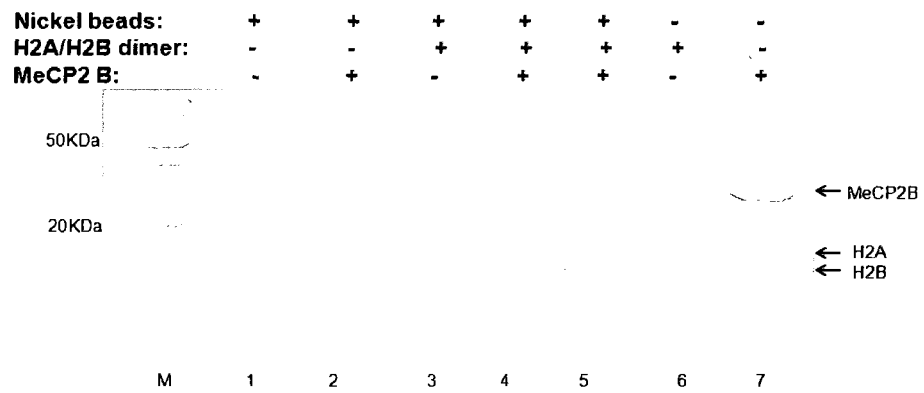


Figure 3.4: His-tagged mouse H2A/H2B dimer pull down assay. No significant amount of MeCP2 B was pulled down by his-tagged mouse histone H2A/H2B dimer.

3.4.3 The interaction between MeCP2 and histones was not detected by

Isothermal Titration Calorimetry (ITC).

Isothermal titration calorimetry (ITC) is a biophysical technique used to determine the thermodynamic parameters of biochemical interactions. It is often used to study the interaction between molecules. Since biochemical interaction events are usually accompanied by heat changes, either releasing heat or absorbing heat, this heat change can be measured by ITC and it also indicates an interaction event.

Our results showed that intein-tagged MeCP2 interacts with histones under 300 mM salt, but the his-tagged mouse H2A/H2B dimer failed to pull down free MeCP2. It is possible that the interaction shown in the intein-tag system was intein tag-dependent. Without intein tag, the interaction between MeCP2 and histones may not exist. So it is important to investigate whether free MeCP2, without the intein tag, can still interact with histones. ITC is a method to probe the interaction between two independent molecules in solution, independent of affinity tags and immobilization. Since MeCP2 B (78-305) showed the interaction with (H3/H4)₂ tetramer similar to that of full length MeCP2, and MeCP2 B has a much better yield than full length MeCP2, the MeCP2 B fragment was used for the initial trial of ITC. (H3/H4)₂ tetramer (375 μM) was titrated into the MeCP2 B fragment (31.8 μM) and the enthalpy change was measured by ITC. (H3/H4)₂ tetramer was also titrated into the reference buffer for baseline determination. The results are shown in figure 3.5. The titration of (H3/H4)₂ tetramer into buffer showed a significant enthalpy change, indicating there is an enthalpy change in the dilution of (H3/H4)₂ tetramer into buffer. However, when (H3/H4)₂ tetramer was titrated into MeCP2 B, the enthalpy change was almost identical with the enthalpy change when (H3/H4)₂ tetramer was titrated into MeCP2 buffer. When the enthalpy change of the dilution of tetramer into

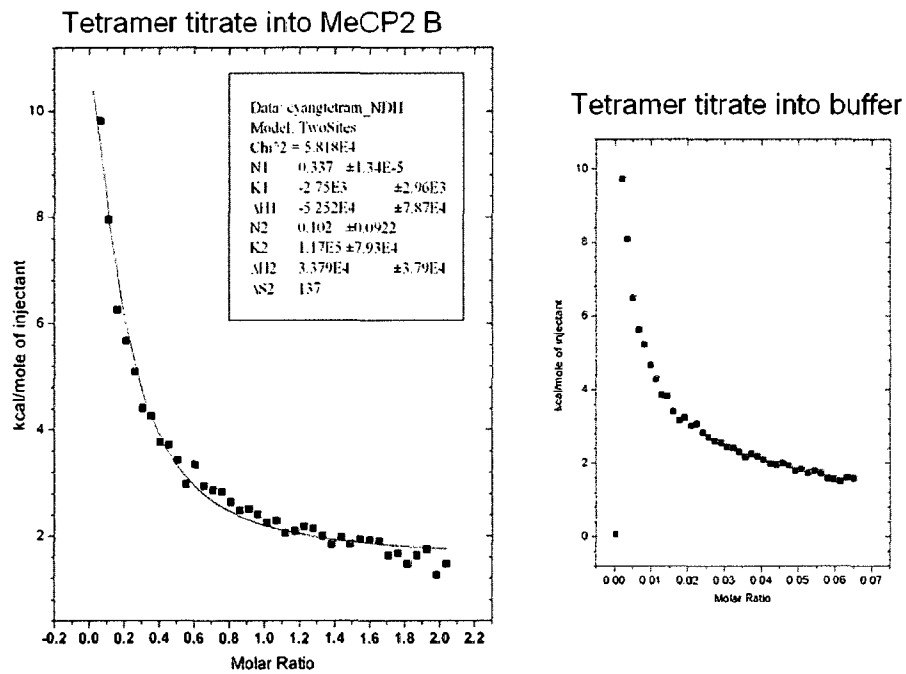


Figure 3.5: Results of ITC experiment suggested no enthalpy change if MeCP2 B interacts with histone tetramer. The left plot shows the enthalpy changes when histone tetramer (375 μM) was titrated into MeCP2 B (31.8 μM), but the plot is identical to that of titrating tetramer into the reference buffer (right plot), which suggested there was very subtle enthalpy change for the interaction, if any, between MeCP2 B and tetramer, given the high protein concentrations used in the ITC experiment.

buffer was subtracted from the titration of tetramer into MeCP2 B, the net enthalpy change was almost zero, which indicates that there is almost no heat change when H3/H4 tetramer was titrated into MeCP2 B. In other words, given the high concentration in the ITC experiment, these results suggested there was a very subtle or no enthalpy change for the interaction. The more likely interpretation is that there was no interaction between MeCP2 B and H3/H4 tetramer.

3.4.4 Sedimentation velocity did not give a conclusive result about the interaction between MeCP2 and histones

When two macromolecule components in solution interact on a timescale that is much faster than the experiment, the migration of the two components is coupled when an external force is applied. In the 1950s, Gilbert and Jenkins developed a theory that describes the migration experiments for rapid reactions with negligible diffusion (Dam and Schuck, 2005). According to the Gilbert-Jenkins theory, sedimentation velocity gradients can be calculated for proteins in self-association and in rapid interaction with other proteins, so sedimentation velocity can be used to probe the interaction between proteins.

Both H2A/H2B dimers and MeCP2 have been characterized by sedimentation velocity before. They have different sedimentation coefficients. In the sedimentation velocity experiment, H2A/H2B dimer and MeCP2WT were both prepared at 3 μ M in 100 mM NaCl. Both components and their mixture at 1:1 molar ratio were subjected to sedimentation velocity experiments in the same rotor. The $g(s)$ plots of the diffusion-corrected sedimentation coefficient distributions are shown in figure 3.6. H2A/H2B dimer sediments at $\sim 1.70s$, MeCP2 sediments at $\sim 2.02s$, which is consistent with published results (Adams et al., 2007). However, the mixture sediments at $\sim 1.95s$, which is

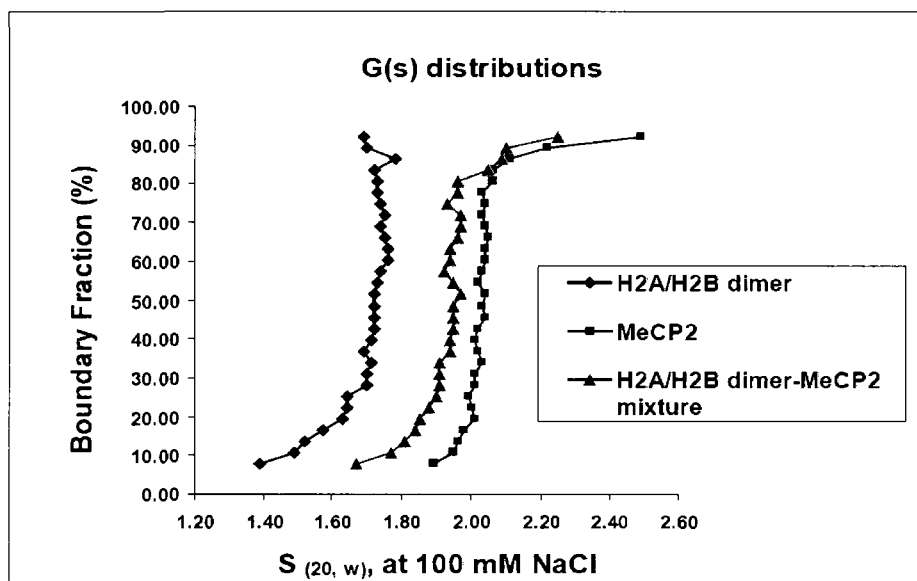


Figure 3.6: Sedimentation coefficient distribution of histone dimer, MeCP2 and their mixture at 100 mM NaCl. 90% of the sedimenting species were homogenous as indicated by the straight lines of the boundary distribution. Histone dimers sediment at ~1.7s, MeCP2WT sediment at ~2.02s, the “mixture” sediment at ~1.9s.

between where the two individual components sediment. The sedimentation coefficient (s) is proportional to M/f (M is the mass of the molecule, f is the frictional coefficient of the molecule). So s depends on both the size (M) and the shape (f) of the molecules. If two molecules are interacting, the size (M) of the complex increases; when the increase in M is larger than the increase in f , M/f increases and s increases; when the increase in M is smaller than the increase in f , M/f decreases and s decreases. If two molecules are not interacting during the sedimentation, two different sedimentation boundaries will be seen, with each boundary corresponding to each molecule. Here in our sedimentation velocity experiment, the ~90% homogeneity of the boundaries for H2A/H2B dimer and MeCP2WT indicated the homogeneity of the samples. The boundary for the mixture also showed a ~90% homogeneity, indicating that ~90% of the sample sediments as one species. Considering that the mixture sediments slower than MeCP2WT, and faster than H2A/H2B dimer, and M should increase if the two molecules are interacting, so if there is interaction between MeCP2WT and H2A/H2B dimer, the frictional coefficient (f) has to increase a lot to offset the increase in M . It is known that MeCP2 is an intrinsically disordered and elongated protein by itself, if MeCP2 forms a complex with histone dimers, they must form an "end-to-end" complex making the complex more elongated, so the frictional coefficient of the complex increases significantly. However, this hypothesis is not validated so far, and no final conclusion regarding the interaction between MeCP2 and H2A/H2B dimer can be made.

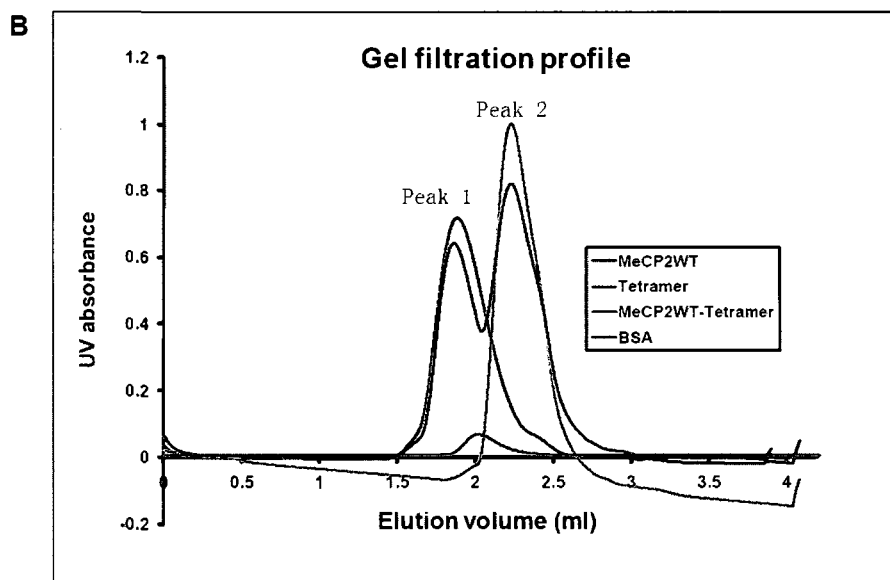
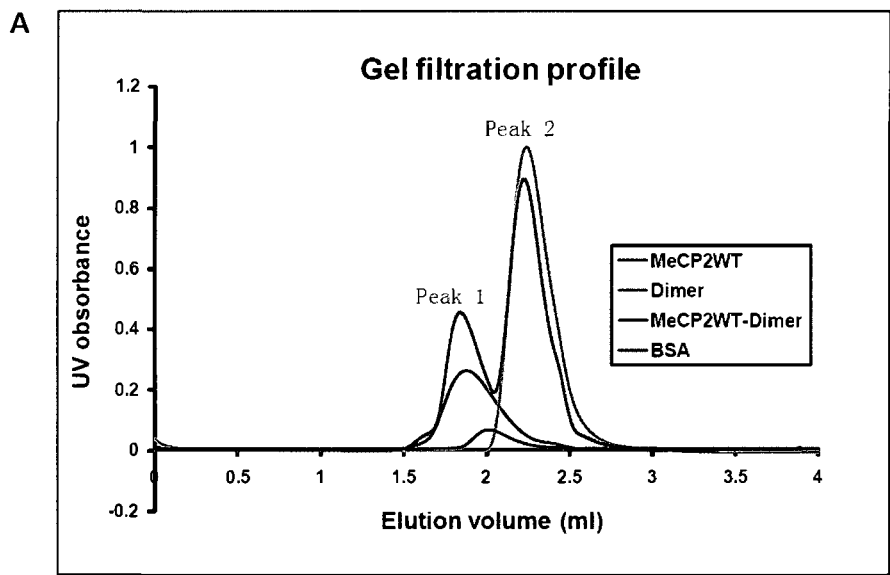
3.4.5 The interaction between MeCP2 and histones cannot be detected by gel filtration

Gel filtration, also referred to as size exclusion chromatography (SEC), is a chromatographic method in which particles are separated based on their size and

shape, or to be more specific, their hydrodynamic volume. Usually the larger molecules elute earlier from the gel filtration column than the smaller molecules of similar shape, due to lesser interaction with the column matrix. The elution volume of a molecule from size exclusion chromatography is determined both by its molar mass and its shape in solution. So SEC is often used to characterize the molar mass and shape of molecules. For example, SEC was used to show MeCP2 to be a very elongated molecule (Klose and Bird, 2004), since MeCP2 elutes from the column much earlier than those molecules with similar molecular weight.

Gel filtration can also be used to probe the interactions between proteins. If two proteins interact with each other, the complex usually elutes earlier or differently than the individual proteins due to the increase in size. The advantage of using gel filtration to detect interactions between proteins is that all the proteins are free in solution, and no tag is needed. The disadvantage of this method is that it cannot detect weak interactions due to the dilution effect of the column.

Gel filtration was used to probe for the interaction between untagged MeCP2 and histones. Initially the gel filtration was done under 100 mM salt, a less stringent condition. Purified MeCP2, without an intein tag, was applied to a Superose 6 3.2/30 gel filtration column, and the elution profile was recorded. Similarly, histone dimer and histone tetramer were applied to the same column. The elution profiles were recorded individually. Then MeCP2 and histone H2A/H2B dimer were mixed at 1:1 ratio and incubated at room temperature for one hour before being applied to the column, the elution profile was compared to the profiles of each component (figure 3.7A). Figure 3.7A shows that MeCP2, a 52.44 KD protein, eluted much earlier than Bovine Serum Albumin (BSA), a 67 KD protein. This is consistent with previous result observed (Klose



C: Molar mass determined by MALS

| sample | MW (measured by MALS) | MW(calculated) |
|-------------------------------|-----------------------|----------------|
| BSA | 69.83 KD(0.9%) | 67.0 KD |
| MeCP2WT | 56.00 KD(4%) | 52.44 KD |
| H2A/H2B Dimer | 26.31 KD(4%) | 27.234 KD |
| (H3/H4) ₂ Tetramer | 54.73 KD(10%) | 53.018 KD |

| Sample | MW(Peak 1) | MW (Peak 2) |
|------------------|---------------|---------------|
| MeCP2WT-Dimer | 52.64 KD (7%) | 24.10 KD (4%) |
| MeCP2WT-Tetramer | 91.52 KD(11%) | 80.33 KD(12%) |

Figure 3.7: Gel filtration and MALS did not detect the interaction between MeCP2 and histone dimer and tetramers in 100 mM NaCl. Panel A shows the gel filtration elution profiles of BSA, MeCP2WT, histone H2A/H2B dimers and MeCP2WT-dimer mixture. The elution peaks of the mixture co-localized with the peak of individual components, indicating no complex formation between the two components. Panel B shows the elution profiles of MeCP2WT, histone (H3/H4)₂ tetramers and the mixture of these two components. The similar results indicated that no interaction was detected between MeCP2WT and histone tetramers. Panel C showed the molar mass for each peak measured by MALS. The numbers in the parentheses are experimental errors. The molar mass of individual protein (e.g. BSA, MeCP2WT and Dimer alone) measured by MALS matched the calculated molar mass based on the amino acid sequences. Molar masses of the two peaks of MeCP2-dimer mixture were close to the molar mass of MeCP2WT and dimer respectively, indicating no complex formation between them. The molar mass of tetramer and MeCP2WT-tetramer mixture measured by MALS had a large error (10-11%), probably because the baselines of the elution profiles of tetramer and its mixture with MeCP2WT were not flat.

and Bird, 2004), demonstrating that MeCP2 is an elongated, random coil-like protein. The elution peak of MeCP2 is distinct from the elution peak of histone dimers (figure 3.7A). This will allow us to distinguish the elution peak for the complex, if there is any, from the peaks for individual proteins. However, when the MeCP2-histone dimer mixture was analyzed, two distinct peaks were observed in the elution profile. These two peaks co-localized exactly with the peaks of each individual component in the mixture, indicating that the two components (MeCP2 and histone dimers) ran separately in the column and did not interact under these conditions. The same results were obtained when MeCP2-histone (H3/H4)₂ tetramer was run through the column (figure 3.7B). No complex formation was observed in the MeCP2-histone (H3/H4)₂ tetramer mixture either.

The molar masses of the elution peaks of MeCP2WT, dimer and MeCP2WT-dimer mixture were measured by MALS followed the gel filtration (figure 3.7C). The molar mass of individual protein (e.g. BSA, MeCP2WT and H2A/H2B dimer alone) measured by MALS matched well with the calculated molar mass based on the amino acid sequences, showing the validity of the method (MALS) to measure the molar mass of proteins. Molar masses of the two peaks of MeCP2-dimer mixture were close to the molar mass of MeCP2WT and dimer respectively, indicating no complex formation between them which served as a confirmation of the gel filtration results. The molar mass of tetramer and MeCP2WT-tetramer mixture measured by MALS had a large error (10-11%), it is probably because the baselines of the elution profiles of tetramer and its mixture with MeCP2WT were not flat.

3.5 Discussion

Proteins are the chief executors of cellular functions. The interactions between different proteins play an important role in many biological functions. For example, signal

transduction from the exterior to the interior of the cell involves extensive protein-protein interactions. Studying protein-protein interactions is important to understand the complex cellular processes. Many methods, including co-immunoprecipitation, pull-down assays, yeast two-hybrid, Bimolecular Fluorescence Complementation, etc., can be used to study protein-protein interactions. Among those, co-immunoprecipitation and pull-down assays are the most widely used.

In this study, we have used the intein tag in the pull-down assay to test the interaction between MeCP2 and histones. The results showed that within the intein tag system, intein-MeCP2 fusion protein can pull down histone H2A/H2B dimers and (H3/H4)₂ tetramers under a rather stringent condition (i.e. 300 mM salt), but the fusion protein failed to pull down the individual histones including H2A, H2B, H3 or H4, suggesting that the interaction between intein-MeCP2 fusion protein and histones does require certain conformations of the histone. The intein tag alone demonstrated no interaction with any of the histones tested under the same conditions. As such, the results of this experiment were entirely consistent and indicated a direct interaction between MeCP2 and folded histone complexes.

However, in the absence of the intein tag, the interaction was not detected between free MeCP2 and histones even under less stringent condition (i.e. 100 mM salt), using a variety of assays including his-tagged reverse pull-down, Isothermal Titration Calorimetry (ITC) and gel filtration combined with MALS. The inconsistency of the results between intein-tag pull-down assays and other experiments suggests that the interaction indicated by the intein-MeCP2 fusion protein pull-down assay may be particular to an epitope for histone binding fortuitously formed between the intein tag and MeCP2. It is

also possible that the interaction between MeCP2 and histones is too weak to be detected by the in-solution assays without the intein-tag.

To further investigate whether the interaction between MeCP2 and histones detected by intein-tagged pull-down assays is an artificial interaction or not, two more important controls are needed. First, the interaction between intein-MeCP2 fusion protein and histones needs to be investigated with the same in-solution assays as an important control. Second, a different tag, e.g. a GST tag, can be used to fuse with MeCP2 in the pull-down assay.

3.6 Acknowledgement

We thank Teresa McLain for help with reagents and Wayne Lilyestrom, Andy Andrews and Uma M Muthurajan for the technical help and discussion which were critical to the progress of this project.

Chapter 4

Crystallographic studies of nucleosome-MeCP2 complex

4.1 Introduction

Methyl-CpG binding protein 2 (MeCP2) is a multifunctional protein. It has been assumed to be only a transcriptional repressor for a long time because of its methyl-DNA binding property (Nan et al., 1997) (Nan et al., 1998); recently, it has also been shown to be a transcriptional activator as well (Chahrour et al., 2008). Other functions of MeCP2, including regulating RNA splicing (Young et al., 2005) and the assembly of transcriptional pre-initiation complex (PIC) (Kaludov and Wolffe, 2000), were also found.

MeCP2 is also an abundant chromatin associated protein. The interaction between MeCP2 and chromatin has been shown *in vivo* and *in vitro* (Nan et al., 1996) (Georgel et al., 2003). Georgel *et al.* have shown that MeCP2 is capable of compacting biochemically defined nucleosomal arrays containing 12 nucleosomes into a higher order structure (Georgel et al., 2003). Horike *et al.* showed that MeCP2 was involved in the formation of a silent chromatin loop between genes (Horike et al., 2005). Taken together, another function of MeCP2 as a chromatin architectural protein has been proposed. It also provides another possible mechanism of MeCP2 in regulating chromatin structure and gene transcription.

The nucleosome is the basic building unit of chromatin. The investigations regarding the interactions between nucleosome and MeCP2 will provide us with insight on how MeCP2 interplays with chromatin and regulates chromatin structure. It has been shown previously that MeCP2 forms a stable complex with the nucleosome (Chandler et al., 1999) (Nikitina et al., 2007). Our results in chapter 2 and the published result that MeCP2 protects ~11bp extra nucleosomal DNA both suggested that the binding site of MeCP2 on nucleosomes is likely on or close to the DNA “entry-exit” site of nucleosomes (Nikitina et al., 2007), but where and how exactly MeCP2 interacts with nucleosome are still unclear, nor is it known which regions in addition to the MBD are involved in the interactions. Additionally, except the MBD region, we have no structural information on the entire MeCP2, a largely disordered protein.

A structure of MeCP2 in complex with the nucleosome core particle will provide essential structural information on MeCP2 that is unlikely to be obtained in any other way due to the intrinsic disorder property of the protein. It will also, for the first time, allow us to visualize the specific interaction between a nuclear protein and the nucleosome.

In this chapter, I will discuss my efforts to determine the crystal structure of a nucleosome-MeCP2 complex. Two different crystallization methods have been applied to obtain the nucleosome-MeCP2 complex crystals. Soaking MeCP2 fragment-I encompassing the MBD into the regular nucleosome crystals was tried first. However, no electron density was observed for MeCP2 in the calculated electron density map. Co-crystallization of the nucleosome-MeCP2

complex was tried next, using nucleosomes reconstituted with a 165 base-pair DNA fragment. Crystals of the complex were obtained and diffracted to 5.2 Å. Molecular replacement searches yielded a good solution with six nucleosomes in the asymmetric unit. The validation of the solution and refinement of the structure are still in progress at the time of this thesis writing.

4.2 Materials and methods

4.2.1 Nucleosome reconstitution

Recombinant *Xenopus laevis* core histones were over-expressed in bacteria and purified individually with previously published protocols (Dyer et al., 2004). Purified histones were refolded into histone octamer and purified by Superdex 200 size exclusion column as described before (Dyer et al., 2004). 147 base pairs of α -satellite DNA (in the case of MeCP2 soaking crystals) or 165 base pairs of strong nucleosome positioning sequence (the 601 DNA) (Lowary and Widom, 1998), (in the case of nucleosome-MeCP2 complex crystals) were prepared and used to reconstitute nucleosomes. Histone octamer and purified DNA (147 bp or 165 bp) at an approximately 1:0.8 ratio were mixed and reconstituted into nucleosome core particles (NCP) by salt gradient dialysis (Dyer et al., 2004). NCPs reconstituted with 147 bp α -satellite DNA were heated at 37 °C for one hour to shift all nucleosomes to a center position (Dyer et al., 2004). For NCPs reconstituted with 165 bp 601 DNA, there is no change in positions when heated at 37 °C. Samples were analyzed on a 5% native polyacrylamide gel.

4.2.2 MeCP2 expression and purification

Recombinant full length human MeCP2 isoform e2 and its fragments 74-172 and 78-305 were expressed and purified as described (Adams et al., 2007) with the IMPACT system (New England Biolab). The purified full length MeCP2 and the fragments were dialyzed into storage buffer (10 mM Tris, pH 7.5, 10% glycerol, 10 mM NaCl, 0.25 mM EDTA, 1 mM β -mercaptoethanol), and stored at 4 °C.

4.2.3 Expression and purification of Selenium labeled MeCP2

To prepare selenium labeled MeCP2, I modified previously used protocols to express and purify recombinant human MeCP2. I used the same strain BL21-CodonPlus(DE3)-RP (Stratagene) from *E. coli* as used in the normal MeCP2 expression grown media, together with the same plasmid construct. At first, cells were cultured in 5 ml Luria-Bertani (LB) broth media (1% tryptone, 0.5% yeast extract and 10% NaCl) for 6 hours and transferred to 100 ml media and grow overnight. 100 ml of overnight cell culture were spun down and resuspended in 8 ml of autoclaved and pre-warmed 37 °C M9 media (6.8g Na_2HPO_4 anhydrous, 3g KH_2PO_4 , 0.59g NaCl, 1g NH_4Cl , 0.4% (w/v) glucose, 2 ml of 1M MgSO_4 , 0.1 ml of 1M CaCl_2 , 0.1 ml of 0.5% (w/v) thiamine (vitamin B1) in 1 liter), and then added to each 1-liter of the same, pre-warmed M9 media containing 50 $\mu\text{g/ml}$ of ampicillin and 17 $\mu\text{g/ml}$ chloramphenicol. 20 ml of 19 amino acid mix (50 x concentrated) containing 2 mg/ml of each of the 19 amino acids, except methionine, prepared with autoclaved water were added per liter of M9 media right before use. The cells were cultured at 37 °C until OD600 reached 0.4~0.6.

Then the selenomethionine amino acid cocktail powder (100 mg each of threonine, lysine-HCl and phenylalanine, 50 mg each of leucine, isoleucine and valine, and 100 mg of L-seleno-methionine per liter) was added. The incubation temperature was decreased to 30 °C thereafter with the procedure similar to that of the unmodified MeCP2B fragment. After 30 minutes, cells were induced with 0.4 mM isopropyl β -D-thiogalactopyranoside (IPTG) for two hours. Then the cells were harvested and lysed. The purification of selenium labeled MeCP2 was the same as described for unmodified MeCP2 purification. The labeling of MeCP2 with selenium was confirmed by mass spectrometry.

4.2.4 Electrophoresis mobility shift assay (EMSA) for interactions between MeCP2 and nucleosome

147NCP or 165NCP (15 μ M) were incubated with increasing amounts of MeCP2 in binding buffer (10 mM Tris, pH 7.5, 1 mM EDTA, 1 mM DTT, 0, 100 or 300 mM NaCl) in 10 μ l reaction volumes at room temperature for 30 minutes. The products were electrophoresed on pre-run 5% polyacrylamide gel (mono/bis ratio of 35:1) in 0.2X TB (45 mM Tris, 45 mM borate pH 8.3) at 150 V for 75 minutes at 4°C. The ability of MeCP2 fragment 74-172 to bind nucleosomes in crystal soaking solution was also checked by gel shift assay in soaking solution (24% methyl-pentane-diol (MPD), 5% trehalose).

4.2.5 Crystallization of nucleosome

NCPs were purified by preparative gel electrophoresis (Dyer et al., 2004) and concentrated to about 12 mg/ml for crystallization. Vapor diffusion hanging and

sitting drop techniques were used to crystallize NCP reconstituted with 147 bp α -satellite DNA (from now on we call this NCP 147NCP). Crystallization conditions were adapted from published conditions (Luger et al., 1997). Diffraction-quality crystals were obtained in 160-180 mM $MnCl_2$, 148-160 mM KCl, and 20 mM K-cacodylate pH 6.0 at 19 °C. Crystals were harvested and soaked stepwise (3% increments, and 10 minutes per step) into cryo-protectant containing a 24% (w/v) methyl-pentane-diol (MPD) and 5% trehalose, as previously described (Luger et al., 1997).

4.2.6 Soaking MeCP2 MBD fragment into nucleosome crystals

147NCP crystals were prepared and soaked in 200 μ l cryo-protectant solution as described above. MeCP2 fragment 74-172 (encompassing the MBD domain) was purified and concentrated to \sim 715 μ M. 50 μ l MeCP2 fragment was mixed with 50 μ l cryo-protectant solution (24%(w/v) MPD and 5% trehalose) and added to the solution containing the nucleosome crystals. The final concentration for MeCP2 fragment in the soaking solution was \sim 119 μ M. MeCP2 was in the soaking solution for one to three days. Crystals soaked with MeCP2 fragment were then harvested and flash cooled without washing, exactly like other nucleosome crystals before data collection (Luger et al., 1997).

4.2.7 Co-crystallization of nucleosome-MeCP2 complex

Nucleosomes reconstituted with 165 base pair positioning sequence (601 DNA) (165NCP) were purified by preparative gel electrophoresis (BioRad) and concentrated to \sim 12-15 mg/ml (Dyer et al., 2004). MeCP2 B fragment (residues

78-305) was purified and concentrated to ~120 μ M. A 10 fold dilution was made to both concentrated 165NCP and MeCP2 B fragment for the titration. MeCP2 B was titrated into 165NCP (from 0.8:1 to 1.8:1) to check for the ratio of MeCP2 B to 165NCP when a single shifted nucleosome band was obtained. The ratio was then used to make a large scale complex for crystallization without further purification. The 165NCP-MeCP2 B complex crystals were grown by hanging and sitting-drop vapor diffusion at a concentration of ~9.4 mg/ml of the complex (~7.52 mg/ml of 165 NCP). The crystals grew within 2-4 weeks at 16 °C in 200~230 mM magnesium acetate, 100 mM MES hydrate, and 13-23% (w/v) methyl-pentane-diol (MPD). The sitting-drop technique yielded several crystals with dimensions of ~0.18 x 0.18 x 0.7 mm. The crystals were soaked in cryo-protectant stepwise (from 14% MPD to 23% MPD, 3% per step; then with addition of 5% glycerol to 20% glycerol, 5% a step; then 2% to 5% trehalose was added in addition to 23% MPD, 20% glycerol). Crystals were allowed to equilibrate for 10 minutes in each step; premade cryoprotectant soaking solution was added to the crystal-containing drop "in situ". This approach prevents the unnecessary manipulation of these fragile crystals. Then the crystals were harvested and flash cooled with nitrogen cryo-stream at -180 °C for data collection.

4.2.8 Heavy atom tetrakis(acetoxymethyl)-methane (TAMM) soaking procedure for nucleosome-MeCP2 complex

It has been shown earlier that *Xenopus laevis* histone H3 C110 residue, while inaccessible in solution in the context of a nucleosome, can be crosslinked by

TAMM by crystal soaking (Luger et al., 1997). TAMM soaking of nucleosome crystals leads to covalent modification of the H3 C110 residue (Luger et al., 1997), making TAMM a valuable reagent in labeling nucleosome crystals with mercury atoms. This approach was adapted in the labeling of nucleosome-MeCP2 crystals. After the last step of soaking the nucleosome-MeCP2 crystals in the cryo-protectant solution “in situ”, several TAMM granules were added directly into the cryo-protectant solution containing the crystals. The TAMM granules dissolved completely in the cryo-protectant solution (23% MPD, 100 mM Magnesium Acetate, 50 mM MES hydrate, 22.5% glycerol, 5% Trehalose) in about one day. Five days were allowed for TAMM to soak into the crystals before the crystals were harvested.

4.2.9 Data collection and structure refinement

X-ray diffraction data for MeCP2 MBD soaked nucleosome crystals were collected at our in-house rotating anode RU-H3R generator and R-Axis IV detector (Rigaku/MSB, Inc.) at a wavelength of 1.5418 Å.

X-ray diffraction data for nucleosome-MeCP2 complex crystals were obtained at the Advanced Light Source, beamline 4.2.2, Berkeley, USA with "NOIR-1" detector.

Data were indexed and scaled with D*TREK (Pflugrath, 1999). Molecular replacement was carried out to obtain crystal phases with AMoRe (Navaza, 1994) or Phaser (McCoy et al., 2007), using Protein Data Bank ID code 1KX5 as the search model. Refinements were done with Refmac 5 (Murshudov et al.,

1997) and model building with COOT (Emsley and Cowtan, 2004). Some of the figures were made by molecular graphics program PYMOL (Delano W.L., 2002, www.pymol.org).

4.3 Results and discussion

4.3.1 Nucleosome crystals soaking with MeCP2 fragment

4.3.1a MeCP2 fragment I (residue 74-172) is stable and active in the soaking solution buffer

Nucleosomes reconstituted with 147mer α -sat DNA and *Xenopus laevis* histones (147NCP) were crystallized using previously published protocols (Luger et al., 1997). Nucleosome crystals were then soaked stepwise into cryo-protectant solutions containing 24% MPD and 5% trehalose. A high concentration (715 μ M, \sim 7.7 mg/ml) of MeCP2 fragment-I was added to the soaking solutions containing nucleosome crystals. Theoretically MeCP2 fragment-I will diffuse homogenously in the soaking solution with a concentration of \sim 120 μ M (\sim 1.3 mg/ml) over time. The concentration of MeCP2 fragment-I in the solution is much higher than in the crystals, and over 60% of the crystal contents are solvent channels, it is possible that MeCP2 fragment-I can diffuse into the crystals through the solvent channels if it is small or adaptive enough to the solvent channels. If MeCP2 fragment-I still retains the ability to bind nucleosomes in the soaking solution, it can interact with nucleosomes and stay in the crystals. To check if MeCP2 fragment-I is still active in the soaking solution, electrophoresis mobility shift assay (EMSA) was used. Increasing amounts of MeCP2 fragment-I

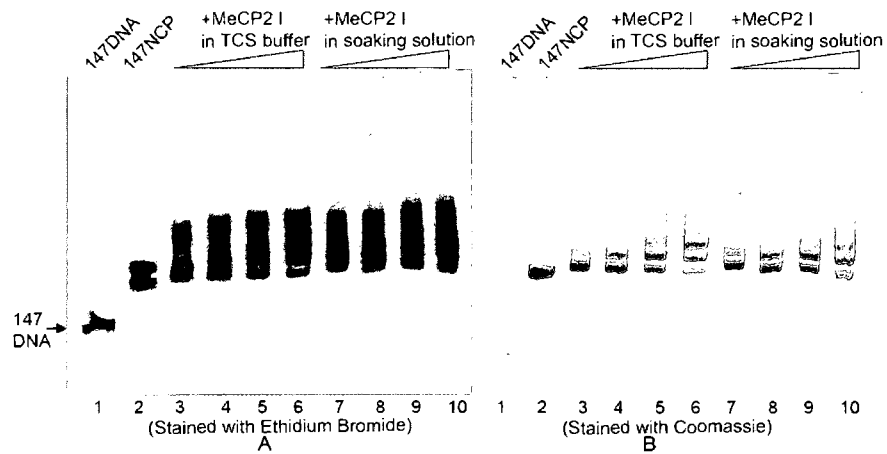


Figure 4.1: MeCP2 fragment-I is still active in soaking solution buffer as in TCS buffer. Increasing amounts (1:0.6, 1:1.0, 1:1.4 and 1:2.0 molar ratio of 147NCP to MeCP2 I) of MeCP2 I fragment were added into 147NCP in TCS buffer (lane 3-6) or in soaking solution (lane 7-10). Similar effects of mobility retardation on 147NCP in both conditions were observed.

were added to nucleosomes in either TCS buffer (10 mM Tris pH 7.5, 1 mM EDTA, 1 mM DTT) or soaking solution (24% MPD and 5% trehalose) and the complexes were resolved in a 5% native PAGE gel. The results are shown in figure 4.1. The mobility of nucleosomes was decreased after the addition of MeCP2, whether in TCS buffer or in soaking solution. This indicated that MeCP2 fragment-I is still as capable of binding nucleosomes in soaking solution as in TCS buffer, so this made it possible that the MeCP2 fragment-I can interact with nucleosomes in the crystal lattice.

4.3.1b Soaking MeCP2 fragment-I into the nucleosome crystals caused minor cracks in the crystals

After 147NCP crystals soaked in soaking solutions containing 24% MPD and 5% trehalose, MeCP2 fragment-I in MeCP2 storage buffer (10 mM Tris, pH 7.5, 10% glycerol, 10 mM NaCl, 0.25 mM EDTA, 1 mM β -mercaptoethanol) was added into the soaking solution containing 147NCP crystals. Some minor but visible cracks formed shortly after MeCP2 fragment-I was added and remained unchanged during the MeCP2 fragment-I soaking process (figure 4.2 A). This crack formation after the addition of MeCP2 fragment-I may have occurred for two different reasons: first, because MeCP2 storage buffer does not contain MPD. When the buffer was added with the addition of MeCP2 fragment-I and contacted with the surface of the crystals, the crystals cracked due to dramatic local environmental changes. The second, more likely explanation is that when MeCP2 fragment-I diffused in to the crystals, it caused some rearrangement of nucleosomes in the crystals so that the crystal lattice changed.

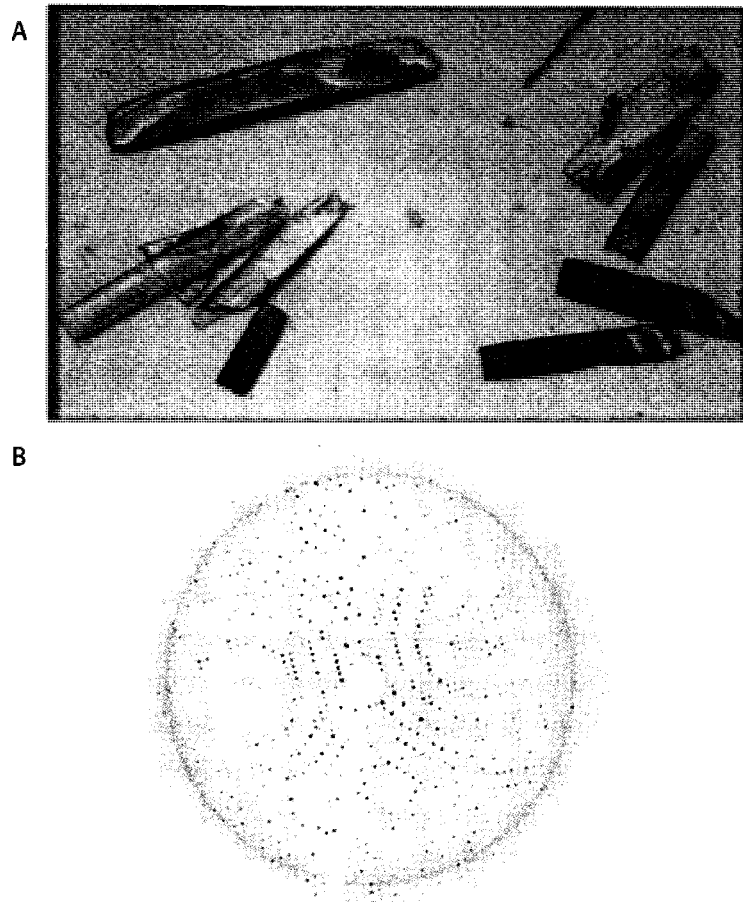


Figure 4.2: Crystals of 147NCP soaked with MeCP2 fragment-I (A) and one of the diffraction pattern images (B). Some minimum cracks developed in the 147NCP crystals after soaking in MeCP2 fragment-I (A).

4.3.1c No electron densities were found for MeCP2

Crystals of 147NCP soaked with MeCP2 fragment-I were harvested and flashed cooled by liquid propane at -125°C followed by nitrogen gas stream at -180°C. Data were collected at a home source X-ray generator with a wavelength of 1.5418 Å. Crystals diffracted to 2.4 Å. A representative diffraction pattern is shown in figure 4.2 B. Data were processed and scaled with D*TREK. Molecular replacement searches in AMoRe (Navaza, 1994) with PDB entry 1KX5 as the search model led to one outstanding solution as expected. The structure model was refined with Refmac 5 and CNS respectively. The statistics from both refinement methods were similar. The data collection and refinement (with Refmac 5) statistics are reported in table 4.1. Model building and visualization was done in COOT. The calculated electron density map matched well with DNA and histones in the model as expected (figure 4.3 A and B). However, no extra density was observed for MeCP2 fragment-I, a peptide of 98 residues. These results suggested that MeCP2 fragment-I did not stably or specifically interact with the 147NCP crystals successfully. It could be that the peptide is too big to get into the crystals through the solvent channels, although MeCP2 fragment-I is mostly disordered. To get the atomic detailed information about the interaction between nucleosome and MeCP2, other methods such as the co-crystallization of the nucleosome-MeCP2 complex are necessary.

Table 4.1: Data collection and refinement statistics of 147NCP crystals soaked with MeCP2 fragment-I

| Data set | 147NCP soaked with MeCP2 fragment-I | | |
|------------------------------|---|---------|--------|
| Data Collection | | | |
| Space group | P2 ₁ 2 ₁ 2 ₁ | | |
| Unit cell dimensions | 106.46 | 109.57 | 181.75 |
| | 90.00 | 90.00 | 90.00 |
| Mosaicity | 1.32 | | |
| Resolution range | 69.12-2.4 (2.49-2.40) | | |
| Total number of reflections | 237536 | | |
| Number of unique reflections | 79932 | | |
| Average redundancy | 2.97 | (2.76) | |
| % completeness | 95.4 | (96.4) | |
| Rmerge | 0.073 | (0.419) | |
| Reduced ChiSquared | 1.01 | (1.19) | |
| Output </sigl> | 8.6 | (2.3) | |
| Refinement Statistics | | | |
| Reflections in test set | 4002 | | |
| Rcryst | 0.256 | | |
| Rfree | 0.284 | | |
| Overall average B-factor | 60.373 | | |

Note: Values in () are for the last resolution shell.

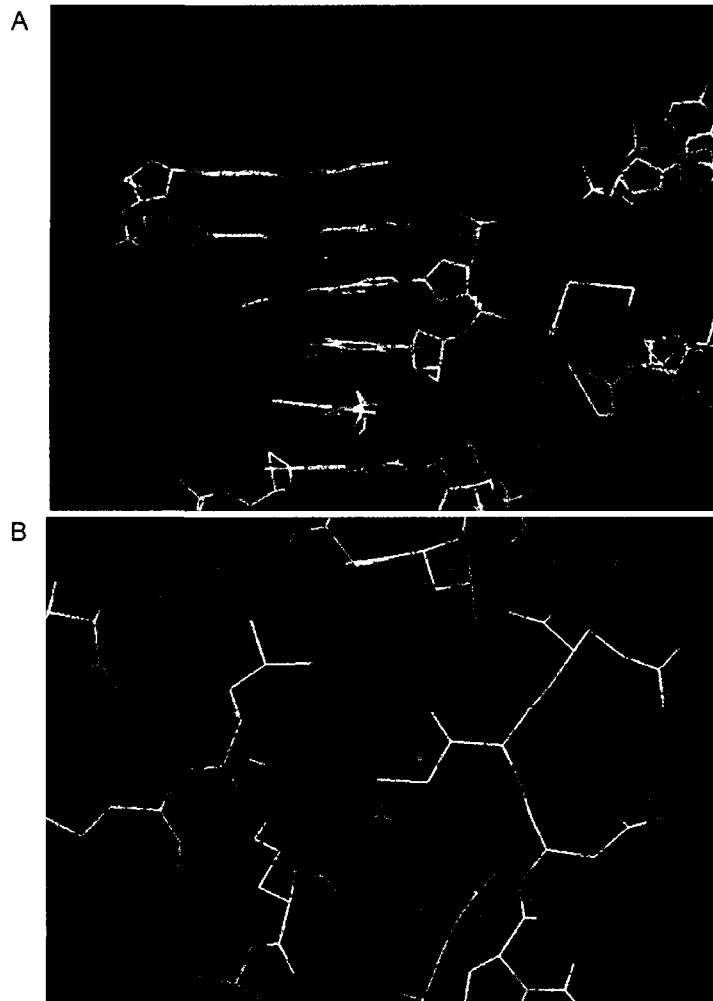


Figure 4.3: Electron density map of 147NCP soaked with MeCP2 fragment-I. The calculated electron density map matched well with DNA (A) and histones (B) in the model as expected.

4.3.2 Co-crystallization of nucleosome-MeCP2 complex

4.3.2a Optimizing the crystals of the nucleosome-MeCP2 complex

Initially, nucleosomes reconstituted with 147 base pair of palindromic α -sat DNA and *Xenopus laevis* histones (147NCP) (Luger et al., 1997) were used in the co-crystallization trials with MeCP2 B fragment (residue 78-305). This fragment encompasses the MBD domain and TRD domain. In the initial screening for crystallization conditions, crystallization suites (PEG II Suite, Nucleix Suite, MPD Suite, Protein Complex Suite) from Qiagen were used. Hits were obtained from MPD Suite with condition of 0.2 M Magnesium Acetate, 0.1 M MES sodium salt pH 6.5, 15% (w/v) MPD. Some other conditions also gave hits, but the crystals were not as good as in this condition. Further 2-D screens were set up around the best hit condition (0.2 M Magnesium Acetate, 0.1 M MES sodium salt pH 6.5, 15% (w/v) MPD) by varying Magnesium Acetate and MPD concentrations, while keeping MES concentrations the same. Bigger crystals were grown at 0.21-0.23 M Magnesium Acetate, 0.1 M MES and 15%-20% MPD. The dimension of the biggest crystals was about 400x72x50 μm . Other precipitants (15%-40% PEG 400, 25%-35% isopropanol) were also tested in replacement of MPD, but no crystals were obtained in any of these conditions.

The best crystal of the 147NCP-MeCP2 complex diffracted to 5 Å with a space group of P222 (table 4.2), but no solutions were obtained when molecular replacement was used to get the phase information for the crystal structure.

Table 4.2: Data collection statistics for the 147NCP-MeCP2 B crystal

| Spacegroup | P222 | | |
|-------------------------------------|--------------|---------------|--------|
| Unit cell dimensions | 109.25 | 108.22 | 189.88 |
| | 90.00 | 90.00 | 90.00 |
| Resolution range | 54.77 - 5.00 | (5.18 - 5.00) | |
| Total number of reflections | 66,658 | | |
| Number of unique reflections | 10,150 | | |
| Average redundancy | 6.57 | (7.04) | |
| % completeness | 99.2 | (100.0) | |
| Rmerge | 0.125 | (0.798) | |
| Reduced ChiSquared | 1.00 | (0.92) | |
| Output $\langle I/\sigma I \rangle$ | 4.6 | (1.3) | |

Note: Values in () are for the last resolution shell.

Therefore, the crystal structure of 147NCP-MeCP2 B complex was not pursued further.

As seen in chapter 2, we have shown that the nucleosome with extra nucleosomal DNA has higher affinity for MeCP2 and that extra nucleosomal DNA is important in organizing the nucleosome-MeCP2 complex to a more compact complex. Therefore, nucleosomes reconstituted with 165 base pair '601' DNA fragment (Lowary and Widom, 1998) and recombinant *Xenopus laevis* histones (165NCP) were also used to crystallize with MeCP2 B fragment. Similar 2-D screening conditions as in the 147NCP-MeCP2 B crystals were used to crystallize the 165NCP-MeCP2 B complex. Crystals of 165NCP-MeCP2 B complex were grown bigger in those conditions (0.21-0.23 M Magnesium Acetate, 0.1 M MES and 15%-20% MPD) (figure 4.4A &B). The morphologies of the crystals were different from that of regular 147NCP. No crystals were obtained in the same condition with 165NCP alone (without MeCP2). The biggest crystals were about 0.7x0.15x0.2 mm. 5.2 Å resolution data was the best data obtained from the 165NCP-MeCP2 B complex.

4.3.2b Optimizing the conditions and methods to cryo-protect the nucleosome-MeCP2 complex

The crystals of 165NCP-MeCP2 B complex were grown in 0.21-0.23 M Magnesium Acetate, 0.1 M MES and 15%-20% MPD. The concentration of MPD is not high enough to protect the crystals from cracking due to ice formation during flash freezing. So transferring the crystals into solutions with higher

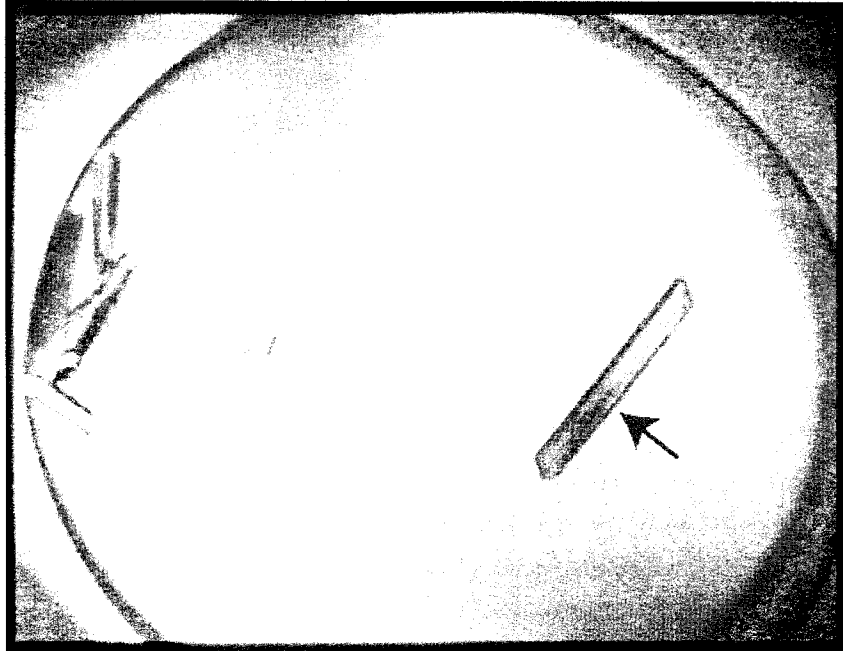
concentrations of cryo-protectant is necessary. First, crystals were harvested and transferred to a depression dish containing the reservoir solutions (e.g. 0.21-0.23 M Magnesium Acetate, 0.1 M MES and 15%-20% MPD). However, the crystals melted quickly in the reservoir solution. Next, mother liquor was used in the depression well to store crystals. Big crystals formed cracks immediately when transferred into the depression well with mother liquor (figure 4.4C).

Two reasons could be responsible for the cracking: the mother liquor condition is not right or crystals do not like the transfer. To test the second hypothesis, 20 μ l of mother liquor were added directly into the crystal well without transferring the crystals. Only minimum cracks formed and healed thereafter in those crystals. Considering the fact that there was a high surface tension when crystals were fished out from the mother liquor, we think it was the transferring process that damaged the crystals. So the cryo-protectant soaking processes were performed "in situ" in the crystal wells where crystals were grown. Mother liquor with increasing concentration of precipitant (MPD, glycerol and trehalose) was exchanged into the well containing crystals in steps, with 3% MPD or 5% glycerol increments in a step. The final soaking solution contains 23% MPD, 20% glycerol, 5% trehalose, 0.1 M Magnesium Acetate, 0.05 M MES.

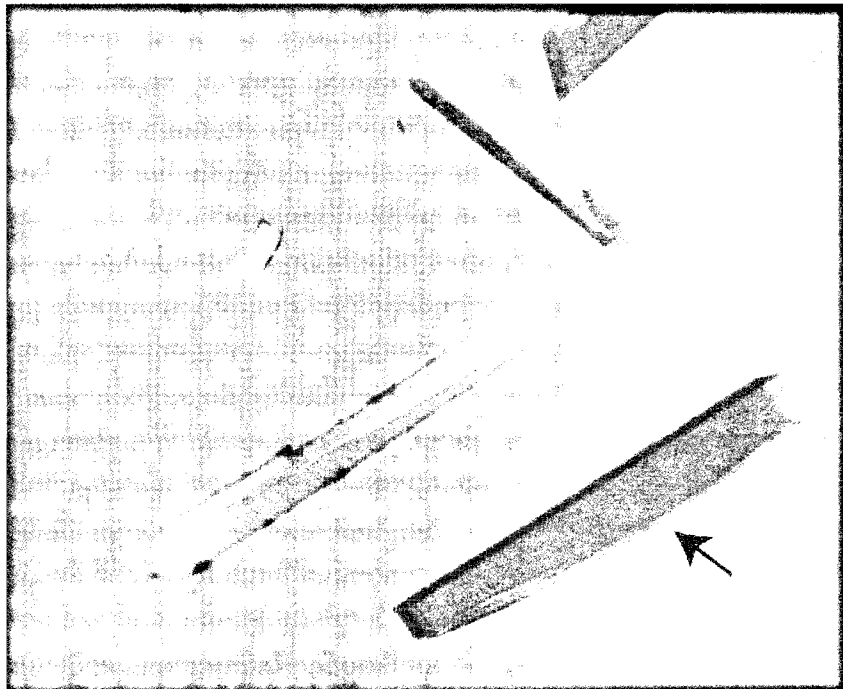
4.3.2c Optimizing flash cooling method of the nucleosome-MeCP2 crystals.

Three different flash cooling methods have been tried to freeze crystals after soaking in cryo-protectant: liquid propane, liquid nitrogen and nitrogen gas

A



B



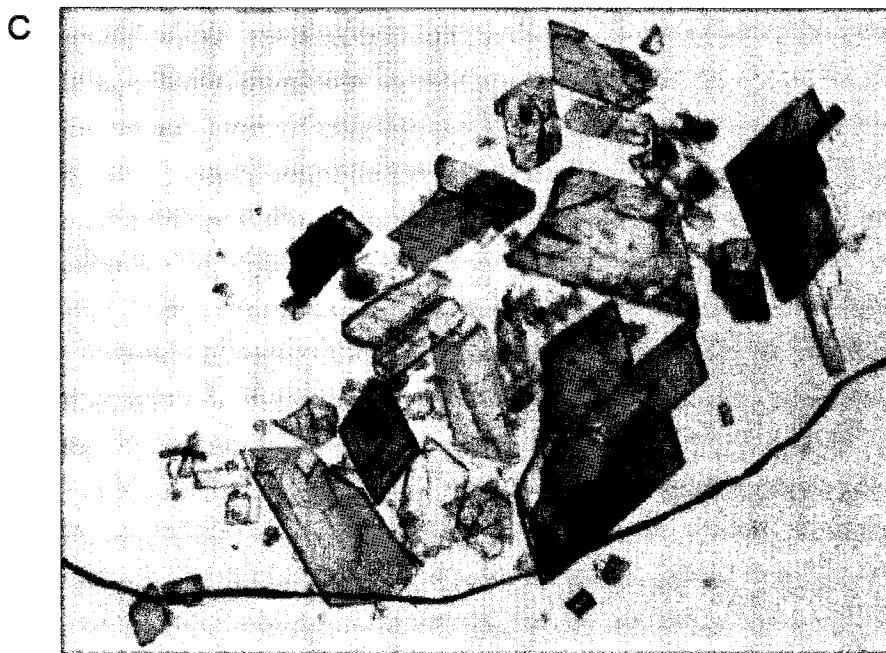


Figure 4.4: Crystals of 165NCP-MeCP2 B complex. Crystals before harvesting (A) and after harvesting (B and C) are shown. Arrows in panel A and panel B indicate the same crystal before and after transferring into a harvest dish containing mother liquor. Rectangular shaped and medium sized crystals formed minimum cracks after transfer, but healed fast afterwards (B). But irregular shaped big crystals formed visible cracks and did not heal (C).

stream. It has been shown that the flash cooling temperature could have a dramatic effect on nucleosome crystals (Edayathumangalam and Luger, 2005). Since the crystals of nucleosome-MeCP2 complex contains nucleosomes, the flash cooling method for regular nucleosome crystals (Luger et al., 1997) was tried first.

Crystals were flash cooled in liquid propane at -125~-150 °C, followed by cooling with liquid nitrogen or nitrogen gas stream at -180 °C. Crystals were also flash frozen by directly plunging them into liquid nitrogen or directly cooled with nitrogen gas stream at -180 °C, but no definite conclusion could be drawn as to which cooling method was better. No obvious ice formation was observed in any of the three flash cooling methods. The diffraction quality varies greatly between crystals. In general, the bigger and thicker the crystal, the better the diffraction is. Among the crystals of similar sizes, no significant difference was observed between the three different methods. Considering the complex manipulations of the propane method, and that the liquid nitrogen method usually caused ice formation at the metal stem of the mounting loop, direct flash cooling with nitrogen gas stream was used mostly. Only two crystals diffracted to 5.2 Å, the highest resolution of 165NCP-MeCP2 complex crystals obtained so far. Both of them were flashed cooled directly with a nitrogen gas stream at -180 °C.

4.3.2d MeCP2 can be washed away from nucleosomes in the crystals

It has been shown that MeCP2 stably associates with mono-nucleosomes in solution (see chapter 2). However, the interaction between MeCP2 and

nucleosomes may be different in the crystal context, and we therefore wanted to verify the presence of MeCP2 in the nucleosome crystals.

Since crystals of nucleosome-MeCP2 complex grew in low cryo-protectant condition (15%-20% MPD), soaking the crystals in solutions containing a higher percentage of cryo-protectant is necessary to protect the crystals from damage caused by ice formation during the flash cooling process. The soaking process is a 10-step process, 20 minutes in each step. So the whole process usually takes about 5-6 hours, including the manipulation time. Crystals were usually left in the last soaking solution overnight before harvesting. Crystal content was checked in different soaking stages: before soaking, right after the penultimate soaking step, after overnight soaking in the last soaking solution. Several crystals from each stage were combined and dissolved in 20 μ l SDS loading buffer and boiled at 95°C for 10 minutes before loading onto an 18% SDS-PAGE gel. The results are shown in figure 4.5. Before soaking, there was a significant amount of MeCP2 B present in the crystals. After ~6 hours soaking, MeCP2B was still present in the crystals (figure 4.5A); however after overnight soaking, MeCP2 B was almost gone from the crystals (figure 4.5B). Since there was no MeCP2 B present in the soaking solutions, and MeCP2 by itself is an intrinsically disordered protein, during the soaking steps the equilibrium: $\text{MeCP2+Nucleosomes} \rightarrow \text{Nucleosome-MeCP2}$ complex shifts toward the left side, the dissociation reaction. Therefore MeCP2 can be dissociated from the crystals and washed away during the soaking procedures, and we conclude that MeCP2 is dynamically associated with

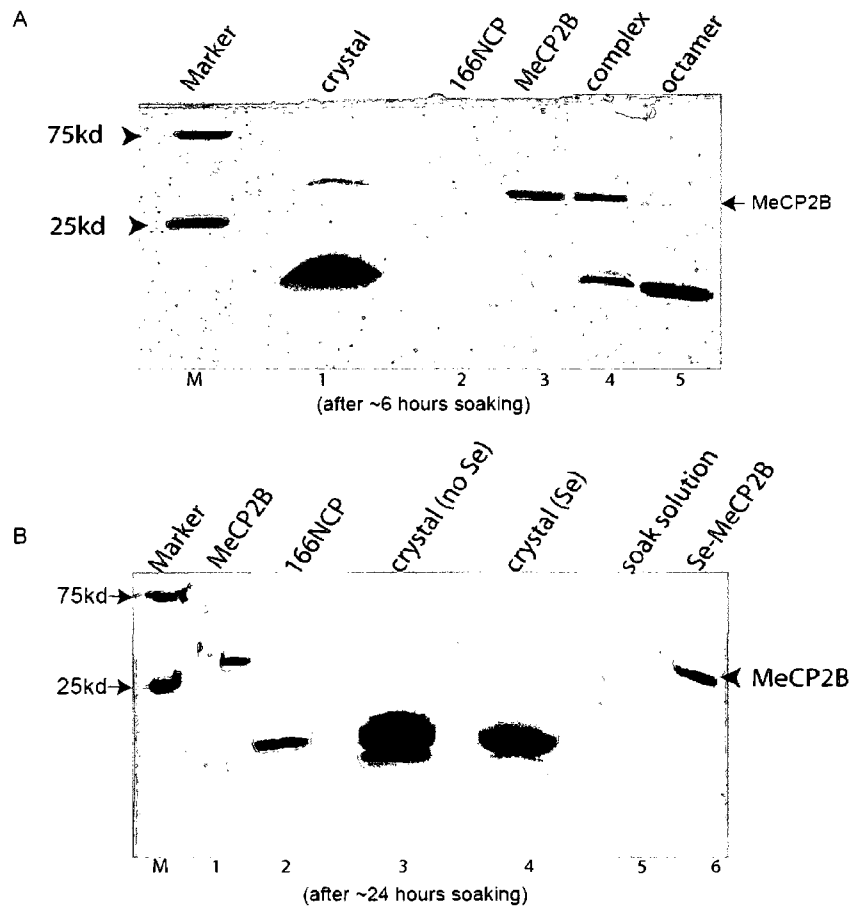


Figure 4.5: Contents check of the 165NCP-MeCP2 B crystals. MeCP2 B was present in the crystals after ~6 hours in the soaking solution (lane 1 in panel A), but was almost gone from the crystals after ~24 hours soaking (lane 3 and 4 in panel B). Crystal (Se) represented the Seleno-methionine labeled MeCP2B-165NCP crystals.

nucleosomes in the crystals and can dissociate from nucleosomes in the low MeCP2-containing solution.

4.3.2e Structure determination and electron density map calculation

To date, almost all nucleosome crystal structures were obtained with either 146 or 147 bp DNA fragments. The morphologies of the crystals obtained from 165NCP-MeCP2 B are different from that of regular nucleosome crystals (figure 4.4A and B). More than a hundred of the crystals were screened. Most crystals diffracted to ~8-17 Å. Only few crystals diffracted to 5.2 Å. Data were collected at ALS beamline 4.2.2 and indexed with D*TREK. The data collection statistics is reported in table 4.2. The crystal of 165NCP-MeCP2 B complex belongs to a monoclinic space group ($P2_1$) with unit cell dimension of $a=108.94$ Å, $b=326.86$ Å, $c=198.47$ Å, $\beta=93.04^\circ$. This is different from canonical nucleosome crystals containing 146/147 base pairs of DNA and histone octamers ($P2_12_12_1$). The loss of symmetry is accompanied by an increase of one of the cell axes and the increase in cell volume as a result (see table 4.3). Molecular replacement searches were used to get phase information of the crystal structure. PDB entry 1KX5 (a 147 bp nucleosome) was used as search model. The searches failed in CNS, Molrep and 'Beast'. However, searches in Phaser program led to one good solution with six nucleosomes in the asymmetric unit (ASU) (figure 4.6). The search for a seventh nucleosome in the ASU did not succeed, indicating that there are six nucleosomes in the ASU. The Matthews Coefficient and solvent content calculation also suggested six nucleosomes in the ASU.

Table 4.3: Data collection statistics of 165NCP-MeCP2B complex crystals

| Space group | P2₁ | | |
|-----------------------------|-----------------------|-------------|--------|
| Unit cell dimension | 108.94 | 326.86 | 198.47 |
| | 90.00 | 93.04 | 90.00 |
| Mosaicity | 1.07 | | |
| Resolution range | 43.73-5.20 | (5.39-5.20) | |
| Total number of reflections | 160,591 | | |
| Number of unique reflection | 50,681 | | |
| Average redundancy | 3.17 | (3.04) | |
| % completeness | 95.5 | (94.2) | |
| Rmerge | 0.051 | (0.449) | |
| Reduced ChiSquared | 0.94 | (1.15) | |
| Output<l/sigI> | 9.0 | (1.8) | |

Note: Values in () are for the last resolution shell

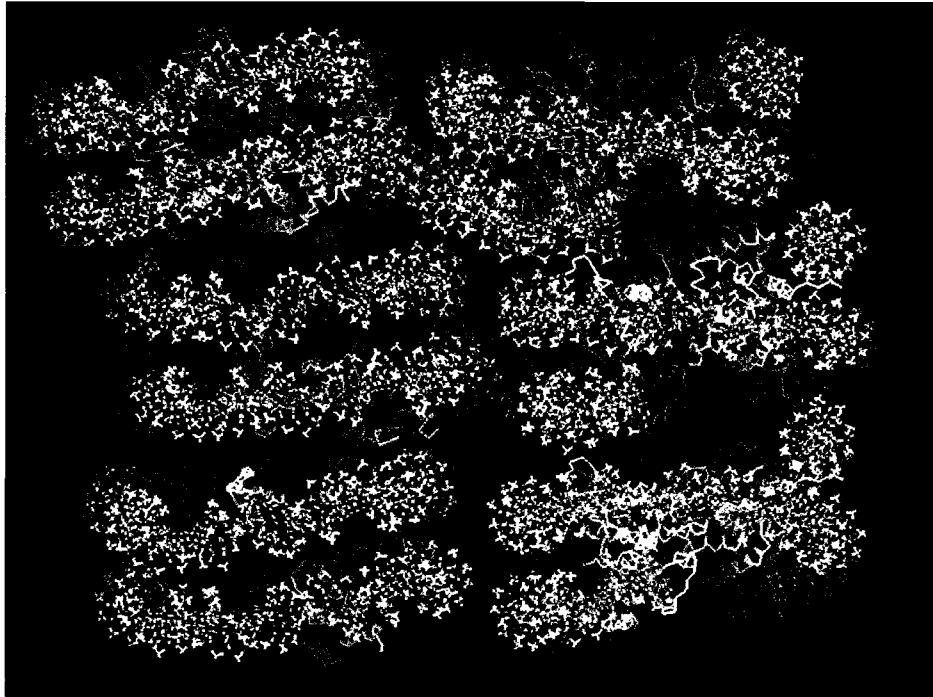


Figure 4.6: The crystals of 165NCP-MeCP2 B complex have six nucleosomes in one asymmetric unit (ASU). Within the ASU, three nucleosomes stack on top of each other facing the same direction, and are related by “pseudo” two-fold symmetry to the other three nucleosomes in the same ASU.

The six nucleosomes in the ASU are not identical to each other. In the ASU, three nucleosomes stack on top of each other and are related by “pseudo” two-fold symmetry to the other three nucleosomes in the other stack. In the initial electron density map generated after molecular replacement, most protein and DNA backbones of the model fit reasonably well into the map, as assessed by visual inspection of the fit of the model into the map. As noted before, there are only 147 base pairs (bp) of DNA in the search model, while in the crystals, there are 165 base pairs of DNA (~9-10 base pairs more extended from either side of the 147 bp DNA). Intriguingly, the initial electron density map generated after molecular replacement showed extra densities with helical shape extending from the two ends of the 147 bp DNA of some nucleosomes in the asymmetric unit (figure 4.7A), indicating the existence of the extra ~9-10 base pair of DNA from each ends of 147 bp DNA. The extra density from the DNA end of one nucleosome appears to be “shaking hands” with the other extra density from DNA end from the next nucleosome (figure 4.7B). From one aspect this validates the initial electron density map. Crystal packing in regular nucleosome crystals involves DNA-DNA stacking and protein-protein interactions. In the 165NCP-MeCP2B crystals, nucleosome packing probably also involves DNA-DNA stacking, since nucleosomes were facing each other with nucleosome generated from unit cell symmetry (figure 4.8). These DNA stacking interactions can be examined after the extra DNA is built into the model and refined.

Molecular replacement with Phaser also generated three other solutions. The only difference between these four solutions is the orientation of the six

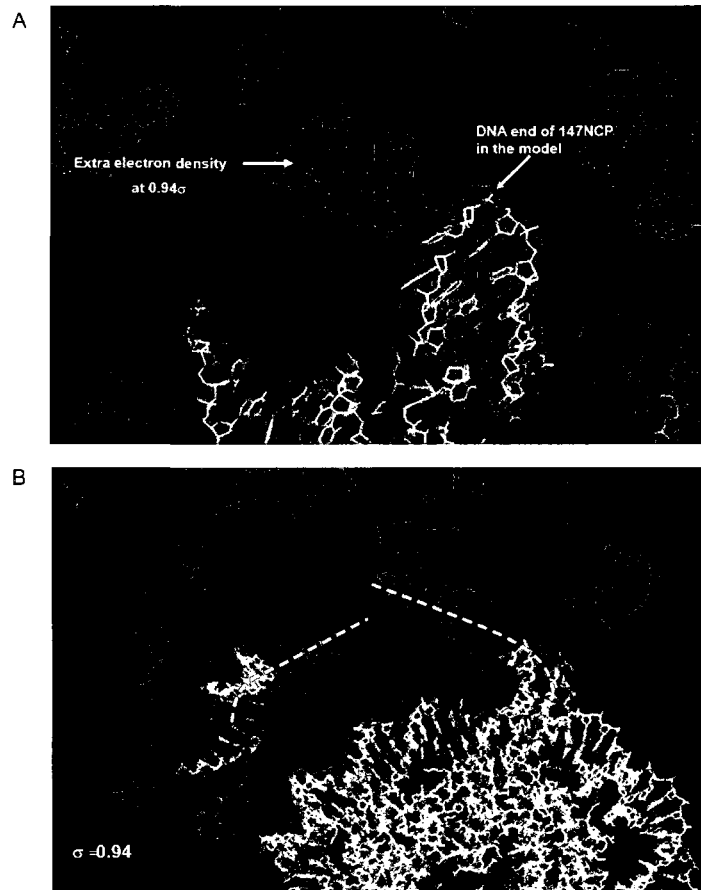


Figure 4.7: Initial electron density map of 165NCP-MeCP2 B complex crystal shown at contour level 0.94. Panel A showed the extra electron density extended from the DNA ends of 147NCP in the model. The extra density also showed the continuous helical feature as the density that covers the DNA in the model. Panel B showed that the extra electron density from one DNA end was approaching the other extra density from one DNA end of the neighboring NCP. The white dotted lines indicate the trace of the extra electron density.

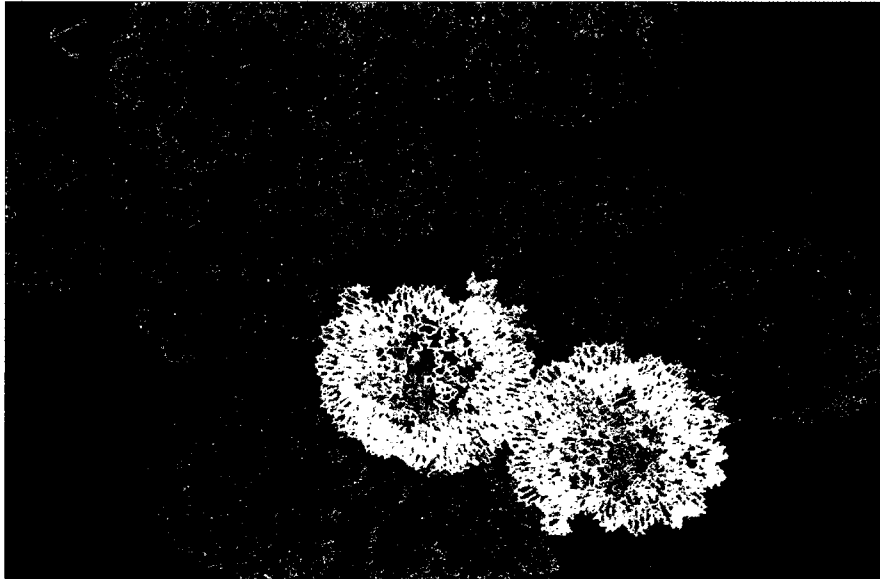


Figure 4.8: Unit Cell symmetry and crystal packing of 165NCP-MeCP2 B crystals. Nucleosomes are packed “face-to-face” or “back-to-back”.

nucleosomes in the ASU: the three nucleosomes in one stack facing the same direction or different directions. The validation of the four solutions is still in process.

Refinement of low resolution crystal structures remains a nearly insurmountable challenge. Refinement of the structure with Refmac was initiated. Density modification and NCS average refinement in Refmac 5.5 did not improve the initial electron density map. More efforts are needed to refine the structure correctly.

Experimental phasing attempts with heavy atom were also made to the 165NCP-MeCP2B structure. Selenomethionine labeled MeCP2B was tried first. The rationale here was that the selenium atoms should be apparent in anomalous difference fourier maps, revealing at least the location of MeCP2 with respect to the nucleosome. There are three methionine residues in the MeCP2 B fragment (figure 4.9A). Substituting methionine residues with supplemented selenomethionine during protein expression results in the selenomethionine labeled MeCP2 B. Purified selenomethionine labeled MeCP2 B was subjected to mass spectrometry. The presence of three selenomethionines was confirmed (figure 4.9B), and labeling procedures did not affect the ability of the protein to interact with nucleosomes. However, although the selenomethionine labeled MeCP2 B was crystallized in complex with 165NCP as normal MeCP2B, due to the soaking processes, the selenomethionine labeled MeCP2 B was “washed” away too as shown in figure 4.5B (lane 5). No selenium absorption peak was observed in the X-ray fluorescence scan.

A

```

ASASPKQRRSIIDRGPMYDDPTLPEGWIRKLEQRKSGRSAGKYDVYLINPQCE
AFRSKVELIAYFEKVGDTSLDPNDFEDFVTGRGSPSRREQKPPKPKSPKAPGTG
RGRGRPKGSGTTRPKAATSEGVQKRVLEKSPGKLLVKMPFQTSPGGKAEGGG
ATTSTQVMVIKRPGRKRKAEADPQAIPKKRGRKPGSVVAAAAAEAKKAVKES
SIRSVQETVLPIKKRKRE

```

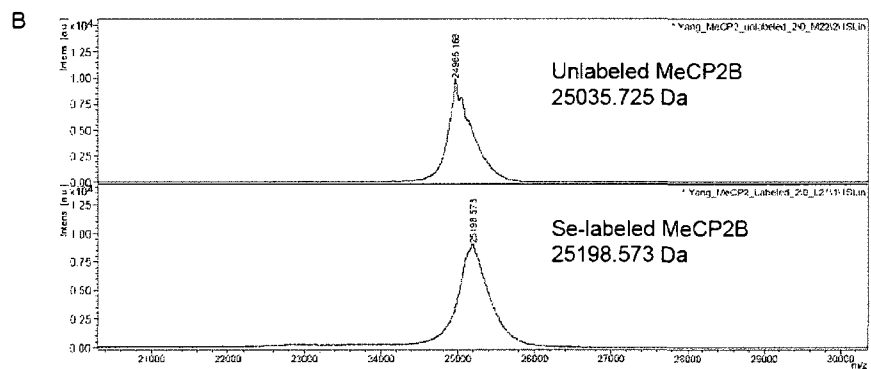


Figure 4.9: MeCP2B was seleno-methionine labeled. Panel A showed the amino acid sequence of MeCP2B. Three Methionine residues are shown in red. Blue and yellow highlights represented the MBD and TRD domain respectively. Panel B showed the mass spectrometry result of Se labeled MeCP2B.

TAMM has been successfully soaked into nucleosome crystals for experimental phasing before (Luger et al., 1997), making TAMM a valuable reagent in labeling nucleosome crystals with mercury atoms. This TAMM soaking method was adapted in the labeling of nucleosome-MeCP2 crystals. TAMM granules were added directly to the soaking solution containing crystals. Usually TAMM granules are hardly dissolved in solutions, but they dissolved completely in the soaking solutions (23% MPD, 100 mM Magnesium Acetate, 50 mM MES hydrate, 22.5% glycerol, 5% Trehalose) in about one day. However, most of the crystals cracked soon after the addition of TAMM granules. This is probably caused by the high concentration of TAMM dissolved in the soaking solution. Two crystals with only a few cracks were harvested and sent to ALS for data collection, but those two crystals did not diffract well. More efforts are needed to find the optimal conditions for the soaking of TAMM to crystals without crack formation, for example, add less TAMM granules or make a TAMM solution and try different TAMM concentrations added to the soaking solution. Other heavy metals can be tried for experimental soaking.

4.4 Discussion

We have shown in this chapter that it is feasible to crystallize the nucleosome-MeCP2 complex. 165NCP in complex with MeCP2B was crystallized and the crystals diffracted to 5.2 Å. Molecular replacement searches in Phaser program led to one good solution with six nucleosomes present in the asymmetric unit. Crystal content check on SDS-PAGE gel showed the presence of MeCP2 in the crystal initially; however, no significant amount of MeCP2 was detected in the

crystal after the cryo-protectant soaking procedures (figure 4.5). Also, the selenomethionine-labeled-MeCP2-containing crystals did not show a selenium absorption peak, indicating that no MeCP2 is present in the crystals. Although MeCP2 was not present in the crystal structure, without MeCP2 165NCP cannot be crystallized under the same condition. So MeCP2 may have an important role in organizing 165NCP in the crystal context.

Thus, in the future, efforts should be made to improve the quality of the complex crystals and prevent the dissociation of MeCP2 from the crystals. The following methods can be tried:

a: 165NCP-MeCP2WT complex was crystallized under the same condition as the 165NCP-MeCP2B complex. But the crystals were very small. However, it is still worthwhile to optimize the crystallization conditions to see if the 165NCP-MeCP2WT complex can be grown bigger and better.

Different MeCP2 fragments can be tried to co-crystallize with 165NCP. It has been shown in chapter 2 that although the 165NCP-MeCP2B complex is more compact than the 147NCP-MeCP2B complex (figure 2.2 and 2.6, table 2.2 and 2.3), the 165NCP-MeCP2B complex still showed some extent of flexibility as indicated by the increased frictional coefficient in the complex when compared to 165NCP itself. So different MeCP2 fragments can be tried to optimize the nucleosome-MeCP2 complex. The C-terminal portion of MeCP2 (residue 206-486) has been indicated to be involved in chromatin compaction (unpublished

data from Hansen lab), so this fragment would be a good candidate to co-crystallize with 165NCP.

b: It has been known that MeCP2 has a higher affinity for methylated DNA. To increase the affinity of MeCP2 for NCP in the crystal context, methylated DNA could be used to reconstitute nucleosomes and crystallize with MeCP2.

c: During the cryo-protectant soaking procedures, MeCP2 dissociated from the crystal context. It is possible that the interaction between MeCP2 and nucleosomes in the crystal is relatively weak and the interaction reaction favors the dissociation side in the soaking solution which has no MeCP2 in it. To prevent this, MeCP2 should be added into the soaking solution in each step to push the reaction towards the association side. Alternately, we can try to crosslink MeCP2 and nucleosomes after the crystals are formed, so that the association state is “frozen” in the crystal.

d: Four-way DNA junction can be used as a “pseudo” nucleosome in the crystallization trials with MeCP2. It has been shown that MeCP2 also binds to unmethylated four-way DNA junctions with a similar affinity to methylated DNA (Galvao and Thomas, 2005), and data in chapter 2 suggested that MeCP2 likely binds to nucleosomes at the DNA “entry-exit” region. So the four-way DNA junction mimics the structure of nucleosomes at the DNA “entry-exit” region where MeCP2 is likely bound. In addition, the four-way DNA junction may be easier to manipulate than nucleosomes, so the four-way DNA junction in complex with MeCP2 would be a good crystallization candidate. The structure of the four-

way DNA junction-MeCP2 complex will shed light on the mechanisms of how MeCP2 interacts with nucleosomes.

We believe that a high resolution structure of MeCP2-nucleosome complex will not only decipher the structure of MeCP2 which has been long delayed, it will also shed light on the functions of MeCP2, how it interacts with nucleosomes in the chromatin context, how it regulates the chromatin structure, and why its mutations cause Rett syndrome.

4.5 Acknowledgement

We thank Jay Nix at the ALS for the help with data collection and Pamela Dyer and Teresa McLain for help with reagents. The technical input, discussion and help offered by Mark van der Woerd and Uma M Muthurajan were critical to the progress of this project.

CHAPTER 5

SUMMARY AND FUTURE DIRECTIONS

The first part of my dissertation focused on the biochemical and biophysical characterization of the nucleosome-MeCP2 complex. It has been shown that MeCP2 is a chromatin architectural protein that can compact chromatin into a higher order structure. Nucleosomes are the basic repeating units of chromatin. To understand the interplay between MeCP2 and chromatin, it is important to understand first how MeCP2 interacts with nucleosomes. Results in chapter 2 demonstrated that MeCP2 prefers to interact with nucleosomes with linker DNA although it can also interact with nucleosomes without linker DNA. The results of various in-solution assays suggested that a single MeCP2 molecule binds to a single nucleosome at the “entry-exit” region and brings linker DNA ends closer to form a “stem” structure. Our data suggest a model in which MeCP2 compacts chromatin by altering the path of the linker DNA. However we do not have direct evidence to verify this model. In the future, high resolution atomic force microscopy (AFM) or Electron microscopy (EM) can be used to visualize the “stem” structure on mononucleosomes upon MeCP2 binding. Although EM has been applied to visualize the mononucleosome-MeCP2 complex structure and no significant “stem” structure was observed (Nikitina et al., 2007), this may be due to the length of the DNA used to reconstitute the nucleosomes. In the EM study with

nucleosomal array and MeCP2, some “stem” and loop formation were observed (Nikitina et al., 2007b). In the study by Nikitina *et al*, they used 208 bp DNA in the mononucleosome reconstitution, so the linker DNA is about 30 bp in each end. When MeCP2 binds to the DNA “entry-exit” region on nucleosome and pulls the two DNA ends closer, it is possible that the short linker DNA has a significant resistance force to the bending caused by MeCP2, so that in solution the bent DNA ends will not be held in place consistently. As a result, no significant amounts of “stem” structures were observed. In contrast, Hamiche *et al* visualized the “stem”-like structure in the ~256bp DNA-containing mononucleosome in the presence of linker histone H5 by EM (Hamiche et al., 1996), so in our case, nucleosomes with longer DNA should be tried in AFM or EM upon addition of MeCP2.

The nucleosomes consist of a histone octamer core as well as of DNA. Whether the histone octamer core also participates in the interaction with MeCP2 is investigated in chapter 3. Intein-tagged MeCP2 pull-down assay showed that MeCP2 interacts with histones in folded forms (for example, H2A/H2B dimer, (H3/H4)₂ tetramer), but not in unfolded forms (individual H2A, H2B, H3 or H4). Results obtained from other in-solution assays without intein tags including gel filtration combined with light scattering did not show the interaction between MeCP2 and histones. The inconsistency in results obtained with intein-tagged pull-down assay and other solution-state assays suggests that the interaction indicated by the intein-MeCP2 fusion protein pull-down assay may be particular to an epitope for histone binding incidentally formed between the intein tag and

MeCP2. To further investigate this hypothesis, the interaction between intein-MeCP2 fusion protein and histones needs to be investigated in the in-solution assays (e.g. gel filtration combined light scattering) as an important control. Alternatively, protein tags like GST tag and/or small peptide tags (for example, FLAG tag) can be used in substitution of the intein-tag in the pull-down assays. If interactions were consistently observed in the pull-down assays with different tags, the interactions between MeCP2 and histones may be true interactions, and other conditions would have to be screened to demonstrate the interaction in solution.

During the crystallographic studies of the nucleosome-MeCP2 complexes, crystals of the 165NCP-MeCP2 complex were obtained that diffracted to 5.2 Å resolution. Molecular replacement searches in Phaser programs led to one good solution with six nucleosomes present in the asymmetric unit. However, crystal content check on SDS-PAGE gel indicated that MeCP2 was dissociated from the crystal after the cryo-protectant soaking procedures. Also, the selenomethionine labeled MeCP2 containing crystals did not show a selenium absorption peak, indicating that no MeCP2 is present in the crystals.

In the future, efforts should be made to improve the quality of the complex crystals and prevent the dissociation of MeCP2 from the crystals. The following approaches should be tried:

a: Optimize MeCP2 or its fragments used to co-crystallize with nucleosomes. 165NCP-MeCP2WT complex was crystallized under the same condition as the

165NCP-MeCP2B complex. Because the 165NCP-MeCP2WT complex crystals were not as big and nice as the 165NCP-MeCP2B complex crystals, no further efforts were given to the 165NCP-MeCP2WT complex crystallization. However, after optimization of the crystallization conditions, the 165NCP-MeCP2WT complex could grow much bigger and nicer and lead to a high resolution crystal structure of nucleosome-MeCP2 complexes.

In addition to MeCP2 fragment B (residue 78-305), different MeCP2 fragments can be tried to optimize the nucleosome-MeCP2 complex. Unpublished data (from Hansen lab and Woodcock lab) has shown that MeCP2 has three different non-specific DNA binding domains (MBD, HMGD2 and TRD) and a C-terminal chromatin interaction region. Some or all of them may be engaged in the interaction with nucleosomes. Fragment B has all 3 DNA binding domains; however, the latest unpublished data (from Woodcock/Hansen labs) suggests that complete chromatin condensation can be accomplished with residues 200-486. So this fragment (residue 200-486) would be a good candidate to co-crystallize with 165NCP.

b: Optimize the nucleosomes used to co-crystallize with MeCP2. This includes the optimization of the length of extra nucleosomal DNA within the nucleosomes. We have shown in chapter 2 that extra nucleosomal DNA is important in organizing the MeCP2-nucleosome complex; however, we did not investigate whether 10 bp extra nucleosomal DNA in each side of nucleosomes is enough to organize the complex. Other lengths of extra nucleosomal DNA need to be tried too.

Also, it is known that MeCP2 has higher affinity for methylated DNA. So nucleosomes reconstituted with methylated DNA can also be tried in the crystallization with MeCP2.

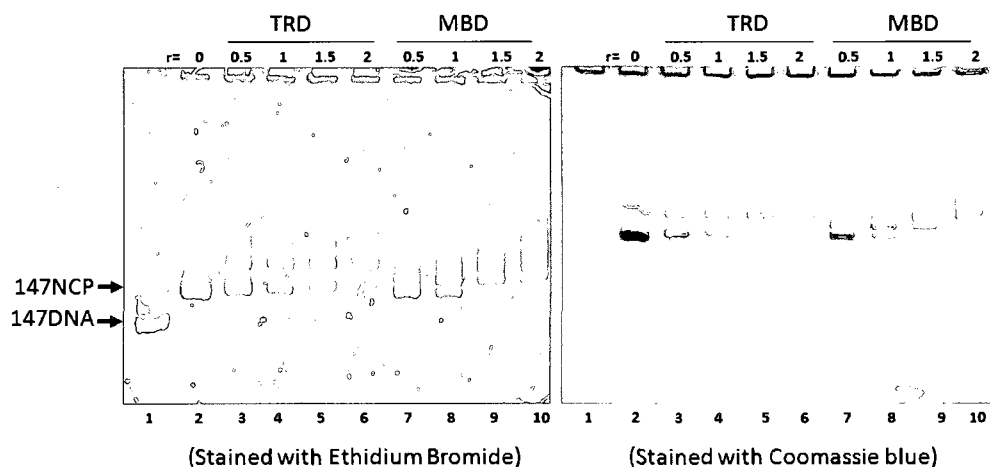
c: During the cryo-protectant soaking procedures, MeCP2 may have dissociated from the crystal. It is possible that the interaction between MeCP2 and nucleosomes in the crystal is relatively weak and therefore favors dissociation since there is no MeCP2 in the soaking solution. To prevent this, MeCP2 should be added into the soaking solution in each step to push the reaction towards the bound state. Alternately, we can try to crosslink MeCP2 and nucleosomes after the crystals are formed, so that the association state is “frozen” in the crystal.

d: A four-way DNA junction could be used as a “pseudo” nucleosome in the crystallization trials with MeCP2. It has been shown that MeCP2 also binds to unmethylated four-way DNA junctions with a similar affinity to methylated DNA (Galvao and Thomas, 2005), and data in chapter 2 suggested that MeCP2 likely binds to nucleosomes at the DNA “entry-exit” region. The four-way DNA junction mimics the structure of nucleosomes at the DNA “entry-exit” region where MeCP2 is likely bound. The structure of a four-way DNA junction-MeCP2 complex will shed light on the mechanisms of how MeCP2 interacts with nucleosomes.

We believe that a high resolution structure of MeCP2-nucleosome complex will not only decipher the structure of MeCP2 which has been long delayed, it will also shed light on the functions of MeCP2, how it interacts with nucleosomes in

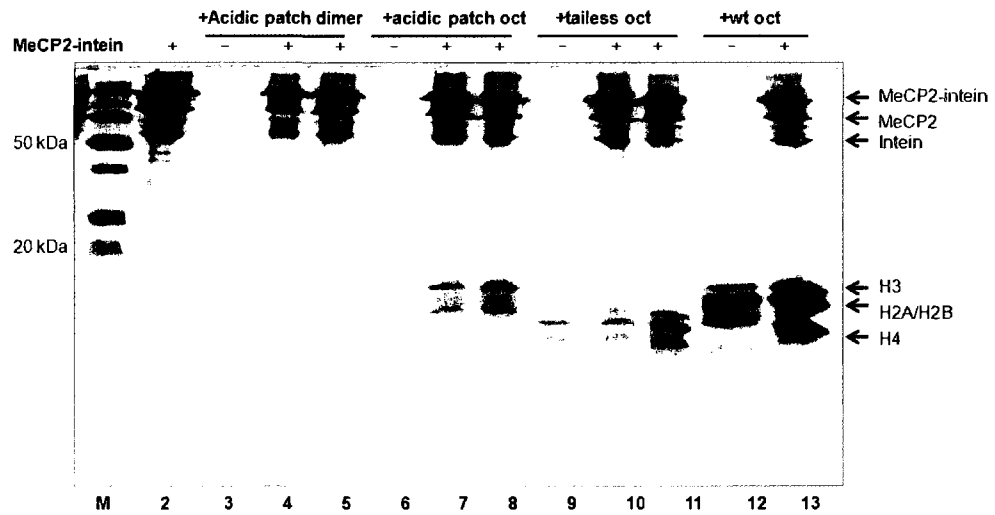
the chromatin context, how it regulates the chromatin structure. More importantly, the details of how MeCP2 function as a chromatin structural protein may also shed light on the mechanisms of Rett Syndrome.

Appendix I



Appendix I figure: MeCP2 TRD and MBD can interact with 147 NCP. Increasing amounts (at molar ratio of 0.5 to 2.0) of MeCP2 TRD or MBD were added to 147NCP, resulting retardation of the mobility of 147NCP. Left panel and right panel show the same 5% native gel stained with different methods (left: Ethidium Bromide staining; right: Coomassie blue staining).

Appendix II



Appendix II figure: Intein-tagged MeCP2 can pull down acidic patch mutant H2A/H2B dimer (lane 4-5) and octamer (lane 7-8), all four histone tailless octamer (lane 10-11) as well as intact histone octamer (lane 13).

References

- Adams, V.H., McBryant, S.J., Wade, P.A., Woodcock, C.L., and Hansen, J.C. (2007). Intrinsic disorder and autonomous domain function in the multifunctional nuclear protein, MeCP2. *J Biol Chem* 282, 15057-15064.
- Adler, D.A., Quaderi, N.A., Brown, S.D., Chapman, V.M., Moore, J., Tate, P., and Disteché, C.M. (1995). The X-linked methylated DNA binding protein, MeCP2, is subject to X inactivation in the mouse. *Mamm Genome* 6, 491-492.
- Akbarian, S., Chen, R.Z., Gribnau, J., Rasmussen, T.P., Fong, H., Jaenisch, R., and Jones, E.G. (2001). Expression pattern of the Rett syndrome gene MeCP2 in primate prefrontal cortex. *Neurobiol Dis* 8, 784-791.
- Amir, R.E., Van den Veyver, I.B., Wan, M., Tran, C.Q., Francke, U., and Zoghbi, H.Y. (1999). Rett syndrome is caused by mutations in X-linked MECP2, encoding methyl-CpG-binding protein 2. *Nat Genet* 23, 185-188.
- Anraku, Y., Mizutani, R., and Satow, Y. (2005). Protein splicing: its discovery and structural insight into novel chemical mechanisms. *IUBMB Life* 57, 563-574.
- Antequera, F., Macleod, D., and Bird, A.P. (1989). Specific protection of methylated CpGs in mammalian nuclei. *Cell* 58, 509-517.
- Archidiacono, N., Lerone, M., Rocchi, M., Anvret, M., Ozcelik, T., Francke, U., and Romeo, G. (1991). Rett syndrome: exclusion mapping following the hypothesis of germinal mosaicism for new X-linked mutations. *Hum Genet* 86, 604-606.
- Ballas, N., Lioy, D.T., Grunseich, C., and Mandel, G. (2009). Non-cell autonomous influence of MeCP2-deficient glia on neuronal dendritic morphology. *Nat Neurosci* 12, 311-317.
- Ballestar, E., Ropero, S., Alaminos, M., Armstrong, J., Setien, F., Agrelo, R., Fraga, M.F., Herranz, M., Avila, S., Pineda, M., *et al.* (2005). The impact of MECP2 mutations in the expression patterns of Rett syndrome patients. *Hum Genet* 116, 91-104.
- Barbera, A.J., Chodaparambil, J.V., Kelley-Clarke, B., Joukov, V., Walter, J.C., Luger, K., and Kaye, K.M. (2006). The nucleosomal surface as a docking station for Kaposi's sarcoma herpesvirus LANA. *Science* 311, 856-861.
- Bates, D.L., and Thomas, J.O. (1981). Histones H1 and H5: one or two molecules per nucleosome? *Nucleic Acids Res* 9, 5883-5894.
- Bednar, J., Horowitz, R.A., Grigoryev, S.A., Carruthers, L.M., Hansen, J.C., Koster, A.J., and Woodcock, C.L. (1998). Nucleosomes, linker DNA, and linker histone form a unique structural motif that directs the higher-order folding and compaction of chromatin. *Proc Natl Acad Sci U S A* 95, 14173-14178.

- Bird, A. (1992). The essentials of DNA methylation. *Cell* 70, 5-8.
- Bird, A.P. (1986). CpG-rich islands and the function of DNA methylation. *Nature* 321, 209-213.
- Bird, A.P., and Wolffe, A.P. (1999). Methylation-induced repression--belts, braces, and chromatin. *Cell* 99, 451-454.
- Boyes, J., and Bird, A. (1991). DNA methylation inhibits transcription indirectly via a methyl-CpG binding protein. *Cell* 64, 1123-1134.
- Buschdorf, J.P., and Stratling, W.H. (2004). A WW domain binding region in methyl-CpG-binding protein MeCP2: impact on Rett syndrome. *J Mol Med* 82, 135-143.
- Butler, P.J.G., and Thomas, J.O. (1998). Dinucleosomes show compaction by ionic strength, consistent with bending of linker DNA. *Journal of Molecular Biology* 281, 401-407.
- Cedar, H. (1988). DNA methylation and gene activity. *Cell* 53, 3-4.
- Chahrour, M., Jung, S.Y., Shaw, C., Zhou, X.B., Wong, S.T.C., Qin, J., and Zoghbi, H.Y. (2008). MeCP2, a key contributor to neurological disease, activates and represses transcription. *Science* 320, 1224-1229.
- Chandler, S.P., Guschin, D., Landsberger, N., and Wolffe, A.P. (1999). The methyl-CpG binding transcriptional repressor MeCP2 stably associates with nucleosomal DNA. *Biochemistry* 38, 7008-7018.
- Chang, Q., Khare, G., Dani, V., Nelson, S., and Jaenisch, R. (2006). The disease progression of Mecp2 mutant mice is affected by the level of BDNF expression. *Neuron* 49, 341-348.
- Cheadle, J.P., Gill, H., Fleming, N., Maynard, J., Kerr, A., Leonard, H., Krawczak, M., Cooper, D.N., Lynch, S., Thomas, N., *et al.* (2000). Long-read sequence analysis of the MECP2 gene in Rett syndrome patients: correlation of disease severity with mutation type and location. *Hum Mol Genet* 9, 1119-1129.
- Chen, R.Z., Pettersson, U., Beard, C., Jackson-Grusby, L., and Jaenisch, R. (1998). DNA hypomethylation leads to elevated mutation rates. *Nature* 395, 89-93.
- Chen, W.G., Chang, Q., Lin, Y., Meissner, A., West, A.E., Griffith, E.C., Jaenisch, R., and Greenberg, M.E. (2003). Derepression of BDNF transcription involves calcium-dependent phosphorylation of MeCP2. *Science* 302, 885-889.
- Chodaparambil, J.V., Barbera, A.J., Lu, X., Kaye, K.M., Hansen, J.C., and Luger, K. (2007). A charged and contoured surface on the nucleosome regulates chromatin compaction. *Nat Struct Mol Biol* 14, 1105-1107.
- Colantuoni, C., Jeon, O.H., Hyder, K., Chenchik, A., Khimani, A.H., Narayanan, V., Hoffman, E.P., Kaufmann, W.E., Naidu, S., and Pevsner, J. (2001). Gene expression profiling in postmortem Rett Syndrome brain: differential gene expression and patient classification. *Neurobiol Dis* 8, 847-865.

Comb, M., and Goodman, H.M. (1990). CpG methylation inhibits proenkephalin gene expression and binding of the transcription factor AP-2. *Nucleic Acids Res* 18, 3975-3982.

Cross, S.H., Meehan, R.R., Nan, X., and Bird, A. (1997). A component of the transcriptional repressor MeCP1 shares a motif with DNA methyltransferase and HRX proteins. *Nat Genet* 16, 256-259.

Curtis, A.R., Headland, S., Lindsay, S., Thomas, N.S., Boye, E., Kamakari, S., Roustan, P., Anvret, M., Wahlstrom, J., McCarthy, G., *et al.* (1993). X chromosome linkage studies in familial Rett syndrome. *Hum Genet* 90, 551-555.

Dam, J., and Schuck, P. (2005). Sedimentation velocity analysis of heterogeneous protein-protein interactions: sedimentation coefficient distributions $c(s)$ and asymptotic boundary profiles from Gilbert-Jenkins theory. *Biophys J* 89, 651-666.

Demeler, B., Behlke, J., and Ristau, O. (2000). Molecular parameters from sedimentation velocity experiments: whole boundary fitting using approximate and numerical solutions of Lamm equation. *Methods Enzymol* 321, 38-66.

Demeler, B., and van Holde, K.E. (2004). Sedimentation velocity analysis of highly heterogeneous systems. *Anal Biochem* 335, 279-288.

D'Esposito, M., Quaderi, N.A., Ciccodicola, A., Bruni, P., Esposito, T., D'Urso, M., and Brown, S.D. (1996). Isolation, physical mapping, and northern analysis of the X-linked human gene encoding methyl CpG-binding protein, MECP2. *Mamm Genome* 7, 533-535.

Dorigo, B., Schalch, T., Bystricky, K., and Richmond, T.J. (2003). Chromatin fiber folding: requirement for the histone H4 N-terminal tail. *J Mol Biol* 327, 85-96.

Dorigo, B., Schalch, T., Kulangara, A., Duda, S., Schroeder, R.R., and Richmond, T.J. (2004). Nucleosome arrays reveal the two-start organization of the chromatin fiber. *Science* 306, 1571-1573.

Dyer, P.N., Edayathumangalam, R.S., White, C.L., Bao, Y., Chakravarthy, S., Muthurajan, U.M., and Luger, K. (2004). Reconstitution of nucleosome core particles from recombinant histones and DNA. *Methods Enzymol* 375, 23-44.

Edayathumangalam, R.S., and Luger, K. (2005). The temperature of flash-cooling has dramatic effects on the diffraction quality of nucleosome crystals. *Acta Crystallogr D Biol Crystallogr* 61, 891-898.

Ehrenhofer-Murray, A.E. (2004). Chromatin dynamics at DNA replication, transcription and repair. *Eur J Biochem* 271, 2335-2349.

Emsley, P., and Cowtan, K. (2004). Coot: model-building tools for molecular graphics. *Acta Crystallogr D Biol Crystallogr* 60, 2126-2132.

Ellison, K.A., Fill, C.P., Terwilliger, J., DeGennaro, L.J., Martin-Gallardo, A., Anvret, M., Percy, A.K., Ott, J., and Zoghbi, H. (1992). Examination of X chromosome markers in Rett syndrome:

exclusion mapping with a novel variation on multilocus linkage analysis. *Am J Hum Genet* 50, 278-287.

Fan, J.Y., Gordon, F., Luger, K., Hansen, J.C., and Tremethick, D.J. (2002). The essential histone variant H2A.Z regulates the equilibrium between different chromatin conformational states. *Nat Struct Biol* 9, 172-176.

Francis, N.J., Kingston, R.E., and Woodcock, C.L. (2004). Chromatin compaction by a polycomb group protein complex. *Science* 306, 1574-1577.

Fujita, N., Takebayashi, S., Okumura, K., Kudo, S., Chiba, T., Saya, H., and Nakao, M. (1999). Methylation-mediated transcriptional silencing in euchromatin by methyl-CpG binding protein MBD1 isoforms. *Mol Cell Biol* 19, 6415-6426.

Fuks, F., Hurd, P.J., Wolf, D., Nan, X.S., Bird, A.P., and Kouzarides, T. (2003). The Methyl-CpG-binding protein MeCP2 links DNA methylation to histone methylation. *Journal of Biological Chemistry* 278, 4035-4040.

Galvao, T.C., and Thomas, J.O. (2005). Structure-specific binding of MeCP2 to four-way junction DNA through its methyl CpG-binding domain. *Nucleic Acids Res* 33, 6603-6609.

Georgel, P.T., Horowitz-Scherer, R.A., Adkins, N., Woodcock, C.L., Wade, P.A., and Hansen, J.C. (2003). Chromatin compaction by human MeCP2. Assembly of novel secondary chromatin structures in the absence of DNA methylation. *J Biol Chem* 278, 32181-32188.

Guideri, F., Acampa, M., Hayek, G., Zappella, M., and Di Perri, T. (1999). Reduced heart rate variability in patients affected with Rett syndrome. A possible explanation for sudden death. *Neuropediatrics* 30, 146-148.

Hagberg, B. (1985). Rett's syndrome: prevalence and impact on progressive severe mental retardation in girls. *Acta Paediatr Scand* 74, 405-408.

Hagberg, B., Aicardi, J., Dias, K., and Ramos, O. (1983). A progressive syndrome of autism, dementia, ataxia, and loss of purposeful hand use in girls: Rett's syndrome: report of 35 cases. *Ann Neurol* 14, 471-479.

Hamiche, A., Schultz, P., Ramakrishnan, V., Oudet, P., and Prunell, A. (1996a). Linker histone-dependent DNA structure in linear mononucleosomes. *J Mol Biol* 257, 30-42.

Hamiche, A., Schultz, P., Ramakrishnan, V., Oudet, P., and Prunell, A. (1996b). Linker histone-dependent DNA structure in linear mononucleosomes. *Journal of Molecular Biology* 257, 30-42.

Hansen, J.C. (2002). Conformational dynamics of the chromatin fiber in solution: determinants, mechanisms, and functions. *Annu Rev Biophys Biomol Struct* 31, 361-392.

Hayes, J.J., and Wolffe, A.P. (1993). Preferential and Asymmetric Interaction of Linker Histones with 5s DNA in the Nucleosome. *Proceedings of the National Academy of Sciences of the United States of America* 90, 6415-6419.

- Hendrich, B., and Bird, A. (1998). Identification and characterization of a family of mammalian methyl-CpG binding proteins. *Mol Cell Biol* 18, 6538-6547.
- Hendrich, B., Hardeland, U., Ng, H.H., Jiricny, J., and Bird, A. (1999). The thymine glycosylase MBD4 can bind to the product of deamination at methylated CpG sites. *Nature* 401, 301-304.
- Hizume, K., Nakai, T., Araki, S., Prieto, E., Yoshikawa, K., and Takeyasu, K. (2009). Removal of histone tails from nucleosome dissects the physical mechanisms of salt-induced aggregation, linker histone H1-induced compaction, and 30-nm fiber formation of the nucleosome array. *Ultramicroscopy*.
- Ho, K.L., Mcnae, L.W., Schmiedeberg, L., Klose, R.J., Bird, A.P., and Walkinshaw, M.D. (2008). MeCP2 binding to DNA depends upon hydration at methyl-CpG. *Molecular Cell* 29, 525-531.
- Horike, S., Cai, S., Miyano, M., Cheng, J.F., and Kohwi-Shigematsu, T. (2005). Loss of silent-chromatin looping and impaired imprinting of DLX5 in Rett syndrome. *Nat Genet* 37, 31-40.
- Iguchi-Ariga, S.M., and Schaffner, W. (1989). CpG methylation of the cAMP-responsive enhancer/promoter sequence TGACGTCA abolishes specific factor binding as well as transcriptional activation. *Genes Dev* 3, 612-619.
- Jaenisch, R. (1997). DNA methylation and imprinting: why bother? *Trends Genet* 13, 323-329.
- Jones, P.L., Veenstra, G.J., Wade, P.A., Vermaak, D., Kass, S.U., Landsberger, N., Strouboulis, J., and Wolffe, A.P. (1998). Methylated DNA and MeCP2 recruit histone deacetylase to repress transcription. *Nat Genet* 19, 187-191.
- Jordan, C., Li, H.H., Kwan, H.C., and Francke, U. (2007). Cerebellar gene expression profiles of mouse models for Rett syndrome reveal novel MeCP2 targets. *BMC Med Genet* 8, 36.
- Kaludov, N.K., and Wolffe, A.P. (2000). MeCP2 driven transcriptional repression in vitro: selectivity for methylated DNA, action at a distance and contacts with the basal transcription machinery. *Nucleic Acids Res* 28, 1921-1928.
- Kato, Y., Nagata, K., Takahashi, M., Lian, L., Herrero, J.J., Sudol, M., and Tanokura, M. (2004). Common mechanism of ligand recognition by group II/III WW domains: redefining their functional classification. *J Biol Chem* 279, 31833-31841.
- Keshet, I., Lieman-Hurwitz, J., and Cedar, H. (1986). DNA methylation affects the formation of active chromatin. *Cell* 44, 535-543.
- Kimura, H., and Shiota, K. (2003). Methyl-CpG-binding protein, MeCP2, is a target molecule for maintenance DNA methyltransferase, Dnmt1. *Journal of Biological Chemistry* 278, 4806-4812.
- Klose, R.J., and Bird, A.P. (2004). MeCP2 behaves as an elongated monomer that does not stably associate with the Sin3a chromatin remodeling complex. *Journal of Biological Chemistry* 279, 46490-46496.

- Kokura, K., Kaul, S.C., Wadhwa, R., Nomura, T., Khan, M.M., Shinagawa, T., Yasukawa, T., Colmenares, C., and Ishii, S. (2001). The ski protein family is required for MeCP2-mediated transcriptional repression. *Journal of Biological Chemistry* 276, 34115-34121.
- Konarev, P.V., Volkov, V.V., Sokolova, A.V., Koch, M.H.J., and Svergun, D.I. (2003). PRIMUS: a Windows PC-based system for small-angle scattering data analysis. *Journal of Applied Crystallography* 36, 1277-1282.
- LaSalle, J.M., Goldstine, J., Balmer, D., and Greco, C.M. (2001). Quantitative localization of heterogeneous methyl-CpG-binding protein 2 (MeCP2) expression phenotypes in normal and Rett syndrome brain by laser scanning cytometry. *Hum Mol Genet* 10, 1729-1740.
- Lewis, J.D., Meehan, R.R., Henzel, W.J., Maurer-Fogy, I., Jeppesen, P., Klein, F., and Bird, A. (1992). Purification, sequence, and cellular localization of a novel chromosomal protein that binds to methylated DNA. *Cell* 69, 905-914.
- Lowary, P.T., and Widom, J. (1998). New DNA sequence rules for high affinity binding to histone octamer and sequence-directed nucleosome positioning. *Journal of Molecular Biology* 276, 19-42.
- Luger, K., Mader, A.W., Richmond, R.K., Sargent, D.F., and Richmond, T.J. (1997). Crystal structure of the nucleosome core particle at 2.8 Å resolution. *Nature* 389, 251-260.
- Mangenot, S., Leforestier, A., Vachette, P., Durand, D., and Livolant, F. (2002). Salt-induced conformation and interaction changes of nucleosome core particles. *Biophysical Journal* 82, 345-356.
- Mccoy, A.J., Grosse-Kunstleve, R.W., Adams, P.D., Winn, M.D., Storoni, L.C., and Read, R.J. (2007). Phaser crystallographic software. *Journal of Applied Crystallography* 40, 658-674.
- Meehan, R.R., Lewis, J.D., and Bird, A.P. (1992). Characterization of MeCP2, a vertebrate DNA binding protein with affinity for methylated DNA. *Nucleic Acids Res* 20, 5085-5092.
- Meehan, R.R., Lewis, J.D., McKay, S., Kleiner, E.L., and Bird, A.P. (1989). Identification of a mammalian protein that binds specifically to DNA containing methylated CpGs. *Cell* 58, 499-507.
- McBryant, S.J., Adams, V.H., and Hansen, J.C. (2006). Chromatin architectural proteins. *Chromosome Res* 14, 39-51.
- Monros, E., Armstrong, J., Aibar, E., Poo, P., Canos, I., and Pineda, M. (2001). Rett syndrome in Spain: mutation analysis and clinical correlations. *Brain Dev* 23 Suppl 1, S251-253.
- Murshudov, G.N., Vagin, A.A., and Dodson, E.J. (1997). Refinement of macromolecular structures by the maximum-likelihood method. *Acta Crystallogr D Biol Crystallogr* 53, 240-255.
- Nakao, M., Matsui, S., Yamamoto, S., Okumura, K., Shirakawa, M., and Fujita, N. (2001). Regulation of transcription and chromatin by methyl-CpG binding protein MBD1. *Brain Dev* 23 Suppl 1, S174-176.

- Nan, X., Campoy, F.J., and Bird, A. (1997). MeCP2 is a transcriptional repressor with abundant binding sites in genomic chromatin. *Cell* *88*, 471-481.
- Nan, X., Ng, H.H., Johnson, C.A., Laherty, C.D., Turner, B.M., Eisenman, R.N., and Bird, A. (1998). Transcriptional repression by the methyl-CpG-binding protein MeCP2 involves a histone deacetylase complex. *Nature* *393*, 386-389.
- Nan, X., Tate, P., Li, E., and Bird, A. (1996). DNA methylation specifies chromosomal localization of MeCP2. *Mol Cell Biol* *16*, 414-421.
- Nan, X.S., Meehan, R.R., and Bird, A. (1993). Dissection of the Methyl-CpG Binding Domain from the Chromosomal Protein Mecp2. *Nucleic Acids Research* *21*, 4886-4892.
- Navaza, J. (1994). Amore - an Automated Package for Molecular Replacement. *Acta Crystallographica Section A* *50*, 157-163.
- Ng, H.H., Zhang, Y., Hendrich, B., Johnson, C.A., Turner, B.M., Erdjument-Bromage, H., Tempst, P., Reinberg, D., and Bird, A. (1999). MBD2 is a transcriptional repressor belonging to the MeCP1 histone deacetylase complex. *Nat Genet* *23*, 58-61.
- Nikitina, T., Ghosh, R.P., Horowitz-Scherer, R.A., Hansen, J.C., Grigoryev, S.A., and Woodcock, C.L. (2007a). MeCP2-chromatin interactions include the formation of chromatosome-like structures and are altered in mutations causing Rett syndrome. *J Biol Chem*.
- Nikitina, T., Shi, X., Ghosh, R.P., Horowitz-Scherer, R.A., Hansen, J.C., and Woodcock, C.L. (2007b). Multiple modes of interaction between the methylated DNA binding protein MeCP2 and chromatin. *Mol Cell Biol* *27*, 864-877.
- Ohki, I., Shimotake, N., Fujita, N., Jee, J., Ikegami, T., Nakao, M., and Shirakawa, M. (2001). Solution structure of the methyl-CpG binding domain of human MBD1 in complex with methylated DNA. *Cell* *105*, 487-497.
- Pflugrath, J.W. (1999). The finer things in X-ray diffraction data collection. *Acta Crystallogr D Biol Crystallogr* *55*, 1718-1725.
- Prilusky, J., Felder, C.E., Zeev-Ben-Mordehai, T., Rydberg, E.H., Man, O., Beckmann, J.S., Silman, I., and Sussman, J.L. (2005). FoldIndex: a simple tool to predict whether a given protein sequence is intrinsically unfolded. *Bioinformatics* *21*, 3435-3438.
- Quaderi, N.A., Meehan, R.R., Tate, P.H., Cross, S.H., Bird, A.P., Chatterjee, A., Herman, G.E., and Brown, S.D. (1994). Genetic and physical mapping of a gene encoding a methyl CpG binding protein, Mecp2, to the mouse X chromosome. *Genomics* *22*, 648-651.
- Razin, A. (1998). CpG methylation, chromatin structure and gene silencing-a three-way connection. *EMBO J* *17*, 4905-4908.
- Rett, A. (1966). [On a unusual brain atrophy syndrome in hyperammonemia in childhood]. *Wien Med Wochenschr* *116*, 723-726.

- Riccio, A., Aaltonen, L.A., Godwin, A.K., Loukola, A., Percesepe, A., Salovaara, R., Masciullo, V., Genuardi, M., Paravatou-Petsotas, M., Bassi, D.E., *et al.* (1999). The DNA repair gene MBD4 (MED1) is mutated in human carcinomas with microsatellite instability. *Nat Genet* 23, 266-268.
- Riggs, A.D., and Pfeifer, G.P. (1992). X-chromosome inactivation and cell memory. *Trends Genet* 8, 169-174.
- Robinson, P.J., Fairall, L., Huynh, V.A., and Rhodes, D. (2006). EM measurements define the dimensions of the "30-nm" chromatin fiber: evidence for a compact, interdigitated structure. *Proc Natl Acad Sci U S A* 103, 6506-6511.
- Robinson, P.J., and Rhodes, D. (2006). Structure of the '30 nm' chromatin fibre: a key role for the linker histone. *Curr Opin Struct Biol* 16, 336-343.
- Routh, A., Sandin, S., and Rhodes, D. (2008). Nucleosome repeat length and linker histone stoichiometry determine chromatin fiber structure. *Proc Natl Acad Sci U S A* 105, 8872-8877.
- Schanen, C., and Francke, U. (1998). A severely affected male born into a Rett syndrome kindred supports X-linked inheritance and allows extension of the exclusion map. *Am J Hum Genet* 63, 267-269.
- Schanen, N.C., Dahle, E.J., Capozzoli, F., Holm, V.A., Zoghbi, H.Y., and Francke, U. (1997). A new Rett syndrome family consistent with X-linked inheritance expands the X chromosome exclusion map. *Am J Hum Genet* 61, 634-641.
- Schwartzman, J.S., Bernardino, A., Nishimura, A., Gomes, R.R., and Zatz, M. (2001). Rett syndrome in a boy with a 47,XXY karyotype confirmed by a rare mutation in the MECP2 gene. *Neuropediatrics* 32, 162-164.
- Schwartzman, J.S., De Souza, A.M., Faiwichow, G., and Hercowitz, L.H. (1998). [Rett phenotype in patient with XXY karyotype: case report]. *Arq Neuropsiquiatr* 56, 824-828.
- Sekul, E.A., Moak, J.P., Schultz, R.J., Glaze, D.G., Dunn, J.K., and Percy, A.K. (1994). Electrocardiographic findings in Rett syndrome: an explanation for sudden death? *J Pediatr* 125, 80-82.
- Shahbazian, M.D., Antalffy, B., Armstrong, D.L., and Zoghbi, H.Y. (2002). Insight into Rett syndrome: MeCP2 levels display tissue- and cell-specific differences and correlate with neuronal maturation. *Hum Mol Genet* 11, 115-124.
- Shahbazian, M.D., and Zoghbi, H.Y. (2001). Molecular genetics of Rett syndrome and clinical spectrum of MECP2 mutations. *Curr Opin Neurol* 14, 171-176.
- Sirianni, N., Naidu, S., Pereira, J., Pillotto, R.F., and Hoffman, E.P. (1998). Rett syndrome: confirmation of X-linked dominant inheritance, and localization of the gene to Xq28. *Am J Hum Genet* 63, 1552-1558.

- Smrt, R.D., Eaves-Egenes, J., Barkho, B.Z., Santistevan, N.J., Zhao, C., Aimone, J.B., Gage, F.H., and Zhao, X. (2007). Mecp2 deficiency leads to delayed maturation and altered gene expression in hippocampal neurons. *Neurobiol Dis* 27, 77-89.
- Springhetti, E.M., Istomina, N.E., Whisstock, J.C., Nikitina, T., Woodcock, C.L., and Grigoryev, S.A. (2003). Role of the M-loop and reactive center loop domains in the folding and bridging of nucleosome arrays by MENT. *J Biol Chem* 278, 43384-43393.
- Svergun, D.I. (1999). Restoring low resolution structure of biological macromolecules from solution scattering using simulated annealing. *Biophys J* 76, 2879-2886.
- Svergun, D.I., Petoukhov, M.V., and Koch, M.H. (2001). Determination of domain structure of proteins from X-ray solution scattering. *Biophys J* 80, 2946-2953.
- Tao, J., Hu, K., Chang, Q., Wu, H., Sherman, N.E., Martinowich, K., Klohe, R.J., Schanen, C., Jaenisch, R., Wang, W., *et al.* (2009). Phosphorylation of MeCP2 at Serine 80 regulates its chromatin association and neurological function. *Proc Natl Acad Sci U S A* 106, 4882-4887.
- Thomas, J.O. (1999). Histone H1: location and role. *Curr Opin Cell Biol* 11, 312-317.
- Toth, K., Brun, N., and Langowski, J. (2001). Trajectory of nucleosomal linker DNA studied by fluorescence resonance energy transfer. *Biochemistry* 40, 6921-6928.
- Trappe, R., Laccone, F., Cobilanschi, J., Meins, M., Huppke, P., Hanefeld, F., and Engel, W. (2001). MECP2 mutations in sporadic cases of Rett syndrome are almost exclusively of paternal origin. *Am J Hum Genet* 68, 1093-1101.
- Tudor, M., Akbarian, S., Chen, R.Z., and Jaenisch, R. (2002). Transcriptional profiling of a mouse model for Rett syndrome reveals subtle transcriptional changes in the brain. *Proc Natl Acad Sci U S A* 99, 15536-15541.
- Vilain, A., Apiou, F., Vogt, N., Dutrillaux, B., and Malfoy, B. (1996). Assignment of the gene for methyl-CpG-binding protein 2 (MECP2) to human chromosome band Xq28 by in situ hybridization. *Cytogenet Cell Genet* 74, 293-294.
- Wade, P.A., Geronne, A., Jones, P.L., Ballestar, E., Aubry, F., and Wolffe, A.P. (1999). Mi-2 complex couples DNA methylation to chromatin remodelling and histone deacetylation. *Nat Genet* 23, 62-66.
- Wakefield, R.I., Smith, B.O., Nan, X., Free, A., Soteriou, A., Uhrin, D., Bird, A.P., and Barlow, P.N. (1999). The solution structure of the domain from MeCP2 that binds to methylated DNA. *J Mol Biol* 291, 1055-1065.
- Wan, M., Lee, S.S., Zhang, X., Houwink-Manville, I., Song, H.R., Amir, R.E., Budden, S., Naidu, S., Pereira, J.L., Lo, I.F., *et al.* (1999). Rett syndrome and beyond: recurrent spontaneous and familial MECP2 mutations at CpG hotspots. *Am J Hum Genet* 65, 1520-1529.
- Woodcock, C.L., Skoultchi, A.I., and Fan, Y. (2006). Role of linker histone in chromatin structure and function: H1 stoichiometry and nucleosome repeat length. *Chromosome Res* 14, 17-25.

Woodcock, C.L. (2006). Chromatin architecture. *Curr Opin Struct Biol* *16*, 213-220.

Yasui, D.H., Peddada, S., Bieda, M.C., Vallerio, R.O., Hogart, A., Nagarajan, R.P., Thatcher, K.N., Farnham, P.J., and LaSalle, J.M. (2007). Integrated epigenomic analyses of neuronal MeCP2 reveal a role for long-range interaction with active genes. *Proceedings of the National Academy of Sciences of the United States of America* *104*, 19416-19421.

Young, J.I., Hong, E.P., Castle, J.C., Crespo-Barreto, J., Bowman, A.B., Rose, M.F., Kang, D., Richman, R., Johnson, J.M., Berget, S., *et al.* (2005). Regulation of RNA splicing by the methylation-dependent transcriptional repressor methyl-CpG binding protein 2. *Proc Natl Acad Sci U S A* *102*, 17551-17558.

Yu, F., Thiesen, J., and Stratling, W.H. (2000). Histone deacetylase-independent transcriptional repression by methyl-CpG-binding protein 2. *Nucleic Acids Res* *28*, 2201-2206.

Zhang, Y., Ng, H.H., Erdjument-Bromage, H., Tempst, P., Bird, A., and Reinberg, D. (1999). Analysis of the NuRD subunits reveals a histone deacetylase core complex and a connection with DNA methylation. *Genes Dev* *13*, 1924-1935.

Zhou, J., Fan, J.Y., Rangasamy, D., and Tremethick, D.J. (2007). The nucleosome surface regulates chromatin compaction and couples it with transcriptional repression. *Nat Struct Mol Biol* *14*, 1070-1076.

Zhou, Z., Hong, E.J., Cohen, S., Zhao, W.N., Ho, H.Y., Schmidt, L., Chen, W.G., Lin, Y., Savner, E., Griffith, E.C., *et al.* (2006). Brain-specific phosphorylation of MeCP2 regulates activity-dependent *Bdnf* transcription, dendritic growth, and spine maturation. *Neuron* *52*, 255-269.